

INFORMATION TO USERS

This was produced from a copy of a document sent to us for microfilming. While the most advanced technological means to photograph and reproduce this document have been used, the quality is heavily dependent upon the quality of the material submitted.

The following explanation of techniques is provided to help you understand markings or notations which may appear on this reproduction.

1. The sign or "target" for pages apparently lacking from the document photographed is "Missing Page(s)". If it was possible to obtain the missing page(s) or section, they are spliced into the film along with adjacent pages. This may have necessitated cutting through an image and duplicating adjacent pages to assure you of complete continuity.
2. When an image on the film is obliterated with a round black mark it is an indication that the film inspector noticed either blurred copy because of movement during exposure, or duplicate copy. Unless we meant to delete copyrighted materials that should not have been filmed, you will find a good image of the page in the adjacent frame. If copyrighted materials were deleted you will find a target note listing the pages in the adjacent frame.
3. When a map, drawing or chart, etc., is part of the material being photographed the photographer has followed a definite method in "sectioning" the material. It is customary to begin filming at the upper left hand corner of a large sheet and to continue from left to right in equal sections with small overlaps. If necessary, sectioning is continued again—beginning below the first row and continuing on until complete.
4. For any illustrations that cannot be reproduced satisfactorily by xerography, photographic prints can be purchased at additional cost and tipped into your xerographic copy. Requests can be made to our Dissertations Customer Services Department.
5. Some pages in any document may have indistinct print. In all cases we have filmed the best available copy.

University
Microfilms
International

300 N. ZEEB RD., ANN ARBOR, MI 48106

8209436

Ofoh, Ebere Paulinus

**DEVELOPMENT OF SUITABLE APPROXIMATION ALGORITHMS TO BE
USED IN THE DESCRIPTION OF HETEROGENEOUS RESERVOIRS FOR
SECONDARY RECOVERY STUDIES**

The University of Oklahoma

PH.D. 1981

**University
Microfilms
International** 300 N. Zeeb Road, Ann Arbor, MI 48106

PLEASE NOTE:

In all cases this material has been filmed in the best possible way from the available copy. Problems encountered with this document have been identified here with a check mark .

1. Glossy photographs or pages _____
2. Colored illustrations, paper or print _____
3. Photographs with dark background
4. Illustrations are poor copy
5. Pages with black marks, not original copy _____
6. Print shows through as there is text on both sides of page _____
7. Indistinct, broken or small print on several pages
8. Print exceeds margin requirements _____
9. Tightly bound copy with print lost in spine _____
10. Computer printout pages with indistinct print _____
11. Page(s) _____ lacking when material received, and not available from school or author.
12. Page(s) _____ seem to be missing in numbering only as text follows.
13. Two pages numbered _____. Text follows.
14. Curling and wrinkled pages _____
15. Other _____

University
Microfilms
International

THE UNIVERSITY OF OKLAHOMA
GRADUATE COLLEGE

DEVELOPMENT OF SUITABLE APPROXIMATION ALGORITHMS
TO BE USED IN THE DESCRIPTION OF HETEROGENEOUS
RESERVOIRS FOR SECONDARY RECOVERY STUDIES

A DISSERTATION
SUBMITTED TO THE GRADUATE FACULTY
in partial fulfillment of the requirements for the
degree of
DOCTOR OF PHILOSOPHY

BY
EBERE PAULINUS OFOH
Norman, Oklahoma
1981

DEVELOPMENT OF SUITABLE APPROXIMATION ALGORITHMS
TO BE USED IN THE DESCRIPTION OF HETEROGENEOUS
RESERVOIRS FOR SECONDARY RECOVERY STUDIES

A DISSERTATION

APPROVED FOR THE DEPARTMENT OF
PETROLEUM ENGINEERING

by

A. E. Menzie

C. K. Bluhm

John M. Kray

Richard V. Andtke

A. W. McGray

DISSERTATION COMMITTEE

ACKNOWLEDGEMENT

I would like to express my gratitude to Dr. D.E. Menzie, Executive Director, Energy Resource Centre, University of Oklahoma in Norman, for his supervision and helpful suggestions in this research effort. The author's appreciation is also warmly extended to Dr. R.M. Knapp, director of the Department of Petroleum and Geological Engineering, for his contributions and helpful suggestions in the mathematical formulation of this study. The author also extends his gratitude to the following members of his Doctoral Committee: Dr. R.V. Andree--a member of Who's Who in American Men of Science, Dr. A.W. McCray and Dr. E.F. Blick, for their kind encouragement through the duration of this study.

I would also like to extend my gratitude to my family, especially to my elder brother, Mr. G.E. Ofoh, for their moral support and patience throughout the course of this investigation.

Lastly, I would like to extend my gratitude to the following organizations for their financial support while the author was in graduate school at Norman: The Nigerian National Petroleum Corporation; Energy Resources Center --University of Oklahoma in Norman; Petroleum Engineering Department for a teaching fellowship.

ABSTRACT

Our current capability to accurately predict the performance of a reservoir given a detailed description of its heterogeneities, calls for an urgent need for an efficient method of describing these non-conformities at any given locations in a reservoir.

In this study, a suitable approximation algorithm was developed for use in the estimation of reservoir performance prior to waterflooding operations. This algorithm, a two dimensional cubic spline, constructs a smooth, and continuous function of the given data values. This smooth function with continuous first and second derivatives, removes the 'wiggly' and undulating characteristics often present in most polynomial approximations.

A number of tests using varying degrees of data contamination shows that the model has the potential to reduce bad data effects. It was also shown that the model can be used to easily determine the reservoir floodable volume, the water injection schedule for secondary recovery operations, and an overall waterflooding performance.

The prediction method makes use of flow capacity distributions in a heterogeneous reservoir.

TABLE OF CONTENTS

	Page
ACKNOWLEDGEMENT	iii
LIST OF FIGURES	vi
LIST OF TABLES	viii
 Chapter	
I. INTRODUCTION	1
1. Review of Previous H ₂ O Flood Applications using core data	3
2. Review of literature on selective plugging	6
II. VARIOUS INTERPOLATION PROCEDURES	9
1. Contour Mapping	9
2. Three Dimensional Projection	10
3. Available Interpolation Technique	12
4. Multi-quadric Equations of Topography and Other Irregular Surfaces	12
5. The Multi-quadric Model	13
6. The Triangular Approach	16
7. Trend Surface Model	16
III. THEORY OF THE WEIGHTED AVERAGES	24
Nomenclature for the weighting technique	34
1. The Weighting Technique	25
2. Vectorial Weighting	28
3. Continuity Weighting	29
4. Influence of Discontinuity	30
5. Practical Example Problem	31
Nomenclature for the cubic spline functions	63
IV. Theory of Cubic Spline	35
1. Reasons for the Cubic Spline Study	37
2. Interpolation using Cubic Spline	38

3.	Sample Problem for One Dimensional Spline (Irregularly distributed data points)	42
4.	Two Dimensional Spline Approach	48
4(a)	Two-dimensional Linear Interpolation.	48
4(b)	Cubic Spline Interpolation in Two-Dimensions.	51
5.	Theoretical Validation of the Procedure Outlined by Use of Hilbert Space Theory.	54
6.	Computation of Derivatives.	56
7.	Sample Problem for Two-dimensional Spline Interpolation (regularly distributed data points).	59
V.	Model Testing	65
VI.	DISCUSSION AND PRACTICAL PETROLEUM ENGINEERING APPLICATION OF THE PROPOSED MODEL.	82
1.	Procedure for Estimation of Flood Performance Using the Results of This Model.	84
	Derivation of Functional Equation	84
	Sample Calculation.	88
2.	Determination of Reservoir Productive Volume	93
3.	Water Injection Plan.	97
4.	Limitations of this Model	100
VII.	CONCLUSIONS AND RECOMMENDATIONS	101
	Recommendations	102
	References.	103
	Appendices.	106
A.	Flow Chart and Nomenclature for the Splint Prediction Algorithm	107
	Flow Chart.	108
	Sub Program	109
	Nomenclature for terms used in the Program	110
B.	Sample Program.	111
C.	Output Program.	113
D.	Program Listing	123

List of Figures

Figure		Page
1.	Prediction of waterflood performance by use of reservoir parameter distribution	4
2.0	The triangular approach.	17
2.1	One, two, and three dimensional representations of surface trend analysis	19
2.2	Trend surface analysis for original gas in place in Woods and Woodward Counties using Symap program	21
2.3	Contour map of a theoretical surface	22
2.4	Trend surface analysis applied to oil bearing structure in Lost Spring area of Kansas	22
3.1	Conceptual procedure for the interpolation of reservoir data.	27
4.1	Deflection of continuous surface	36
4.2	Linear relation of $M(x)$ versus X	38
4.3	Comparison of the result of sample calculation and linear interpolation with original curve.	47
4.4	2-Dimensional linear interpolation	49
4.5	Two-dimensional spline interpolation	52
5.1	Comparison of Lagrange interpolation method with the method of this study	67
5.2	Contour plots of the two-dimensional approach of this study and the Hermite Interpolation Method	69
5.3	Flow capacity distribution in the Sitio Grand field.	71
5.4	3-D plot of flow-capacity distribution Sitio Grand field.	73
5.5	3-Dimensional plot of waveform distribution	75
5.6	Original surface	76
5.7	Surface obtained by replacing 5% of data values with zeros (extreme cases)	77
5.8	Surface obtained by replacing 10% of data values with zeros	79
5.9	Surface obtained by replacing 20% of data values with zeros (extreme cases)	80
5.10	Surface obtained by replacing 30% of data points with zeros (extreme cases)	81

6.1	Flow capacity distribution in the Sitio Grand field.	85
6.2	3-Dimensional plot of flow capacity distribution in Sitio Grand field. . . .	86
6.3	Diagram showing parts of a	90
6.4	Plot of water cut versus oil recovery. .	90
6.5	Plot of flow capacity versus oil recovery	91
6.6	Plot of flow capacity versus water cut.	92
6.7	Plot of cumulative capacity versus cumulative volume.	95
6.8	Plot of water injection versus water cut.	98
A-1	Flow chart for this model--main. : . . .	107
A-2	Flow chart for subroutine splint	108
4.6	Interpolation along X-axis first, and then Y axis.	61
4.7	Interpolation along Y axis first, and then Y axis.	62

List of Tables

Table		Page
3.1	Values of parameters calculation	33
4.1	Sample data.	45
4.2	Two dimensional interpolation method	60
5.1	Data for comparison of Lagrange interpolation method with the method of this study	66
5.2	Reservoir data from Sitio Grand field in New Mexico.	68
5.3	Wave form study data	72
6.1	Calculation of reservoir performance	89
6.2	Determination of reservoir productive volume (Planimeter method).	94
6.3	Calculation of reservoir volume.	96
6.4	Water injection plan	99
A-1	Input data for sample program.	112
4.3	Solution values - interpolation of X, first.	60
4.4	Solution values - interpolating Y first, then, X.	60

CHAPTER I

INTRODUCTION

Our present capability to accurately predict the performance of a reservoir given a detailed description of its heterogeneities, calls for an urgent need for an improved description of these non-conformities at given locations in a field. Good waterflood engineering can be achieved by a precise and quantitative description of these reservoir heterogeneities. This need has become more critical particularly now that the industry has turned its attention to the low permeability regions of the field. Since it is now certain that the probability of obtaining a homogeneous reservoir structure is remote, experts are developing different mathematical models to define reservoirs in terms of their intensive properties. This is just part of the unending effort by researchers to continuously evaluate factors affecting waterflood performance in order to reduce operating costs and increase ultimate recovery. In practice, a reservoir may be non-uniform in all its intensive properties such as pore size distribution, wettability, connate water saturations, crude properties, permeability, porosity and thickness. This study recognizes the last three parameters: permeability,

porosity and thickness as important tools needed in the planning of waterflood projects when we have available core analysis data. Various techniques for describing a reservoir by means of these basic properties are well documented in the literature.

Kruger [18] was the first to quantitatively describe areal permeability distributions using observed differences in well production history. Jacquard and Jain [13] used field pressure data in their numerical technique model. Jans [14] developed a regression analysis technique and used pressure interference test data. Johnson et al published a method [15], "Pulse testing," for describing reservoir flow properties between wells. Their technique showed promise for providing a measure of storage capacity (ϕh), and formation flow capacity (kh). Hutchinson [11] suggested that formation outcrop be carefully examined to obtain information on such factors as continuity of zones of specific permeability, extent of shale breaks, and the degree of stratification.

The use of core data in the study of reservoir properties has been controversial. Kruger [18] remarked that the use of core analysis and/or well flow tests give sparse, spotty, and doubtful information that are difficult to interpret. However, Miller and Lenta [20] by use of a 'Positional Approach' method had disproved this belief. Using the positional approach model, they were able to determine the

layering properties of Cotton-Valley reservoir project from core data obtained from different wells. Skov, et al⁹ also reported success when they used a similar technique to match the performance of a number of fluid injection projects.

1.1 Review of Previous Waterflood Applications Using Core Data

One of the earliest attempts to use a two-dimensional approach of parameter distributions to predict waterflood performance in depleted or nearly depleted reservoirs was by Stiles [28]. He studied the lateral flow of fluids in formations of irregular permeability. He represented patterns of irregularities by a smoothed permeability distribution curve and a flow capacity distribution curve. The permeability values were arranged in order of decreasing values. Dimensionless values of permeability ratios were plotted against the cumulative thickness (ratio). Similarly he plotted dimensionless capacity ratio against cumulative thickness (ratio). He also calculated water cut values and recovery values using appropriate equations. Water Cut-Recovery Curve was then used to predict the behavior of a well. The prediction model, however did not consider the structural nature of the reservoir under study. To obtain better results, such other factors as the shape of field, the structural position of the individual wells, and well spacing should be considered by the model.

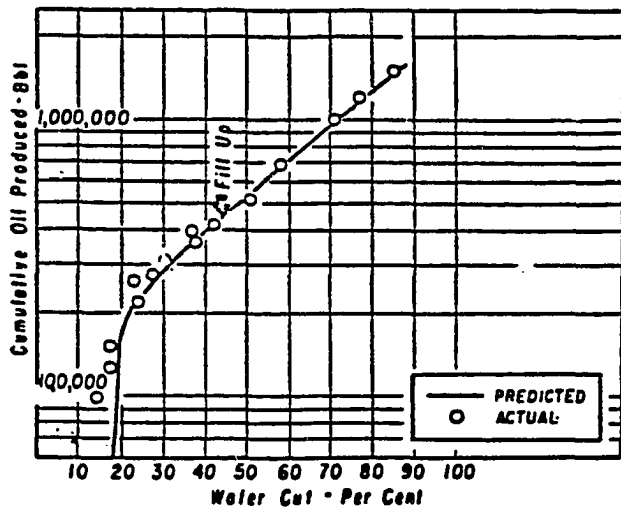
In his two dimensional approach Johnson [16] used a graphical representation of porosity and permeability

distribution to predict waterflood performance. His technique was able to predict cumulative water injected and cumulative oil produced in terms of percent water-cut by use of permeability-porosity relationship. Classifying the reservoir permeability data (from core analysis) in order of decreasing values, he made a plot of cumulative flow capacity versus the logarithm of the corresponding cumulative volume. He observed that the above plot is similar to the plot of logarithm of cumulative oil recovery versus water cut. By this finding, Johnson [16] is confirming the work of Stiles [28]. He also observed that in highly stratified reservoirs, adjusting the slope of the flow capacity-volume curves for mobility ratio will produce a slope approximating the slope of the performance curve (figure 1).

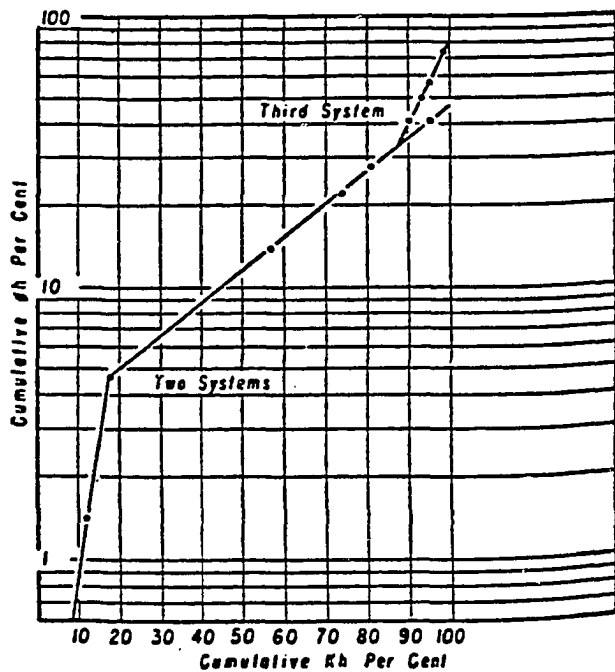
Here again, Johnson [16] did not consider the effect of the well structure and pattern. The accuracy of his work may be limited.

Schmalz and Rahme [25] studied the degree and the magnitude of variation in waterflood performance with variation in permeability profile. Using several precise mathematical regression models such as straight lines of varying slope and/or various continuous curves, they calculated a composite group of waterflood predictions under constant reservoir conditions.

By obtaining a plot of Lorenz coefficient versus percent recovery (of recoverable oil), they made a preliminary quantitative estimate of the expected performance of a flood,



A—Project 1 performance.



B—Project 1 classification composite.

Figure 1: Prediction of waterflood performance by use of reservoir parameter distribution (after Johnson [16]).

given only the permeability data. This general review shows the extent to which core data can be stretched to profit the petroleum industry. That oil wells perform in accordance with their joint parameter distributions has been demonstrated [14, 16, 20, 25, 28].

1.2 Review of Literature on Selective Plugging

In most oil reservoirs, the oil saturated formations have strata of varying permeabilities and thicknesses. In the waterflood process, the more permeable strata are depleted of oil first, and thereafter they continue to take large quantities of water even though they produce no more oil. This situation eventually results in large quantities of water circulating through depleted formations. This results in an unnecessary expense in the way of water costs and pumping. High back pressure in the vicinity of the producing well will interfere with the flow of oil from the less permeable strata.

Selective plugging is a practical method for preventing the wasteful circulation of water through most permeable strata. It generally involves the injection of dispersed solids and semi-solids of such a particle size that they will enter the pores of the most permeable strata (or fractures). The dispersed solids will travel some distance and then stop. Particles keep building up behind this stop point until they form a plug which stops the flow of water into the strata. Wayne et al, [32] reported an unusually high degree of success

over a variety of field conditions using selective plugging technique. Joseph [17] reported the case history of a number of field tests as successful.

However, his procedure has some major drawbacks:

1. Where there is no bedding planes to isolate the plugged zone, the injection water may go round the surface plug and enter the zone of highest permeability. This means waste of a large quantity of water.
2. An injection well may develop a backflow which will wash away the surface plugging chemicals and thus reopen the offending zone to accept flood water again.
3. Field trials are limited since operators are reluctant to treat the formation selectively when they cannot determine quickly the location and effectiveness of such a treatment.
4. Selective plugging chemicals can get so costly that the application of the technique becomes uneconomic.
5. Irregular absorption of chemicals to the formation rock can cause the blocking of the wrong zones -- hence defeating the purpose of the technique.

In view of these difficulties and the fact that the first stage of selective plugging requires an accurate knowledge of waterflood profile, the method of this study proves advantageous and superior. All we need to know in this

investigation is the core data, then from the interpolation algorithm and the resulting graphical display of the reservoir parameter, we can isolate zones of interest where special treatment may be necessary.

CHAPTER II

MAPPING AND VARIOUS INTERPOLATION PROCEDURES

2.1 Contour Mapping

Contouring is a way of representing pictorially values of a variable at various points in a study area. Contour maps are frequently used to obtain detailed pictorial representation of a function of two variables whose values are known at discrete points.

In geographical research, contour maps are used to represent terrain surfaces. In crystallography, contour maps are employed extensively to map electron density. Imaginary surfaces comprising of a continuum of all possible parameter values can be employed in reservoir engineering studies to map reservoir parameter distributions. Unlike the surface trend analysis employed in geographical studies, contour mapping in petroleum engineering studies is difficult to obtain due to the problem of limited data resources. Thus, we must therefore rely on some kind of an approximation theory to generate the much needed data matrix by interpolation procedure.

The approximation technique considered suitable for this sort of investigation is one that would represent the data information as a continuous function of two variables.

The continuity condition is desirable to eliminate the presence of maxima points at the nodes of given data points, and the existence of saddle points at the unknown data points -- both of which are present in other interpolation methods. The result is a curve, smooth and differentiable at all points. This mathematical approach is also considered noise free -- resulting in smooth contours.

Contour plotting involves the drawing of contour lines through equal values in a two-dimensional surface. A contour plotting algorithm [29] may be constructed by following contours from some starting points until they either close or intersect a boundary. Alternatively each cell of the grid can be examined in turn and then all contours found inside the cell are drawn.

Linear or non-linear interpolation procedures may be used in the execution of a contour. All contours intersecting the boundaries are drawn first and then all contours which do not intersect the boundaries are drawn later.

The contouring algorithm modified and used in this study is due to Synder [29]. It is presented under the Statistical Analysis System [24].

2.2 The Three Dimensional Projection

A conceptual surface is often obtained when a function whose points are related by some two-dimensional system of co-ordinates is associated, point to point, with the corresponding value of variable, Z_i , say. The implication

of the above is that as many conceptual surfaces are possible as there are variables.

In engineering, the determination and variation of these conceptual surfaces can be related to the variation of corresponding non-spatial functions from point to point. This variation can be regarded as the flow on the conceptual surface, and thus, the generation of this conceptual surface can replace the physical system.

In petroleum engineering, this conceptual surface can range from flow capacity (kh) to flow volume (ϕh). An understanding of how the peaks, pits and beds associated with these projections are related to one another, will give the engineer the desired insight into the flow of the non-spatial variable.

A sequence of points in three-space is usually connected together by linear interpolation between adjacent points. The three dimensional plot adopts a masking technique. Those lines or portions of lines which should be hidden by previous lines are masked. This means that lines in the foreground in the positive Z-direction are plotted before lines in the background. A line or portion of a line is hidden if it lies within the region bounded by previously plotted lines.

The three dimensional algorithm modified and used in this study is due to Watkins [31]. His algorithm was modified under the SAS [24]. The algorithm accepts three dimensional data in various forms rotated in three dimensional

space. The projection of the resulting figure is plotted on to the x-y plane.

2.3 Available Interpolation Techniques

To be very effective, a good interpolation algorithm should provide some or all of the following conditions:

1. It should reduce estimation errors to a minimum and give exact values at the data points.
2. It should be simple and manageable so that the evaluation of data points is not tedious.
3. The interpolation function should be nice and continuously differentiable.

Two-dimensional approaches briefly discussed in this study include:

The multi-quadric approach

The trend surface model

The normal distribution model

The triangular model

Unfortunately most of the above models are inadequate for use.

2.4 Multiquadric Equations of Topography and Other Irregular Surfaces¹⁰

This is an analytical method that involves the summation of equations of quadric surfaces having unknown coefficients. The quadric surfaces are located at significant points throughout the region to be mapped. Contoured multi-quadric surfaces are compared with topography and other

irregular surfaces from which the multiquadric equation was derived.

Topography can be represented by various analytical, numerical, and digital methods, in addition to the classical contour map.

Earliest work in topography solved the problem stated thusly: given continuous topographic information in a certain region, reduce it to an equivalent set of discrete data example spherical harmonic coefficients or digital terrain increments.

My study among others [10,23] is concerned with the procedural inverse of the above statement, thus: given a set of discrete data on a topographic surface (or reservoir parameter), reduce it to a satisfactory continuous function representing the topographic surface (or reservoir parameter).

2.5 The Multi-Quadric Model

The multi-quadric model is an approach introduced by Hardy [10] for obtaining the equations of irregular surfaces. This technique has been modified for the purpose of this review to be applicable to cases of heterogeneous reservoirs. The procedure requires a set of discrete reservoir data. The algorithm reduces the data into a satisfactory continuous function representing a quadric surface having unknown coefficients. The summation of a number of quadric surfaces will give the profile of the physical system.

Consider a function Z with co-ordinates X and Y from

a class of quadric surfaces Q,

$$Z = \sum_{i=1}^n A_i [Q(X_i, Y_i, X, Y)] \quad 2(1)$$

where A_i is a constant determining the algebraic sign or flatness of the quadric term.

For a multi-quadric surface defined by circular hyperboloids in two sheets: 2(1) becomes

$$Z_j = \sum_{i=1}^n A_i [(X_j - X_i)^2 + (Y_j - Y_i)^2 + C]^{\frac{1}{2}} \quad 2(2)$$

For the case of cones and straight lines segments $C = 0$ and 2(2) becomes

$$Z_j = \sum_{i=1}^n A_i [(X_j - X_i)^2 + (Y_i - Y_i)^2]^{\frac{1}{2}} \quad 2(3)$$

For an ellipse (Ellipsoid), $0 < C < 1$, a good approximation is considered here to be $C = .5$

Then

$$Z_j = \sum_{i=1}^n A_i [(X_j - X_i)^2 + (Y_j - Y_i)^2 + 0.5]^{\frac{1}{2}} \quad 2(4)$$

If we assume that reservoir parameter are normally distributed; (Gaussian distribution) we have: assumptions similar to this has been reported [10, 11, 14, 23].

$$\log_e Z_j = - \sum_{i=1}^n A_i [(X_j - X_i)^2 + (Y_j - Y_i)^2 + .5]^{\frac{1}{2}} \quad 2(5)$$

$$Z_i = e^{-[A_i \sum [(X_j - X_i)^2 + (Y_j - Y_i)^2 + .5]^{\frac{1}{2}}]} \quad 2(6)$$

$$Z_j = \sum_{i=1}^n c_i e^{-\frac{1}{2} \left[\frac{(X_j - X_i)^2 + (Y_j - Y_i)^2 + .5}{\lambda^2} \right]} \quad 2(7)$$

or

$$Z_j = \sum_{i=1}^n c_i e^{\frac{[-(X_j - X_i)^2 - (Y_j - Y_i)^2 + 0.5]}{\lambda^2}} \quad 2(8)$$

Where λ is the average spacing between data point positions ($\lambda_x = \lambda_y = \lambda$), equation 2(8) is similar to 2(4) but it has been modified to handle normally distributed random variables consisting of reservoir parameters for an elliptical system.

2(8) is the same as $f(t) = \sum c e^{-r^2/\lambda^2}$ 2(8a)

Thus a circle of radius r is a theoretical contour containing essentially all the variables of the population.

The solution of 2(8) will yield

$$AX = B \quad 2(9)$$

where

$$\begin{bmatrix} c_1 \\ c_2 \\ \vdots \\ c_n \end{bmatrix} = X \quad 2(10)$$

and

$$\begin{bmatrix} Z_1 \\ \vdots \\ Z_n \end{bmatrix} = Zi = B \quad 2(11)$$

The matrix $[A_{ij}] = A$ (which is $n \times n$) 2(12)

from 2(8) - 2(12)

$$AX = B \quad 2(13)$$

$$X = A^{-1}B \quad 2(14)$$

When the known values of C_i are substituted into equation 2(8)

we have the required equation of the surface - which fits the data points exactly and provides a logical interpolation at intermediate points. However, the real problem in multi-quadratic approach is the placement of a saddle in a region with no data information. Questions regarding the continuity of the first and second derivatives of the function may be raised.

One important aspect of the multivariate approach is that it can handle cases where the data points are irregularly distributed.

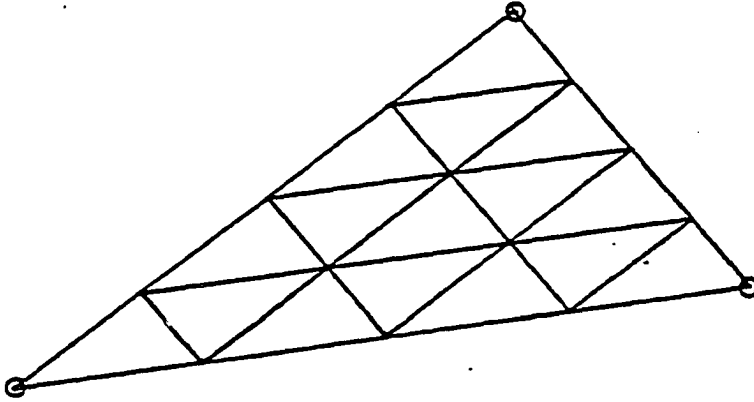
2.6 The Triangular Approach

Bengtsson and Nordbeck (2) recommended partitioning the domain under study into triangles having data points as vertices. A plane is then passed through the values at each of the data points. The approach calls for ordered or random data with series of triangles having data point at each vertex (see figure 2.0). Each side of the triangle is subdivided into "J" equal parts. Hence the number of vertices for any triangle is given by

$$N = (J + 1)(J + 2)/2 \text{ vertices} \quad 2(15)$$

2.7 Trend Surface Model

A Trend Surface is a statistically derived equation to explain variations in given data values distributed regularly or irregularly in X-Y space. It displays data by fitting a continuous surface which can be described by a polynomial equation. The parameters for an equation representing



- ⊙ Triangle Vertex - Surface value known (data point)
- Triangle Vertex - Surface value unknown

Fig 2.0 - Triangular Approach

a surface is estimated by use of least squares fit. Hence the surface is fitted to data values in such a way that the sum of the squared deviations between the given values at data points position and the value of the computed surface at same points are minimized. A contour map displays data as a continuous surface interpolated from discrete data as a function of the distance of neighboring data points and their associated values. The difference between a contour map and a Trend Surface map using same data is the Residual map. A perfect fit is unlikely using this model.

Equations describing Trend Surfaces can be linear, quadratic, cubic--et cetera (figure 2.1).

The general form of the above surfaces using polynomial representation has been noted by Krumbein [19].

$$f(Z) = B_1 + B_2U + B_3V + B_4U^2 + B_5UV + B_6V^2 + B_7U^3 + B_8U^2V + B_8V^2U + B_9V^3 \quad 2(16)$$

Figure 2.1 gives the relationship of four orders of two-dimensional polynomial curves to their three dimensional counterparts [19].

It was pointed out [8] that the lower order surfaces are very effective in isolating important local trends from those that exist over a larger area while the higher order surfaces will reflect the Z-values very accurately. Trend Surface analysis is therefore considered as a filter which filters an input signal. The surface then represents the

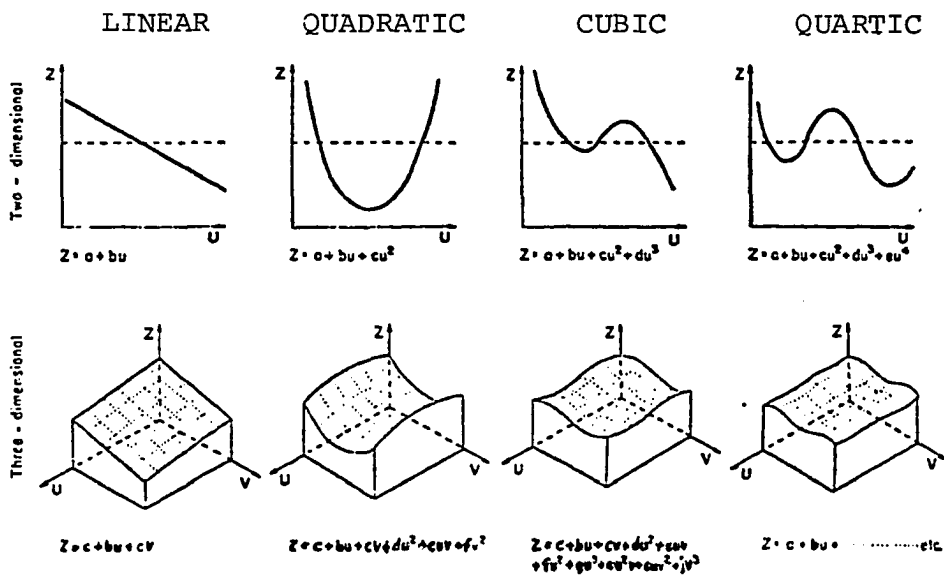


Fig. 2.1 Two and three dimensional representative of surface trend analysis (19).

result of this filtering process. As the order of the surfaces gets higher, the quantity of the input data that passes through the filter gets bigger.

Figure 2.2 shows a trend surface map of Woods and Woodward counties in Oklahoma. Raw data for this program was obtained from Dwight's Natural Gas Data⁷ and modified appropriately for Symap Program.⁸ For the interest of this review, figure 2.2 shows what happens to the data distribution when the order of surfaces is varied from one to six. When the order of the surfaces is one, very few data enter through the filter but when the order of the surfaces is increased to six, more data enter the system for analysis. Hence more description of the data is reflected in the latter.

Figure 2.3 is a contour map of a theoretical surface using Symap Method.⁸ The contour plot shows how the relative heights of the theoretical can be displayed for informational purposes. Figure 2.4 is a trend surface analysis applied to an oil bearing structure in Lost Springs area of Kansas.²² It is important to note that using a trend surface model, one can identify oil bearing structure. This being the case, the study of trend surface capabilities seems to be a cause worth taking. But the trend surface procedure has a big handicap. It is an inexact method and is only fairly acceptable when the number of data points is large. But since in Petroleum engineering we are faced with the problem of limited data information, trend surface analysis is not very suitable.



A: order one

B: order three

C: order six

Fig. 2.2: Trend surface analysis for original gas in place in Woods and Woodward counties using symap program(8)

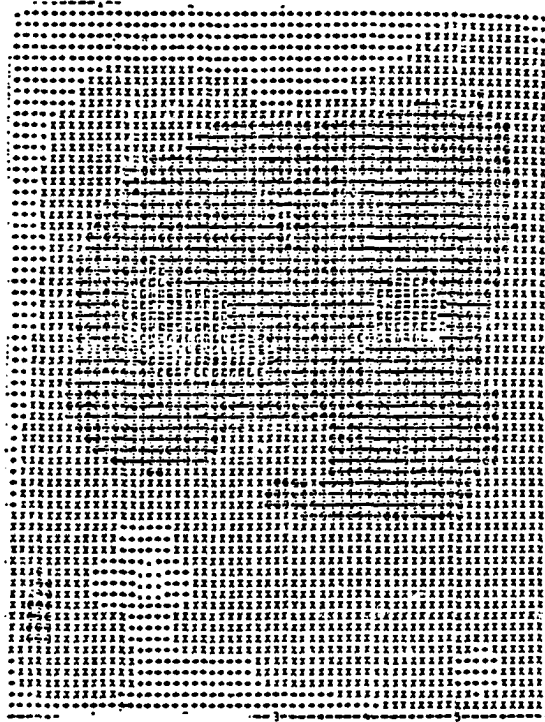


Fig. 2.3: Contour map of a theoretical surface using reference (8).

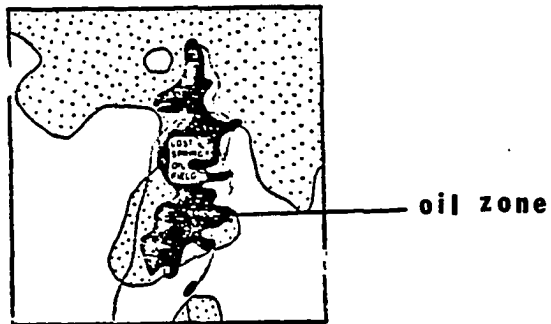


Fig. 2.4: Trend surface analysis applied to oil bearing structure in Lost Spring area of Kansas. (ref. 22).

Exact interpolation methods give exact values at data point positions. Two types of exact interpolation methods exist. One employs a single global function in describing a surface. The other uses a piecewise procedure. The approach of the former is generally unacceptable because of problems of "unmanageable complexity" associated with it, when data values get very large.²⁷ The latter is popular for its simplicity and ease of use. Many problems mask the results of most exact interpolation procedures. If the interpolating algorithm is one that does not have continuous derivatives, the interpolated points can develop saddle points, and unnecessary minima points.

The weighted average approach introduced in Chapter III was designed to correct most of the defects in exact interpolation procedure. It is adequately suited for heterogeneous reservoir application since it can comfortably handle irregularly spaced data. Similar procedure has been followed elsewhere,²⁷ but Shepard worked on topographic surfaces instead of reservoir parameters distribution.

CHAPTER III

Theory of the Weighted Averages

The weighted average procedure is an exact interpolation method which puts into consideration a number of factors which affects interpolated parameters in a reservoir. Such factors as distance between data points, the direction of a desired interpolation value from the given data points, the length and effect of discontinuities as they affect the interpolation point, and the direction of the desired unknown parameter value from the given data point locations, have been considered in the formulation of the governing equation. The governing equation is simply stated as:

$$f(z) = \frac{\sum_{i=1}^N (W_i Z_i)}{\sum_{i=1}^N W_i} \quad 3(1a)$$

The result of this formulation is a curve that passes through all the given data points. The curve is continuous and so is its first and second derivatives. These properties make an investigation of this algorithm worthwhile especially when considering the estimation of reservoir parameters using data points that are irregularly positioned.

3.1 The weighting technique ²⁷

Define a basic interpolation function as

$$f(P) = \left[\frac{\sum_{i=1}^N (d_i)^{-2} z_i}{\sum_{i=1}^N d_i^{-2}} \right] \quad 3(1)$$

where:

d_i = distance from point of interpolation to data point position

P_i = interpolation point

Z_i = data point value.

Implication of the inverse square distance expression used in 3(1):

higher weighting is placed on nearby data points with the result that the effect of far away data points is negligible. What this means is that depending on the point of interpolation, only nearby data points influence our results.

3.2 Conceptual procedure of the method

Define a standard radius as:

$$r_s = \left[\frac{n_p}{\pi} \left(\frac{A}{N} \right) \right]^{0.5}$$

where

$A = \pi R^2$ = area of the largest circle enclosing the reservoir

n_p = Number of data points to be used in the interpolation

N = Total number of data points

To successfully interpolate a value for P_i we do the following:

- (1) Specified minimum number of points required for interpolation (n_{\min})
- (2) Maximum number of points required for interpolation (n_{\max})
- (3) if $n_p < n_{\min} \rightarrow n_p = n_{\min}, d_i = d_{\min}$
 if $n_p > n_{\max} \rightarrow n_p = n_{\max}, d_i = d_{\max}$
 if $n_{\min} < n_p < n_{\max} \rightarrow n_p = \frac{n_{\min} + n_{\max}}{2}$

From figure 3.1,

we shall find an interpolated value of p by weighting the values at the data point positions while accounting for the following parameters.

- (a) distance
- (b) direction
- (c) slope
- (d) presence of discontinuity.

The overall weightings will give an estimate for P_i .

Boundary conditions: The boundary can be completely defined by assuming an impermeable boundary layer. This means that flow capacity, flow volume or rock permeability will be treated as zero at the boundary.

If however, a flow boundary is assumed then some values of permeability defining the boundary should be provided.

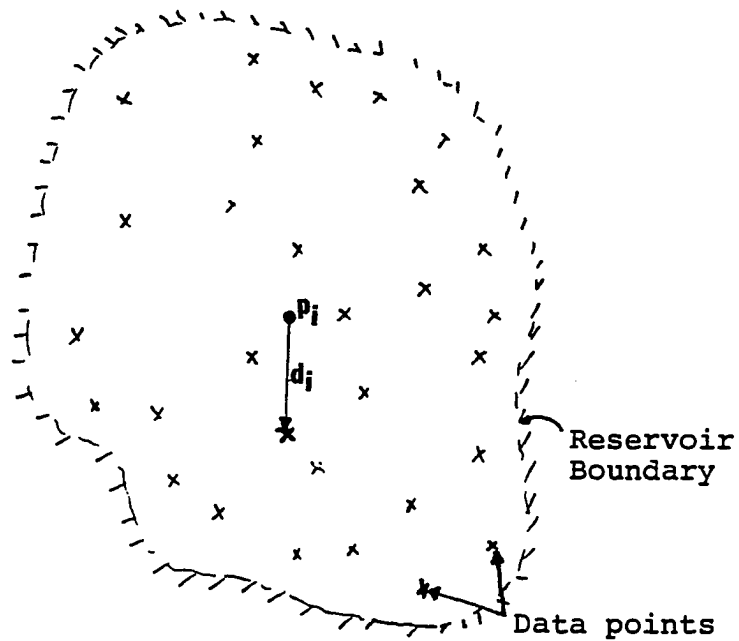


Figure 3.1: Conceptual procedure for the interpolation of reservoir data.

If l_i is a weighting function defined as :

$$l_i = 1/d_i, \quad d_i \neq 0 \quad 3(2a)$$

Then 3(1) becomes

$$f(p) = \left| \frac{\sum l_i^2 z_i}{\sum l_i^2} \right| \quad 3(2)$$

Restrictions :

$$f(p) = \left[\begin{array}{ll} 0 & \text{if } d_i > r_p \\ f(.8r_p) & \text{if } d_i > 0.5 r_p \\ z_i & \text{if } d_i = 0 \end{array} \right] \quad 3(3)$$

3.2 Vectorial weighting:

let S_i be a directional weighting term

where $0 < S_i < 1$

$$g_i = S_i / \sum_{\substack{i=1 \\ j \neq i}}^{N_p} d_i \quad 3(4)$$

where $S_i = \frac{1}{2} (1 - \cos\theta)$, and is such that

$S_i = 0$ for points in same direction

$S_i = 1$ for weighting in opposite direction.

$$S_i = \frac{1}{2} (1 - \cos\theta) \quad 3(5)$$

$\cos\theta = \text{Angle } D_i \text{ P } D_j$

$D_i \equiv x_i, y_i = \text{data point Coordinate } i$

$D_j \equiv x_j, y_j = \text{data point Coordinates } j$

$P \equiv P(x, y) = \text{interpolation point } x, y$

$$\cos\theta = \vec{D_i P} \cdot \vec{D_j P}$$

$$\cos\theta = \frac{1}{2d_i d_j} \left[\Delta x_i \cdot \Delta x_j + \Delta y_i \cdot \Delta y_j \right] \quad 3(6)$$

where: d_i, d_j are distances of P from data point positions D_i, D_j

$\Delta x_i, \Delta x_j$ are coordinate differences from P.

Thus $\Delta x_i = (x - x_i)$.

Let the new weighting function be W_i

$$W_i = \frac{1}{d_i^2} (1 + g_i) = L_i^2 (1 + g^2) \quad 3(7)$$

Then

$$f(P) = \left[\begin{array}{ll} \sum_{i=1}^{N_p} (W_i Z_i) / \sum_{i=1}^{N_p} W_i & \text{if } d_i \neq 0 \\ Z_i & \text{if } d_i = 0 \end{array} \right] \quad 3(8)$$

3.3 Continuity Weighting

let

$$p^i = \sum_{\substack{k=0 \\ i=0}}^{N_p} \frac{\Delta Z_i}{d_k} \cdot dx_i \quad 3(9)$$

$$q^j = \sum_{\substack{k=0 \\ i=0}}^{N_p} \frac{\Delta Z_i}{d_k} \cdot dy_i \quad 3(10)$$

where: p^i = weighting of derivative of Z with respect
 $\times \text{dir}^n$

q^j = weighting derivative of Z in $y - \text{dir}^n$

d_k = distance between any two data points con-
 tained in P_n .

$$\text{Let } M = (p^{i2} + q^{j2})^{0.5}$$

define an increase in data point value:

$$\Delta Z_i = (p^i \Delta x_i + q^j \Delta y_i) (\lambda_i) \quad 3(12)$$

$$\text{where } \lambda_i = \frac{\alpha}{c_i} \quad 3(13)$$

$$c_i = \alpha + |d_i|$$

$$\alpha = \frac{\Delta Z_{\max}}{M \cdot N_h} \quad 3(14)$$

N_h = Maximum number of data points allowable
for each point interpolation

The final equation is

$$f(Z) = \left[\begin{array}{l} \sum_{i=1}^{N_p} W_i Z_i' / \sum_{i=1}^{N_p} W_i \quad \text{if } d_i \neq 0 \\ Z_i \quad \text{if } d_i = 0 \end{array} \right] \quad 3(15)$$

$$\text{where } Z_i' = Z_i + \Delta Z_i \quad 3(16)$$

3.4 Influence of Discontinuities

If d_c is the length of discontinuity and d_i is the length from P to data point position

Then

$$d_i' = (d_i^2 + d_c^2)^{0.5} \quad 3(17)$$

This value of distance in 3(17) is then used in 3(2), 3(3) and 3(4).

3.6 Practical Example Problem

Find an interpolated value of flow capacity at a point P with co-ordinates at the origin, given the values at two other points A(2,0) with k_h value 300 md-ft, and B(4,0) with k_h value 500 md-ft.

Solution:

$$\cosine \theta = (0-4)(0+2)/(4)(2) = -1 \text{ or } \theta = 180^\circ$$

$$S_i = \frac{1}{2}(2) = 1.0$$

$$g_i = S_i/d_i = \frac{1}{4}$$

$$g_2 = -\frac{1}{4}$$

$$W_1 = \frac{1}{(4)^2} (1+\frac{1}{4}) = \frac{5}{64}$$

$$W_2 = \frac{1}{8}$$

$$P_1 = \frac{(500-300)}{(4+2)^2} (4) = \underline{\underline{22.22}}$$

$$P_2 = \frac{(500-300)(2)}{6^2} = \underline{\underline{11.11}}$$

$$P^i = \frac{2}{1} P_i = \underline{\underline{33.33}}$$

$$\mu = (33.33^2 + 0^2)^{0.5} = 33.33$$

$$\alpha = \frac{200}{333.3} = 0.6$$

$$C_1 = 0.6 + 4 = 4.6$$

$$C_2 = 0.6 + 2 = 2.6$$

$$\lambda_1 = \frac{0.6}{4.6} = 0.13043$$

$$\lambda_2 = \frac{0.6}{2.6} = 0.23077$$

$$\Delta Z_1 = ((22.22)(4) + 0)(0.13032) = 11.59262$$

$$\Delta Z_2 = ((11.11)(2) + 0)(0.23077) = 5.1277$$

$$Z'_1 = Z_1 + \Delta Z_1 = 500 + 11.59262 = 511.59262$$

$$Z'_2 = Z_2 + \Delta Z_2 = 300 + 5.1277 = 305.1277$$

$$f(P) = \frac{W_1 Z'_1 + W_2 Z'_2}{W_1 + W_2} = \frac{\frac{5}{64} (511.59262) + (\frac{1}{8}) (305.1277)}{\frac{5}{64} + \frac{1}{8}}$$

$$f(P) = \frac{39.97 + 38.141}{\frac{5}{64} + \frac{1}{8}} = \underline{\underline{384.54}}$$

An example of a case where a discontinuity exists:

($d_c = 3$ units)

$$d_i^1 = (d_i^2 + 3^2)^{0.5}$$

$$d_1^1 = (16 + 9)^{0.5} = 5$$

$$d_2^1 = (4 + 9)^{0.5} = 3.61$$

$$L_1 = 1/5 = 0.2$$

$$L_2 = (1/3.61) = 0.277$$

with these new values of L_1 and L_2 we can calculate the required interpolation function.

NOMENCLATURE—WEIGHTED AVERAGE

- d_i = distance from interpolation point to data point position
 P_i = An interpolation point
 Z_i = data point value
 A = Area of the largest circle enclosed by the data points
 N_p = Number of data points to be used in the interpolation process
 N = Total number of data points
 N_{max} = Maximum number of points needed for interpolation
 N_m = Minimum number of points required for interpolation
 L_i = weighting function associated with distance
 S_i = directional weighting symbol
 D_i, D_j = Data point position
 d_j = distance of P from data point positions
 W_i = a weighting function
 θ = Angle made by D_i P D_j
 λ_i = Constant
 N_h = Max. number of data points allowable for each point interpolation.
 P^i, q^j = Partial derivatives of Z with respect to X, Y respectively
 d_i' = equivalent distance used to account for discontinuity effect
 M = a function of P^i, q^j .

CHAPTER IV

THEORY OF THE CUBIC SPLINE

Any third degree polynomial function which is continuous on an interval $a \leq x \leq b$, and has continuous first and second derivatives is referred to as a cubic spline.

For many years draftsmen used thin splines to smoothly connect points of interest in a given surface. These connections were made possible by means of weights or 'ducks' attached at specified points. Figure 4.1 is an example of what happens to a spline under various load conditions.

The forces tending to bend the spline can be accounted for by the Bernoulli-Euler Law:

$$Y''(x) = \delta M(x) \qquad 4(1)$$

$$Y''(x) = M(x) \quad 1/EI \qquad 4(1a)$$

$$EI Y''(x) = M(x)$$

where:

$M(x)$ = Bending moment

$Y''(x)$ = Function Deflection

E = Young's modulus of Elasticity

I = Geometric moment of Inertia

α = Proportionality symbol

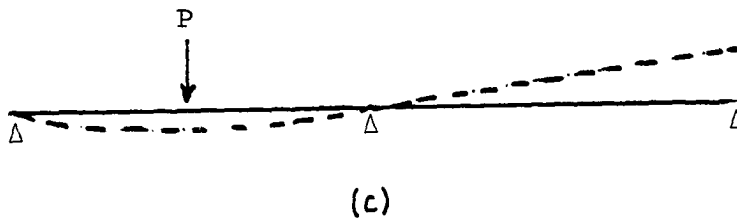
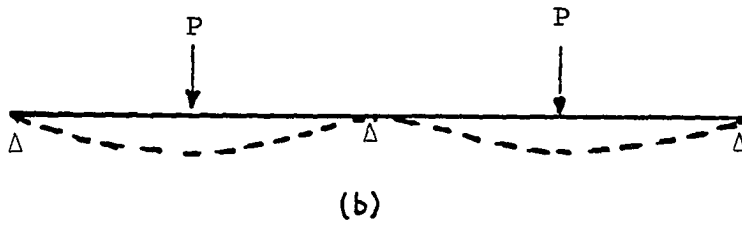
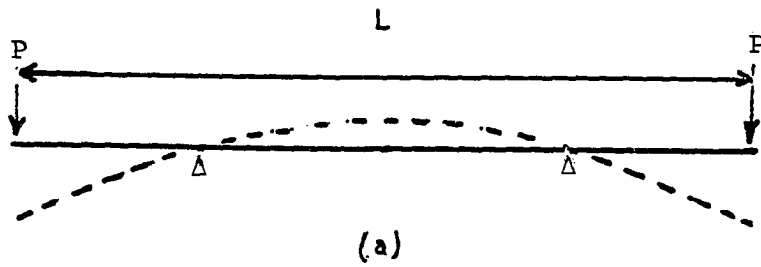


Figure 4.1: Deflection of a continuous beam under various load conditions.

4.1 Reasons for the Cubic Spline Study

Since conventional polynomial approximations produce results that are highly inflected, the cubic spline approach is desirable for more reliable results. Whereas conventional polynomial approximations give simple continuous function, the cubic spline approach gives a continuous function whose first and second derivatives are continuous. These additional properties make the cubic spline approach capable of handling derivative dependent functions such as velocity in potential flow, and slopes to streamline curvature. The cubic spline approach can smooth the surface and also can represent curved sections with very few nodes.

An improved reservoir description is possible by assuming that the reservoir parameter forms smooth spline surfaces which are continuous. The nature of these surfaces may represent the degree of communication between different rock layers.

The two dimensional spline interpolator is a function of co-ordinate axes. Since reservoir heterogeneity can vary entirely with the co-ordinate axes, the spline approach is a good asset to reservoir engineers.

Finally interpolation using the cubic spline properties is currently very popular, particularly for interpolating relatively noise-free tables of physical data.

4.2 : Interpolation Using Cubic Spline

Due to the inflected or "Wiggly" character often developed by the conventional polynomial interpolation, the cubic spline function is developed to produce smoother contours. In view of this, conditions for an interpolating cubic spline have been given as follows:

- | | | | |
|--------------------------------|---|---|---------------------------------|
| a) $F_i(X_i) = f(X_i)$ | } | → | Function $f(X_i)$ is continuous |
| b) $F_i(X_{i+1}) = f(X_{i+1})$ | | | |
| c) $F_i'(X_i) = F'(X_{i-1})$ | } | → | Derivatives of X_i same when |
| d) $F_i''(X_i) = F''(X_{i-1})$ | | | |

All four conditions indicate that both the function, and its first and second derivatives are continuous in the interval $X_0 < X < X_n$.

Figure 4.2 shows a linear function of the second derivative $M_{(x)}$.

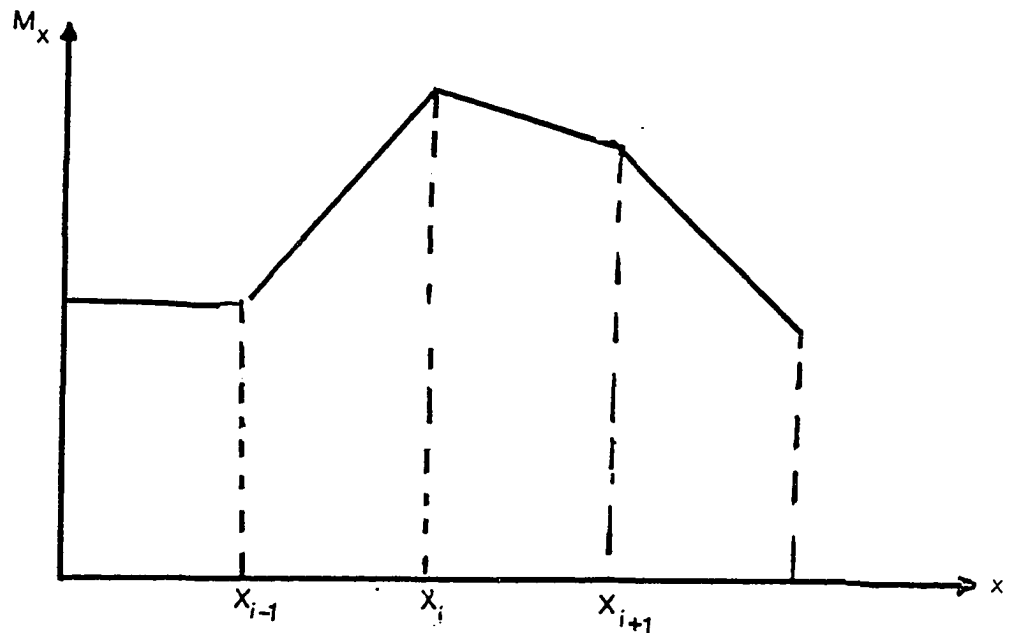


Figure 4.2: Linear relation of $M_{(x)}$ vs X

By linear interpolation, define the second derivative of the interpolation function at any point X as

$$S''(x) = M_{j-1} + \frac{x-x_{j-1}}{x_j-x_{j-1}} [M_j - M_{j-1}] \quad 4(2)$$

$$S''(x) = M_{j-1} \frac{(x_j-x)}{h_j} + M_j \frac{x-x_{j-1}}{h_j} \quad 4(3)$$

where :

$$h_j = x_j - x_{j-1}$$

$$S''(x) = M_{j-1} \frac{(x_j-x)}{h_j} + M_j \frac{(x-x_{j-1})}{h_j} \quad 4(3)$$

Integrate with respect to $(x-x_{j-1})$ or (x_j-x)

$$S'(x) = -M_{j-1} \frac{(x_j-x)^2}{2h_j} + \frac{m_j(x-x_{j-1})^2}{2h_j} + C_1 \quad 4(4)$$

integrating again we have

$$S(x) = \frac{M_{j-1}(x_j-x)^3}{6h_j} + \frac{m_j(x-x_{j-1})^3}{6h_j} + C_1(x-x_{j-1}) + C_2 \quad 4(B)$$

at $x = x_{j-1}$, $S(x) = Y_{j-1}$; 4(B) becomes

$$Y_{j-1} = \frac{M_{j-1}(x_j-x_{j-1})^3}{6h_j} + m_j(0) + C_1(0) + C_2 \quad 4[C]$$

$$C_2 = Y_{j-1} - M_{j-1} \frac{(x_j-x_{j-1})^2}{6} \quad 4[D]$$

when $x=x_j$, $S(x) = Y_j$

$$Y_j = M_{j-1}(0) + \frac{M_j h^2}{6} + C_1(h_j) + C_2$$

$$C_1 h_j = Y_j - \frac{M_j h^2}{6} - Y_{j-1} + M_{j-1} \frac{h^2}{6}$$

$$C_1 = \frac{Y_j - Y_{j-1}}{h_j} - \frac{(M_j - M_{j-1})h_j}{6} \quad 4[E]$$

Putting in values of C_1 and C_2 in 4(B) we have:

$$S(x) = \frac{M_{j-1}(x_j-x)^3}{6h_j} + M_j \frac{(x-x_{j-1})^3}{6h_j} + (Y_{j-1} - \frac{M_{j-1}h_j^2}{6})$$

$$\left(\frac{x_j-x}{h_j}\right) + (Y_j - \frac{M_j h_j^2}{6}) \frac{x-x_{j-1}}{h_j} \dots\dots\dots 4[F]$$

Now we can list the equations that obtain

$$S''(x) = M_{j-1} + \frac{x-x_{j-1}}{x_j-x_{j-1}} [M_j - M_{j-1}] \dots\dots\dots 4(2)$$

$$S''(x) = M_{j-1} \frac{(x_j-x)}{h_j} + M_j \frac{x-x_{j-1}}{h_j} \dots\dots\dots 4(3)$$

$$S'(x) = -M_{j-1} \frac{(x_j-x)^2}{2h_j} + M_j \frac{(x-x_{j-1})^2}{2h_j} + \frac{Y_j-Y_{j-1}}{h_j} -$$

$$\frac{(M_j-M_{j-1})}{6} h_j \dots\dots\dots 4(4)$$

$$S(x) = M_{j-1} \frac{(x_j-x)^3}{6h_j} + M_j \frac{(x-x_{j-1})^3}{6h_j} + (Y_{j-1} -$$

$$\frac{M_{j-1}h_j^2}{6}) \frac{(x_j-x)}{h_j} + (Y_j - \frac{M_j h_j^2}{6}) \frac{(x-x_{j-1})}{h_j} \dots\dots\dots 4(5)$$

or

$$S(x) = \frac{M_{j-1}}{6} \left[\frac{(x_j-x)^3}{h_j} - (x_j-x)h_j \right] + \frac{M_j}{6} \left[\frac{(x-x_{j-1})^3}{h_j} -$$

$$(x-x_{j-1})h_j \right] + Y_{j-1} \left(\frac{x_j-x}{h_j} \right) + Y_j \left(\frac{x-x_{j-1}}{h_j} \right) \dots\dots\dots 4(6)$$

Putting the condition $S'_{j-1} = S'_j(x_j)$ in 4(4) we have

$$S'_{j-1}(x_j) = \frac{h_j}{6} M_{j-1} + \frac{h_j}{3} M_j + \frac{Y_j-Y_{j-1}}{h_j} \dots\dots\dots 4(7)$$

$$S'_j(x_j) = \frac{-M_j}{3} h_{j+1} + 0 + \frac{Y_{j+1}-Y_j}{h_{j+1}} - \frac{(M_{j+1}-M_j)}{6} h_{j+1}$$

$$S'_j(x_j) = -M_j \left(\frac{h_{j+1}}{3} \right) - M_{j+1} \left(\frac{h_{j+1}}{6} \right) + \frac{Y_{j+1}-Y_j}{h_{j+1}} \dots\dots\dots 4(8)$$

Equating 4[F] and 4(8) we have:

$$h_j M_{j-1} + 2(h_j+h_{j+1})M_j + h_{j+1}M_{j+1} = 6 \left[\frac{Y_{j+1}-Y_j}{h_{j+1}} - \frac{Y_j-Y_{j-1}}{h_j} \right] \quad 4(9)$$

$$\frac{h_j}{h_j+h_{j+1}} M_{j-1} + 2M_j + \frac{h_{j+1}}{h_j+h_{j+1}} M_{j+1} = \left[6 \left[\frac{Y_{j+1}-Y_j}{h_{j+1}(h_{j+1}+h_j)} - \frac{Y_j-Y_{j-1}}{h_j(h_{j+1}+h_j)} \right] \right] \quad 4(10)$$

$$\text{or } \mu_j M_{j-1} + 2M_j + \lambda_j M_{j+1} = d_j \quad 4(11)$$

where:

$$\mu_j = \frac{h_j}{h_j+h_{j+1}} = 1-\lambda_j \quad 4(12)$$

$$\lambda_j = \frac{h_{j+1}}{h_j+h_{j+1}} \quad 4(13)$$

$$d_j = 6 \left[\frac{(Y_{j+1}-Y_j)/h_{j+1}}{h_{j+1}+h_j} - \frac{(Y_j-Y_{j-1})/h_j}{h_{j+1}+h_j} \right] \quad 4(14)$$

Applying boundary conditions to 4(11) at boundaries $j=0$, and $j=N$:

$$(\mu_0)M_{-1} + 2M_0 + \lambda_0 M_1 = d_0 \quad 4(15)$$

$$M_{N-1} + 2M_N + \lambda_N M_{N+1} = d_N \quad 4(16)$$

Solve for $M_0, M_1, M_2, \dots, M_{N-1}$ by matrix using Gauss-Elimination

$$\begin{bmatrix}
 2 & \lambda_0 & 0 & \dots & 0 & 0 & 0 \\
 \mu_1 & 2 & \lambda_1 & \dots & 0 & 0 & 0 \\
 \vdots & \vdots & \vdots & \dots & \vdots & \vdots & \vdots \\
 \vdots & \vdots & \vdots & \dots & \vdots & \vdots & \vdots \\
 \vdots & \vdots & \vdots & \dots & \vdots & \vdots & \vdots \\
 0 & 0 & 0 & \dots & 2 & \lambda_{n-2} & 0 \\
 0 & 0 & 0 & \dots & \mu_{n-1} & 2 & \lambda_{n-2} \\
 0 & 0 & 0 & \dots & 0 & n & \mu_2
 \end{bmatrix}
 \begin{bmatrix}
 M_0 \\
 M_1 \\
 \vdots \\
 \vdots \\
 \vdots \\
 M_{n-2} \\
 M_{n-1} \\
 M_n
 \end{bmatrix}
 =
 \begin{bmatrix}
 d_0 \\
 d_1 \\
 \vdots \\
 \vdots \\
 \vdots \\
 d_{n-2} \\
 d_{n-1} \\
 d_n
 \end{bmatrix}$$

Knowing M_j ($j = 0, 1, \dots, N$), we
can now apply our interpolation function:

$$\begin{aligned}
 g(x) &= \frac{M_{j-1}}{6} \left[\frac{(x_j - x)^3}{h_j} - h_j (x_j - x) \right] \\
 &+ \frac{M_j}{6} \left[\frac{(x - x_{j-1})^3}{h_j} - h_j (x - x_{j-1}) \right] \\
 &+ y_{j-1} \left[\frac{x_j - x}{h_j} \right] + y_j \left[\frac{x - x_{j-1}}{h_j} \right] \quad 4(18)
 \end{aligned}$$

We can now interpolate values of interest.

4.3 Sample Problem for one dimensional spline (Irregularly distributed data points)

Obtain an approximate value for $g(7)$, and $g(10)$ by interpolation (Table 4.1). Given a natural spline boundary conditions ($M_1 = M_6 = 0$).

Divide equation 4(9) by h_{j+1} and we get

$$\begin{aligned} \frac{h_j}{h_{j+1}} [M_{j-1}] + \frac{2(h_j + h_{j+1})}{h_{j+1}} [M_j] + M_{j+1} \\ = 6 \left[\frac{y_{j+1} - y_j}{(h_{j+1})^2} - \frac{y_j - y_{j-1}}{h_j (h_{j+1})} \right] \end{aligned} \quad 4(19)$$

For:

$$j=2; h_j=4; h_{j+1}=3; y_{j-1}=4; y_j=10; y_{j+1}=15$$

$$\frac{4}{3}[M_{j-1}] + \frac{7}{2}[M_j] + M_{j+1} = 6 \left[\frac{5}{9} - \frac{1}{2} \right] = \frac{1}{3} \quad 4(20)$$

Since $M_1 = 0$ 4(20) becomes:

$$21 M_2 + 6 M_3 = 2 \quad 4(21)$$

For:

$$j=3; h_j=3; h_{j+1}=3; y_{j-1}=10; y_j=15; y_{j+1}=8$$

$$M_2 + 2 M_3 + M_4 = -8 \quad 4(22)$$

For:

$$j=4; h_j=3; h_{j+1}=4; y_{j-1}=15; y_j=8; y_{j+1}=3$$

$$\frac{3}{4} M_3 + \frac{7}{2} M_4 + M_5 = \frac{13}{8} \quad 4(23)$$

$$18 M_3 + 84 M_4 + 24 M_5 = 39 \quad 4(24)$$

$$\text{But } M_1 = M_5 = 0$$

$$18 M_3 + 84 M_4 = 39 \quad 4(25)$$

from 4(21) and 4(22) we get

$$-36 M_3 - 21 M_4 = 168 \quad 4(26)$$

$$4 \times (4(25)) + (4(26))$$

$$-126 M_3 = 711$$

$$M_3 = -5.643$$

4(27)

$$M_4 = 1.673$$

$$M_2 = 1.612$$

$$M_1 = M_5 = 0.0$$

Since we want to interpolate the function value when $X_i = 7.0$, we must use the cubic approximation to the interval between $j=2$, and $j=3$ (or $6 \leq x \leq 9$)

From equation 4(18), we can calculate $g(7)$ using node $j=2$

Thus:

$$h_j = 4; h_{j+1} = 3; \quad x_{j-1} = 2; x_j = 6; x_{j+1} = 9$$

$$y_j = 10; y_{j+1} = 15$$

$$g(7) = \frac{M_1}{6} \left[\frac{(6-7)^3}{4} - 4(6-7) \right]$$

$$+ \frac{M_2}{6} \left[\frac{(7-2)^3}{4} - 4(7-2) \right]$$

$$+ 4 \left[\frac{6-7}{4} \right] + 10 \left[\frac{7-2}{4} \right]$$

$$g(7) = 0 + 3.02 + 11.5 = 14.52$$

Using linear interpolation $g(7) = 11.86$

Exact value is 14.0

$$\text{Similarly } g(10) = \frac{M_2}{6} \left[\frac{(9-10)^3}{3} - 3(9-10) \right]$$

$$\begin{aligned}
& + \frac{M_3}{6} \left[\left(\frac{10-6}{3} \right)^3 - 3 \left(\frac{10-6}{3} \right) \right] \\
& + 10 \left(\frac{9-10}{3} \right) + 15 \left(\frac{10-6}{3} \right) \\
& = \left(\frac{1.612}{6} \right) (2 \frac{2}{3}) + \left(\frac{-5.64}{6} \right) \left(\frac{64}{3} - 12 \right) - \frac{10}{3} + 20
\end{aligned}$$

$$g(10) = 8.61$$

By linear interpolation $g(10) = 12.7$

Exact value is $g(10) = 9.3$

Figure 4.3 shows how the one-dimensional method of this study approximates the original curve. The closeness of the values obtained to the exact values explains the quality of this approach as compared to other approaches such as linear interpolation method. The method of this study is recommendable to problems dealing with curvatures, etcetera.

Table 4.1. Sample Data.

j	x_j	Y_i
1	2	4
2	6	10
3	9	15
4	12	8
5	16	3

$$\begin{array}{cccccc}
 M_1 & M_2 & M_3 & M_4 & M_5 & M_6 & M & d_j \\
 \left[\begin{array}{ccccc}
 0 & 2 & 3/7 & 0 & 0 \\
 0 & 4/7 & 2 & \frac{1}{2} & 0 \\
 0 & 0 & \frac{1}{2} & 2 & 4/7
 \end{array} \right] & & & & & & \left[\begin{array}{c}
 M_1 \\
 M_2 \\
 M_3 \\
 M_4 \\
 M_5
 \end{array} \right] & = & \left[\begin{array}{c}
 1/7 \\
 -4 \\
 13/14
 \end{array} \right]
 \end{array}$$

Solutions:

$$M_1 = 0.0$$

$$M_2 = 1.612$$

$$M_3 = 5.643$$

$$M_4 = 1.673$$

$$M_5 = 0.0$$

$$g(10) = 8.61$$

$$\text{Exact solution } g(10) = 9.3$$

$$\text{By Linear interpolation } g(10) = 12.7$$

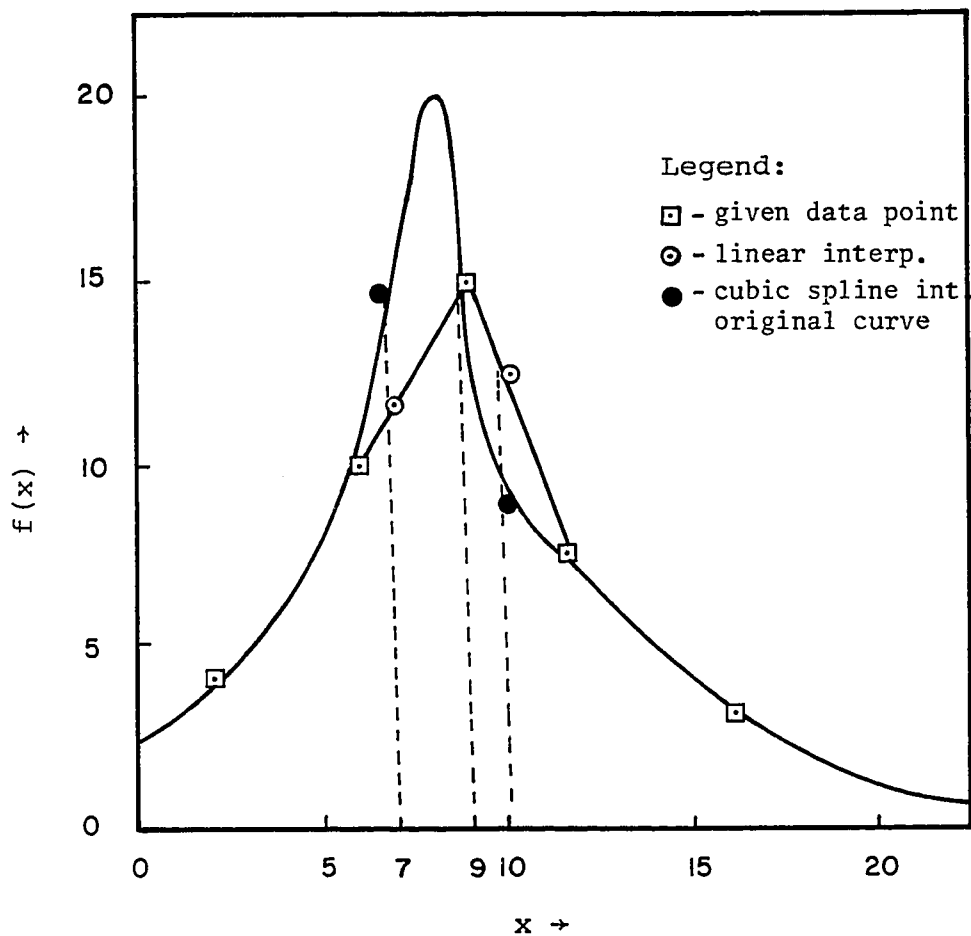


Figure 4.3 Comparison of the result of sample calc. and linear interpolation with original curve.

4.4 Two Dimensional Spline Approach

In the one dimensional spline procedure, we constructed an interpolating spline of the form $g(x)$ as a function of a single variable x . In the two dimensional approach, our interpolating spline will be a function $S(x,y)$ which is dependent on the x and y co-ordinate axes. However, the two dimensional approach is essentially an extension of the one dimensional case applied in two dimensions. The major difference between the one dimensional method and the two dimensional approach is that the latter is mesh dependent as can be seen later in this development.

The procedure for the two-dimensional development of the cubic spline interpolation is similar to that of the two dimensional linear interpolation. Both use the basic theory of Hilbert Space [1]. Because of its simplicity, one can present the development of the two-dimensional linear interpolation first for illustrative purposes.

4.4.(a) Two-Dimensional Linear Interpolation

The procedure for obtaining the two dimensional linear interpolation is represented in figure 4.4. First, carry out linear interpolation along the x -axis to obtain values for f_A and f_B . Then interpolate between f_A and f_B linearly along the y direction while keeping x constant to obtain the approximation value $f(x,y)$.

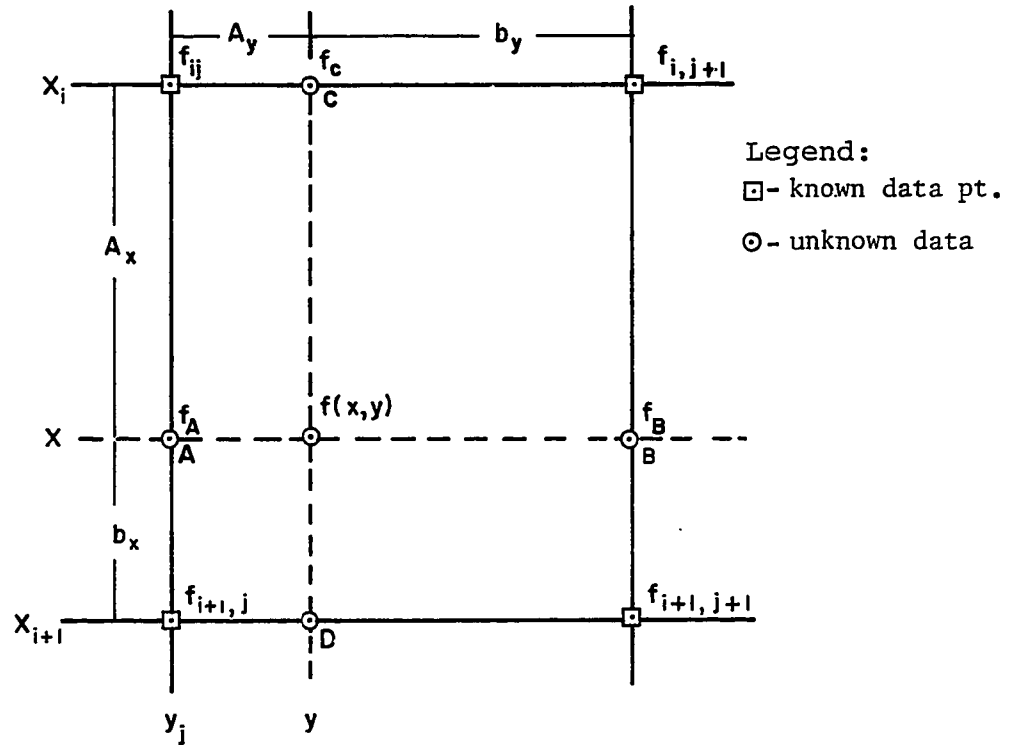


Figure 4.4 2-Dimensional linear interpolation (rectangular mesh system).

Derivations:

$$x_i < x < x_{i+1}; y_i < y < y_{j+1}$$

$$\text{Let } A_x = x - x_i; A_y = y - y_j$$

$$b_x = x_{i+1} - x$$

$$b_y = y_{i+1, j+1} - y$$

$$f_A = f_{ij} + (f_{i+1, j} - f_{i, j}) \left(\frac{A_x}{A_x + b_x} \right) \quad 4(28)$$

$$f_A = \left(1 - \frac{A_x}{A_x + b_x} \right) f_{ij} = \left(\frac{A_x}{A_x + b_x} \right) f_{i+1, j} \quad 4(29)$$

Similarly

$$f_B = \left(- \frac{A_x}{A_x + b_x} \right) f_{i, j+1} + \left(\frac{A_x}{A_x + b_x} \right) f_{i+1, j+1} \quad 4(30)$$

$$f(x, y) = f_A + (f_B - f_A) \left(\frac{A_y}{A_y + b_y} \right) \quad 4(31)$$

$$f(x, y) = (1 - \beta) f_A + \beta f_B \quad 4(32)$$

where:

$$\beta = \frac{A_y}{A_y + b_y}, \quad \alpha = \frac{A_x}{A_x + b_x}$$

then

$$f_A = (1 - \alpha) f_{ij} + \alpha f_{i+1, j} \quad 4(33)$$

$$f_B = (1 - \alpha) f_{i, j+1} + \alpha f_{i+1, j+1} \quad 4(34)$$

$$\begin{aligned} f(x, y) &= (1 - \beta)(1 - \alpha) f_{ij} + \beta(1 - \alpha) f_{i, j+1} \\ &\quad + \alpha(1 - \beta) f_{i+1, j} + (\alpha\beta) f_{i+1, j+1} \end{aligned} \quad 4(35)$$

4.4.(b) Cubic Spline Interpolation in Two-dimensions:

The two dimensional spline interpolation like its two dimensional linear counterpart will first interpolate values of S_A , S_B , S_C and S_D in the x-direction while holding y axis constant. The one dimensional spline approach is further applied in the y-direction using known values of f_A , f_B , f_C and f_D to obtain an estimate of $S(x,y)$ at the desired points.

The interpolating function is as given in 4(6) for x axis:

$$\begin{aligned}
 S(x) = & \frac{M_{i-1}}{6} \left[\frac{(x_i - x)^3}{h_i} - (x_i - x) h_i \right] \\
 & + \frac{M_i}{6} \left[\frac{(x - x_{i-1})^3}{h_i} - (x - x_{i-1}) h_i \right] \\
 & + f_{i-1} \left(\frac{x_i - x}{h_i} \right) + f_i \left(\frac{x - x_{i-1}}{h_i} \right)
 \end{aligned} \tag{4(6)}$$

where f_i are the function values (Figure 4.5).

By putting appropriate values of distances A, B, C, D, we can determine f_A , f_B , f_C , f_D where x is such that $x_{i-1} < x < x_i$

NOTE: $f_A \equiv f_{j-1}$, $f_B \equiv f_j$, $f_C \equiv f_{j+1}$, $f_D \equiv f_{j+2}$

These values thus determined form new data points for a one-dimensional interpolation along the y-axis.

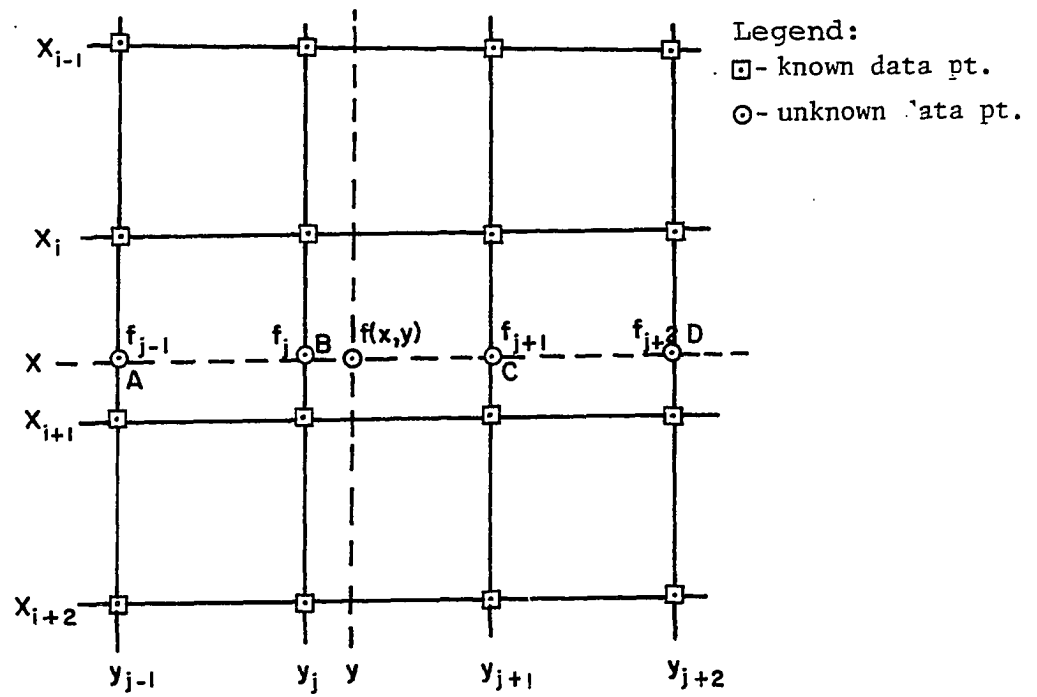


Figure 4.5 Two Dimensional Spline Interpolation (mesh system).

Let $S^*(y)$ represent an independent interpolation along the y -axis.

$$\begin{aligned}
 S^*(y) = & \frac{M_{j-1}}{6} \left[\frac{(y_j - y)^3}{h_j} - (y_j - y)h_j \right] \\
 & + \frac{M_j}{6} \left[\frac{(y - y_{j-1})^3}{h_j} - (y - y_{j-1})h_j \right] \\
 & + f_{j-1} \left(\frac{y_j - y}{h_j} \right) + f_j \left(\frac{y - y_{j-1}}{h_j} \right)
 \end{aligned} \tag{4(37)}$$

Where f_j are the function values represented by f_A, f_B, f_C and f_D

y is such that $y_{j-1} < y < y_j$

Since f_A, f_B, f_C and f_D are functions of x , then $S^*(y)$ is a function also of x

$$S^*(y) = S(x, y).$$

Theoretically we can look at the overall relationship as a product of two one dimensional splines given by the relation (from 4(6)).

$$S^*(y) = S(x, y) = \sum_{i=0}^3 \sum_{j=0}^3 K_{ij} (x-x_i)^i (y-y_j)^j \tag{4(38)}$$

where K_{ij} is the coefficient to be determined.

Alternatively we can apply a Hilbert Space theory to the problem.

4.5 Theoretical Validation of the Procedure

Outlined by Use of Hilbert Space Theory [1]

Let L_x, L_y represent two differential operators in a rectangular mesh, R_{ij} , operating in the x and y directions respectively.

$$L_x = A_n(x) D_x^m + A_{n-1}(x) D_x^{m-1} + \dots + A D(x) \quad 4(39)$$

$$L_y = B_n(y) D_y^n + B_{n-1}(y) D_y^{n-1} + \dots + B D(y) \quad 4(40)$$

where:

$A_m(x), B_n(y)$ possess continuous $m^{\text{th}}, n^{\text{th}}$ derivatives respectively.

D_x, D_y = partial derivatives with respect to x, y respectively.

Then

$$L_x \cdot L_x S(x,y) = 0 \quad 4(41)$$

$$L_y \cdot L_y S(x,y) = 0 \quad 4(42)$$

If the fundamental solutions of the above are given by $U_i(x), U_j(y)$ respectively

Then we can solve for $S(x,y)$ from the $U_i(x)$ solution.

$$S(x,y) = A_i(x) U_i(x) \quad 4(43)$$

putting this value of $S(x,y)$ into the second equation will give the relation for the y-direction [cross product relation]

$$S(x,y) = \sum_{i=0}^m \sum_{j=0}^n A_i U_i(x) B_j U_j(y) \quad 4(44)$$

where:

A_i, B_j are functions of x, y respectively with the property of continuous n^{th} derivatives. m, n are no. of terms in x, y respectively

$U_i(x), U_j(y)$ are functions of x , and y respectively

However looking at equation 4(6) one can rightly say this:

$$S(x, y) = \sum_{i=0}^3 \sum_{j=0}^3 k_{ij} (x-x_i)^i (y-y_j)^j \quad 4(45)$$

where:

$$K_{i,j} = f(f(x,y), P_{ij}, q_{ij}, e_{ij}) \quad 4(46)$$

$f(x,y)$ is the functional cubic equation in x and y

P_{ij} = partial derivation of the interpolation equation with respect to x

q_{ij} = partial derivative of the interpolation equation with respect to y

e_{ij} = Second derivative of the interpolation equation with respect to x, y .

Finally we can define the coefficient k_{ij} thusly:

$$k_{ij} = \sum_{i=0}^3 \sum_{j=0}^3 C_{ij} \cdot 1/H_{ij} \quad 4(47)$$

where:

$$C_{ij} = \begin{vmatrix} f(x,y) & P_{ij} \\ q_{i,j} & e_{ij} \end{vmatrix} \quad 4(48)$$

$$H_{ij} = \sum_{i=0}^3 \sum_{j=0}^3 [h_i]^i [h_j]^j \quad 4(49)$$

where:

$$h_i = x_i - x_{i-1} \quad 4(50)$$

$$h_j = y_j - y_{j-1} \quad 4(51)$$

The computation of $P_{i,j}$, $q_{i,j}$ and $e_{i,j}$ are presented in the succeeding pages.

4.6 Computation of Derivatives

The partial derivatives needed at each of the four corners of the subrectangle are defined thus:

Let

$$P_{ij} = \frac{\delta S}{\delta x}$$

$$q_{ij} = \frac{\delta S}{\delta y} \quad 4(52)$$

$$e_{ij} = \frac{\delta^2 S}{\delta y \delta x}$$

Then as in 4(10) for P_{ij} :

$$\begin{aligned} & \Delta X_{i-1} P_{i-1,j} + 2(\Delta X_{i-1} + \Delta X_i) P_{ij} + \Delta X_i P_{i+1,j} \\ &= 6 \left[\frac{1}{\Delta X_i} (U_{i+1,j} - U_{i,j}) - \frac{1}{\Delta X_{i-1}} (U_{i,j} - U_{i-1,j}) \right] \quad 4(53) \end{aligned}$$

In y-direction : q_{ij}

$$\begin{aligned} & \Delta Y_{j-1} q_{i,j-1} + 2(\Delta Y_{j-1} + \Delta Y_j) q_{i,j} + \Delta Y_j q_{i,j+1} \\ & = 6 \left[\frac{1}{\Delta Y_j} (U_{i,j+1} - U_{i,j}) - \frac{1}{\Delta Y_{j-1}} (U_{i,j} - U_{i,j-1}) \right] \end{aligned} \quad 4(54)$$

for second derivative e_{ij} :

$$\begin{aligned} & \Delta X_{i-1} e_{i-1,j} + 2(\Delta X_{i-1} + \Delta X_i) e_{ij} + \Delta X_i e_{i+1,j} \\ & = 6 \left[\frac{1}{\Delta X_i} (q_{i+1,j} - q_{ij}) - \frac{1}{\Delta X_{i-1}} (q_{ij} - q_{i-1,j}) \right] \end{aligned} \quad 4(55)$$

Equations 4(52) through 4(55) can be solved independently using a tridiagonal matrix as in 4(17) to calculate values for P_{ij} , q_{ij} and e_{ij} respectively.

Thus:

$$\begin{bmatrix} 2 & \lambda_0 & 0 & \dots & 0 & 0 & 0 \\ \mu & 2 & \lambda_1 & \dots & 0 & 0 & 0 \\ \cdot & \cdot & \cdot & & \cdot & \cdot & \cdot \\ \cdot & \cdot & \cdot & & \cdot & \cdot & \cdot \\ \cdot & \cdot & \cdot & & \cdot & \cdot & \cdot \\ \cdot & \cdot & \cdot & & \cdot & \cdot & \cdot \\ \cdot & \cdot & \cdot & & \cdot & \cdot & \cdot \\ \cdot & \cdot & \cdot & & \cdot & \cdot & \cdot \\ \cdot & \cdot & \cdot & & \cdot & \cdot & \cdot \\ \cdot & \cdot & \cdot & & \cdot & \cdot & \cdot \\ 0 & 0 & 0 & \dots & 2 & \lambda_{n-2} & 0 \\ 0 & 0 & 0 & \dots & \mu_{n-1} & 2 & \lambda_{n-1} \\ 0 & 0 & 0 & \dots & 0 & 0 & 2 \end{bmatrix} \begin{bmatrix} P_0 \\ P_1 \\ \cdot \\ P_{m-2} \\ P_{m-1} \\ P_m \end{bmatrix} = \begin{bmatrix} d_0 \\ d_1 \\ \cdot \\ d_{m-2} \\ d_{m-1} \\ d_m \end{bmatrix} \quad 4(56)$$

Similar approach can be used to obtain q_{ij} and e_{ij}

The above is equivalent to

$$AX = D \quad 4(57)$$

$$X = A^{-1}D \quad 4(58)$$

where:

$$X = P_1, P_2, \dots, P_{m-1} \quad 4(59)$$

$$D = d_1, d_2, \dots, d_{m-1} \quad 4(60)$$

The divided difference version for calculating the partial derivatives can also be used to simplify calculations.

$$\frac{\delta S}{\delta x} = P_{ij} = [S_{i+1,j} - S_{i,j}] / (X_{i+1} - X_i) \quad 4(61)$$

$$\frac{\delta S}{\delta y} = q_{ij} = [S_{i,j+1} - S_{i,j}] / (Y_{j+1} - Y_j) \quad 4(62)$$

$$\frac{\delta^2 S}{\delta y \delta x} = e_{ij} = [P_{i,j+1} - P_{ij}] / (Y_{j+1} - Y_j) \quad 4(63)$$

$$= [q_{i+1,j} - q_{ij}] / (X_{i+1} - X_i) \quad 4(64)$$

4.7 Sample Problem for two-dimensional Spline Interpolation (regularly distributed Data Points)

Obtain an approximate value at $f(1.5,1.5)$ using a two-dimensional cubic spline interpolation. Data values are tabulated in table 4.2.

Assume a natural spline condition.

Solution:

Start the solution by noting that

$$\lambda = \mu = \frac{1}{2}$$

$$d_j = 3(f_{j-1} - 2f_j + f_{j+1})$$

$$h_j = h_{j+1} = 1.0$$

- a. Interpolate x first, and then y .

(see figure 4.6 and table 4.3)

- b. Y first then x (figure 4.7 and table 4.4)

The two values obtained by reversing the axes are same .

Table 4.2: Two Dimensional Interpolation Method

X_i	Y_j			
	0	1	2	3
0	4	6	8	12
1	9	10	18	20
2	15	16	30	32
3	7	8	14	16

Table 4.3: Solution values--interpolation of X, first.

Y_j	M_1	M_2	M_3	M_4	$g_x(1.5)$
0	0.0	7.2	-11.8	0.0	12.98
1	0.0	8.8	-23.2	0.0	13.9
2	0.0	5.433	-15.73	0.0	24.644
3	0.0	17.6	-46.4	0.0	27.8

Interpolate in the x direction:

from $g_x(1.5)$, $M_2 = 18.743$, $M_3 = -16.065$, $f(x,y) = [19.6]$

Table 4.4: Solution values--interpolating y first, then x.

j	x_j	m_1	m_2	m_3	m_4	$g_y(1.5)$
1	0	0.0	0.0	0.0	0.0	7
2	1	0.0	13.6	-12.4	0.0	13.925
3	2	0.0	25.6	-24.4	0.0	22.425
4	3	0.0	9.6	-8.4	0.0	10.925

Interpolate in the x direction using value of

$g_y(1.5)$: $M_2 = 11.72$, $M_3 = -34.43$, $f(y,x) = [19.6]$

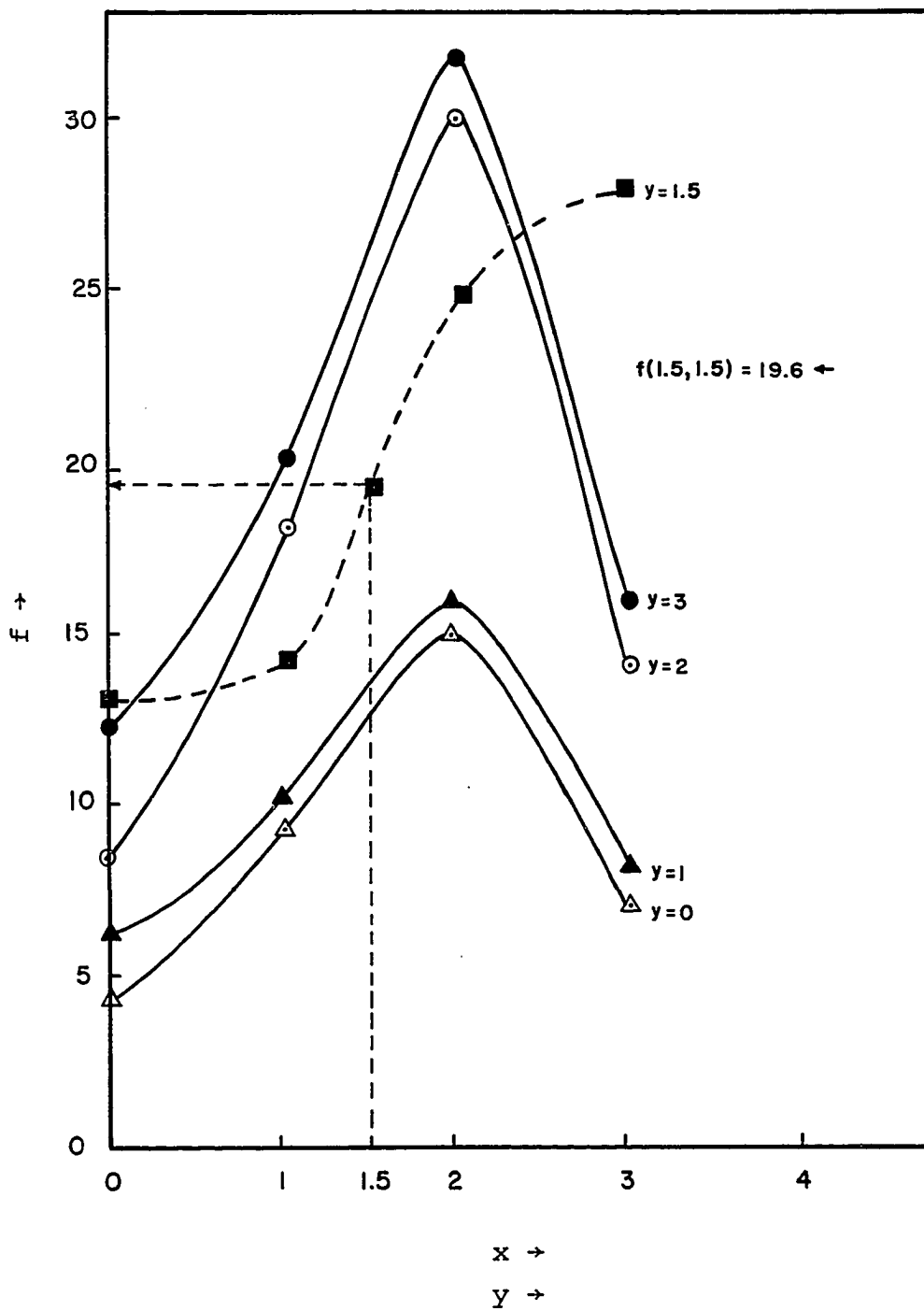


Figure 4.6 Interpolation along x axis, first and then along y axis.

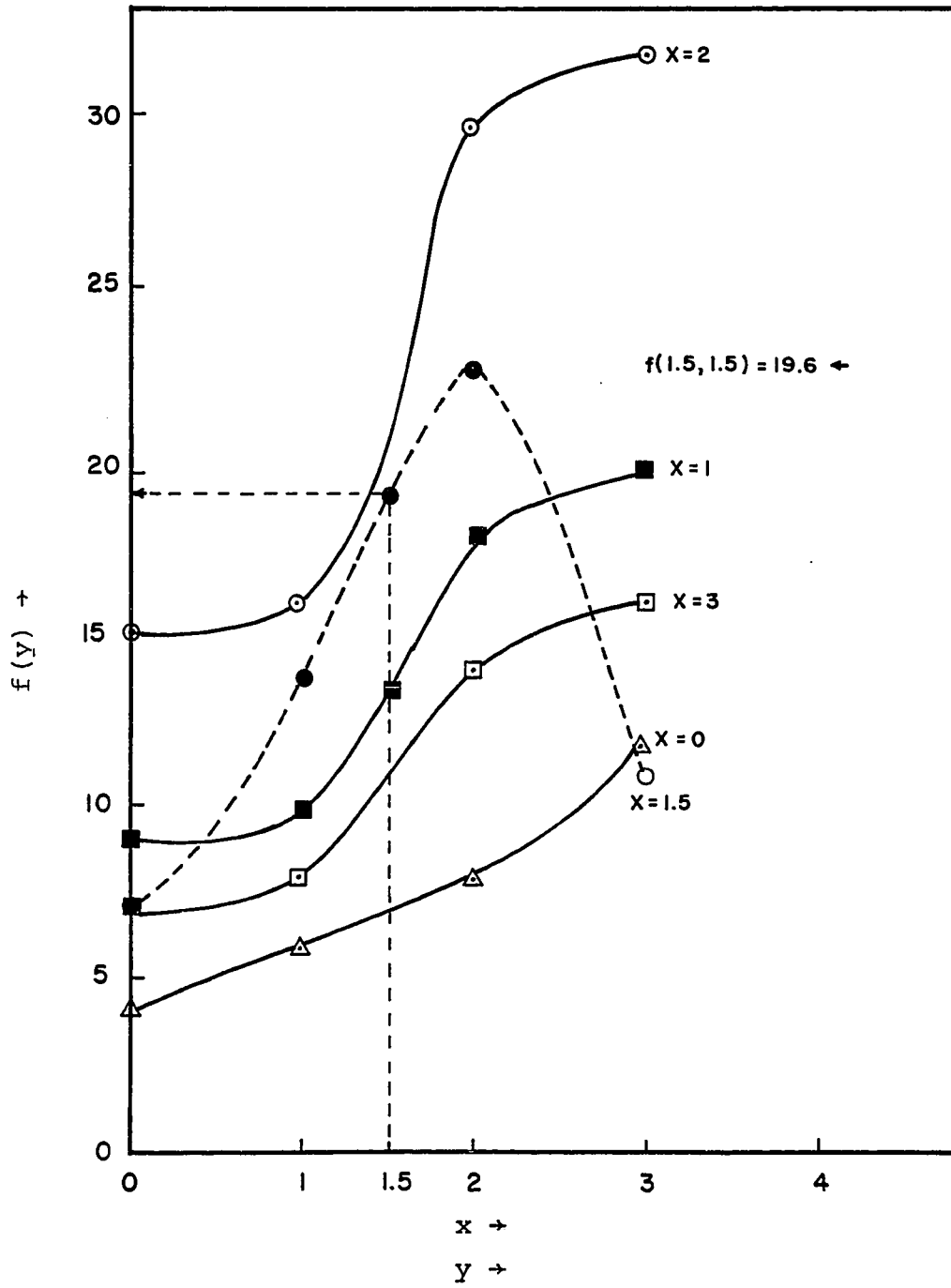


Figure 4.7 Interpolation along y axis first and then x axis.

NOMENCLATURE FOR THE CUBIC SPLINE FUNCTIONS

- $y(x)$ = functional value of x
 $y''(x)$ = Second derivative of y with respect to x
 $y'(x)$ = first derivative of function y with respect to x
 $M(x)$ = 'Bending moment' function
 E = Young's modulus of Elasticity
 I = Geometric moment of Inertia
 α = Proportionality symbol
 C_1, C_2 = constants of integration
 $\mu \quad \lambda$ = constants
 d_j = $n \times 1$ matrix
 M_j = "Bending moment" at node $j \rightarrow$ a constant
 y_j = functional value at node j
 h_j = interval constant between node at j and node at $j-1$
 $g(x)$ = One-dimensional interpolation function
 $S(x,y)$ = Two-dimensional interpolation function
 f_A, f_B, f_C, f_D = Interpolation values obtained by interpolation along the x -axis.
 α, β = Proportional constants in the two dimensional linear interpolation
 $f_{i,j}$ = Two-dimensional functional values at coordinate nodes i, j .
 $S^*(y)$ = An interpolating function along the y -axis.

- $K_{i,j}$ = Coefficient matrix
 L_x, L_y = Differential operators in x and y
 A_m, B_n = functions in x , and y possessing continuous
 m^{th} and n^{th} derivatives respectively
 U_i, U_j = fundamental solutions of sets of equations in
the x , and y directions.
 $P_{i,j}$ = Partial derivative of the interpolation equa-
tion with respect to x
 Q_{ij} = Partial derivative of the interpolation equa-
tion with respect to y .
 $\rho_{i,j}$ = Partial derivative of the interpolation equa-
tion with respect to x, y
 $H_{i,j}$ = Coefficient Matrix

CHAPTER V

MODEL TESTING

In order to show the superiority of this study model over some of the conventional approaches, a few tests were run. The first test, figure 5.1, is a plot that compares the quality of the Lagrange interpolator with the one dimensional approach of this study. The results are tabulated in table 5.1, and figure 5.1 is the resulting plot. A comparison of both plots with the original curve shows that the one-dimensional method of this study is a much closer approximator than the Lagrange polynomial interpolator. One of the possible reasons for this outcome is the fact that the first and the second derivatives of the method of this study are continuous. These properties make it easier for the Spline model to closely approximate curvatures than the conventional polynomial approximations.

The two dimensional approach of this study was also compared with the two-dimensional Hermite interpolation method. Hermite interpolation method has a continuous first derivative. Figure 5.2 A is the result of the Hermite interpolation method while figure 5.2 B is the result of interpolation using the method of this study. Data for this test is presented in table 5.2. A comparison of both methods shows

Table 5.1. Data for Comparison of Lagrange interpolation method versus the method of this study.

X	Y		
	Original curve	Lagrange method	This study
*2	4.0	4.0	4.0
*6	10.0	10.0	10.0
7	14.0	11.6	14.5
8	20.0	10.0	21.0
*9	15.0	15.0	15.0
10	9.5	9.3	8.8
11	--	--	--
*12	8.0	8.0	8.0
*16	3.0	3.0	3.0

*Supplied data points.

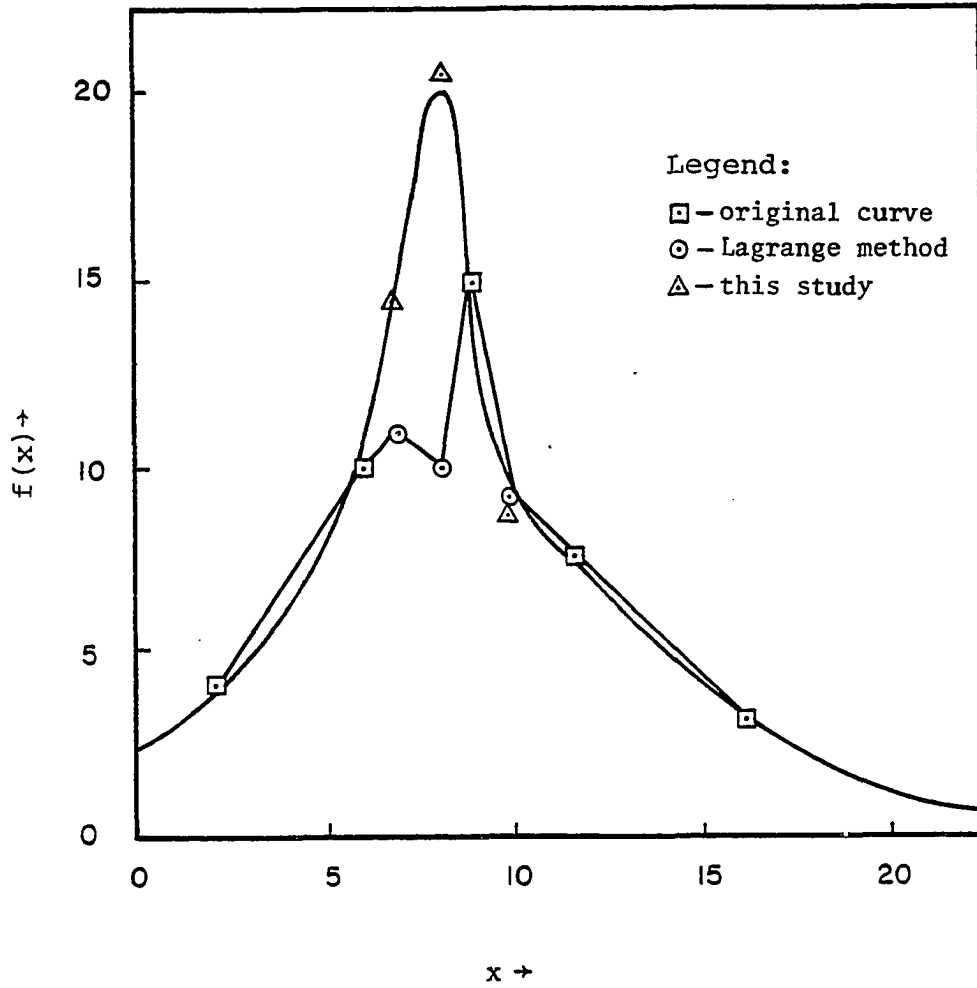
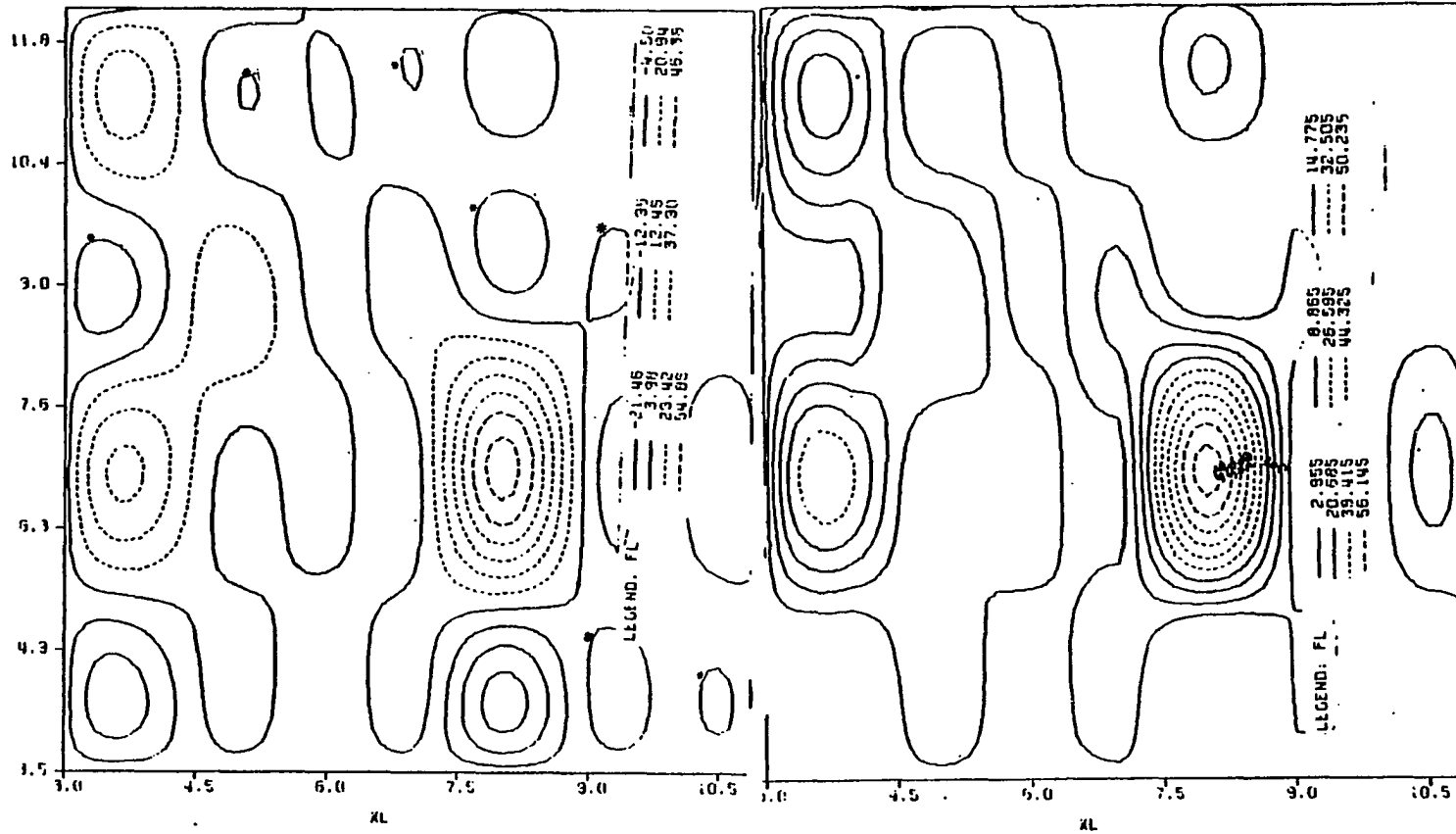


Figure 5.1. Comparison of Lagrange interpolation method with the method of this study.

Table 5.2: Reservoir data from Sitio Grand Field in New Mexico (data of Perez (23)).

X	Y	kh
2.95	12.3	0.4
4.	11	16.3
4	7	27
5	12.3	14.
5	8.8	19.4
5	5.3	6.5
6	11	4.2
6	7	10.0
7	12.3	0.31
7	8.8	11.2
7	5.3	6.82
8	11.	1.2
8	7	59.1
9	8.8	4.1
9	5.3	3.2
10	7	1.45
10	3.5	0.15
11	5.3	4.2

Legend:
 • minima



that the Hermite interpolation method exhibits some undesirable minima contour values which are absent in the contours produced by the method of this study. The exhibition of minima contour values (indicated by '*') is often referred to as undulations. One big advantage of the model of this study over the Hermite interpolator is the elimination of excessive undulations often present in the latter. It can be easily said that most polynomial approximations exhibit excessive undulations which are caused by interpolated values that are much smaller than the lowest available data values.

A test of how this model will behave in the presence of real reservoir parameter was carried out using data given in table 5.2. The data was obtained from Sitio Grand Field²³ which is producing from limestone of Cretaceous age. It is located in southeast Mexico. The results are shown in figure 5.3. Figure 5.3 is a contour map showing the flow capacity values at different positions of the field. This sort of distribution is desirable especially for a researcher who may need some flow capacity information at different points in the field. A three dimensional plot is presented in figure 5.4. The three dimensional plot shows zones of the field with peaks and pits. These phenomena elicit information as to those areas of the field or reservoir where high or low values of flow potential are expected.

Further tests were carried out using data from table 5.3. The data is a waveform studies information given in ref. (4).

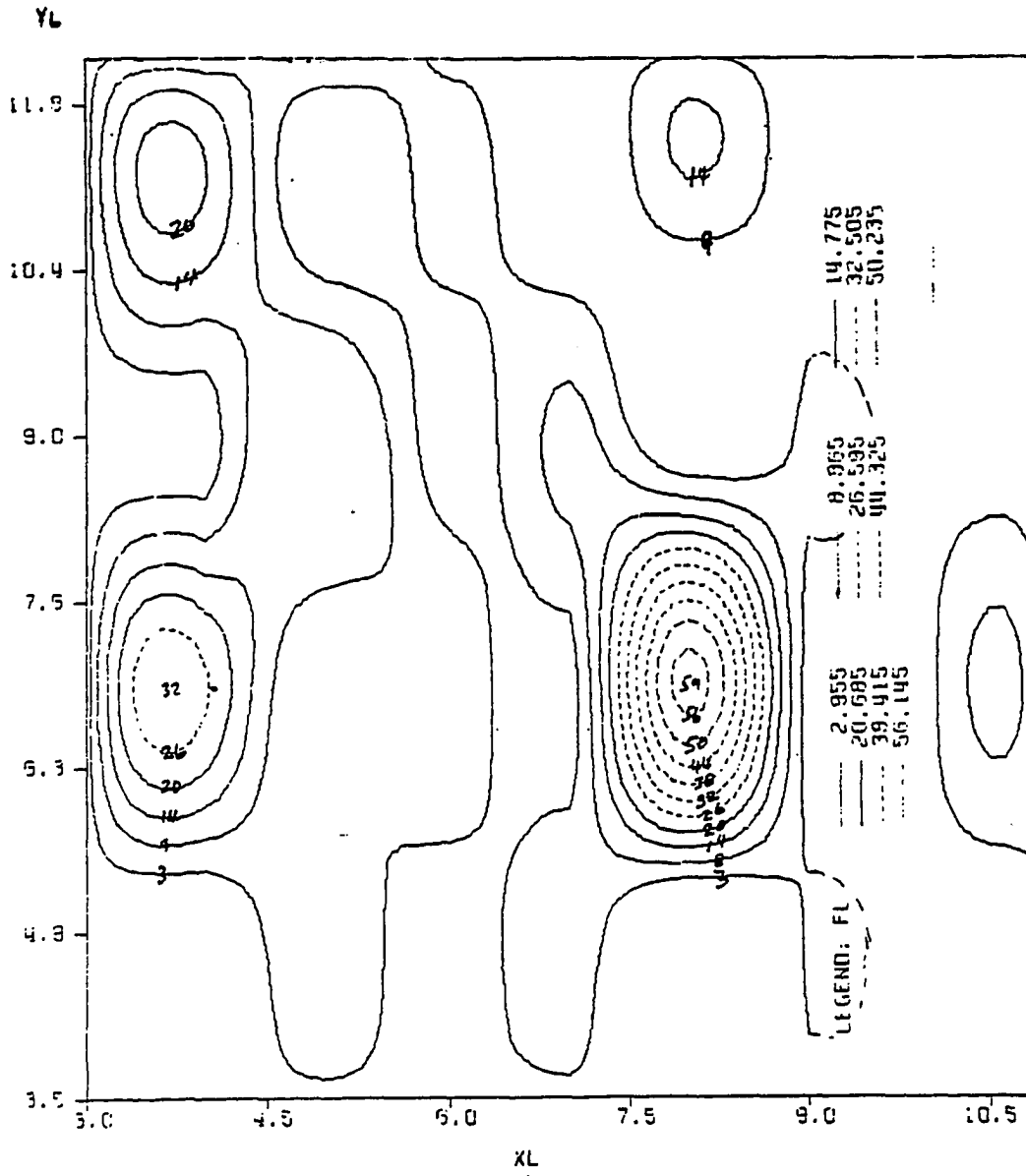


Fig. 5.3: Flow-capacity distribution in the Sitio Grand field.

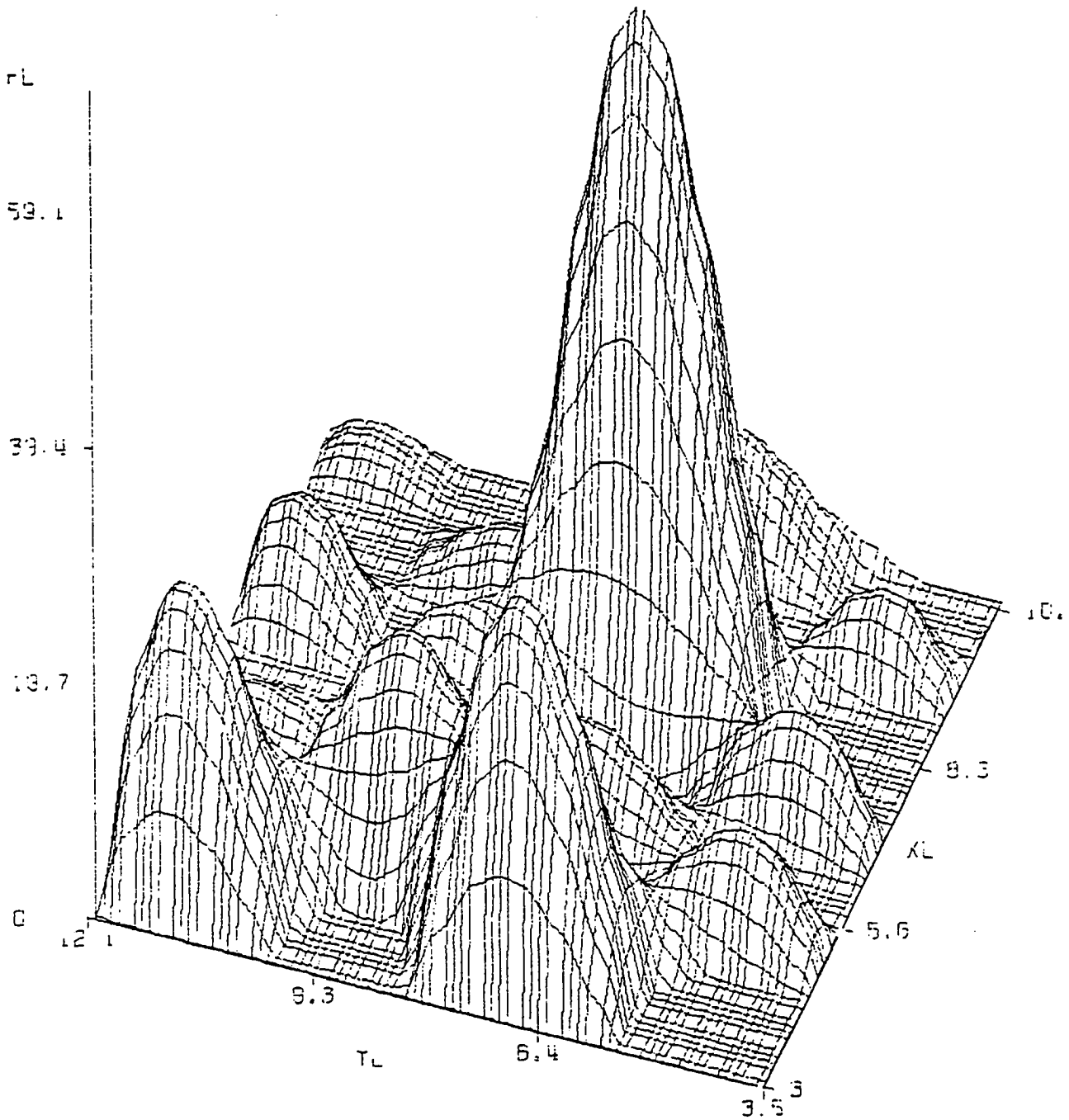


Fig. 5.4: 3-D plot of Flow-Capacity distribution--Sitio
Grand field

Here again, high peaks indicating high wave conditions were observed. Similarly, low pits indicating low wave conditions were observed (figure 5.5). Since wave condition may affect the way debris for off-shore hydrocarbon accumulation are distributed in the ocean the approach of this study can be used to influence the future of various off-shore prospecting.

In an attempt to see what happens to the ability of this model to approximate an original surface and identify parameter 'high points', varying percentages of known error were introduced into the original data constituting the known surface. Figure 5.6 is the original data as given in table 5.3. Figure 5.7 is the result obtained using the model of this study after replacing 5 percent of the original data values by zeros. Zero values were purposely chosen in order to amplify the results in each situation. Figure 5.7(A) shows smooth contours of the resulting surface. A comparison of the contours of figure 5.7(A) and those of the original data shows no marked differences, apart from the recognition that the former are smoother contours.

Figure 5.7(B) is a three dimensional projection of the data. The three dimensional plot of figure 5.7(B) carefully identifies areas having very high and very low parameter values which correspond to those indicated by the contours of figure 5.7(A). The importance of the three dimensional plot is to afford an easy recognition of anomalous portions

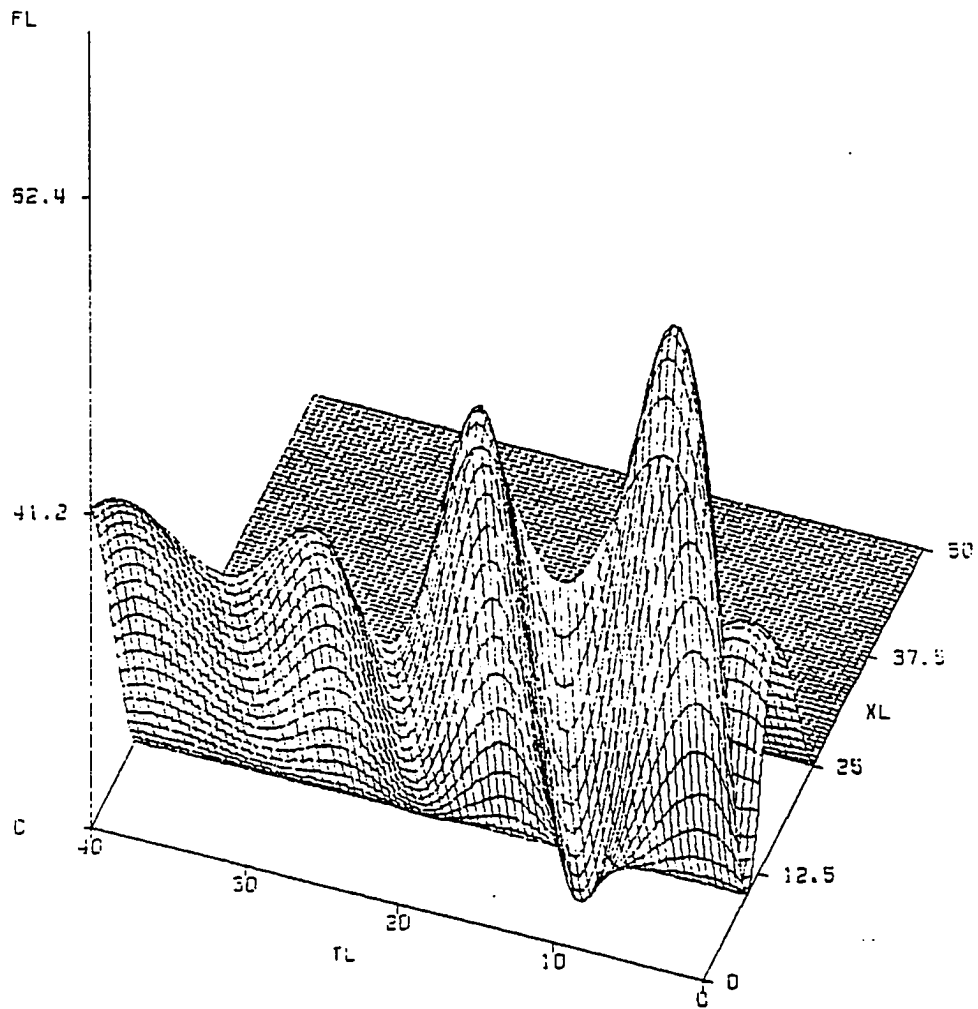
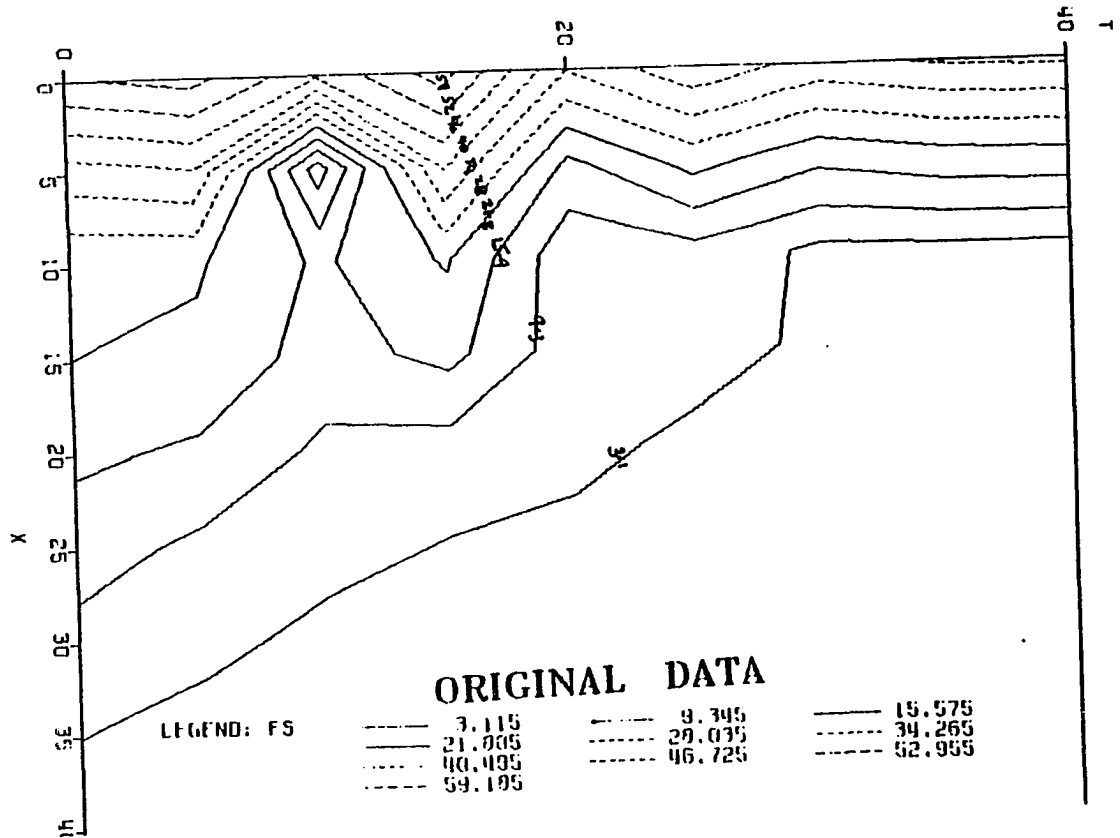


Fig. 5.5: 3-Dim. plot of waveform distribution

Fig. 5.6: Original surface



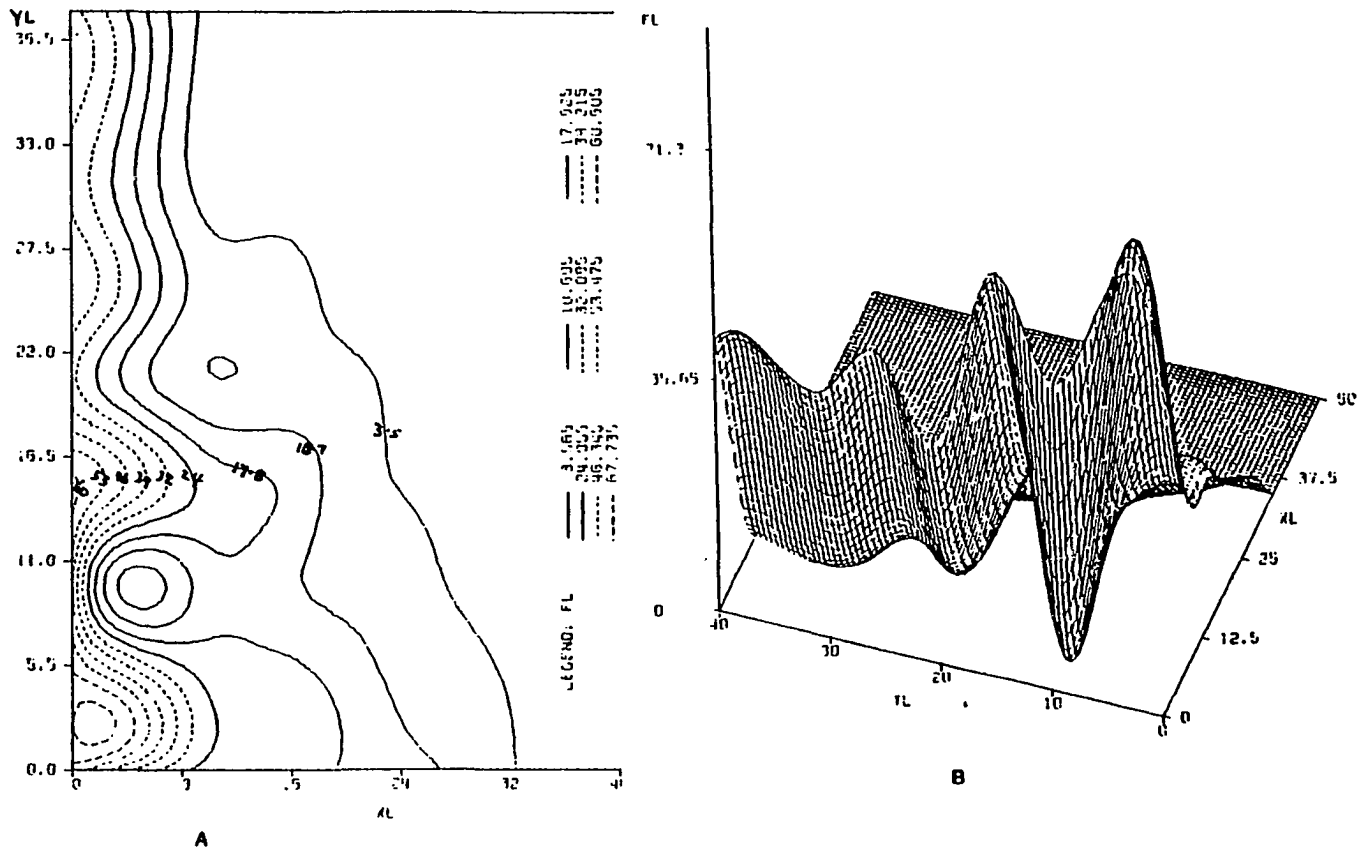


Fig. 5.7: Surface obtained by replacing 5% of data values with zeros (extreme cases).

of a field or reservoir where special attention may be necessary.

Figure 5.8 shows the result of contaminating 10 percent of the original data. This was done as before by replacing 10 percent of the original data with zeros. Comparison of the produced contours with the contours obtained using the original data does not easily reveal any obvious differences. The resulting contours and the corresponding three dimensional display are very closely similar to those of figure 5.7. This means that the model of this study can closely approximate the original data distribution even when 10 percent of the data information are faulty.

A further test was carried out using 80 percent of the correct data information and 20 percent data contamination. The result of this operation is shown in figure 5.9. A comparison of this result with that of the original data shows some little differences. However the actual positions of the peaks and 'pits' were not basically changed. As the contamination was increased beyond 20 percent, marked differences were observed. Figure 5.10 is the result of introducing a 30 percent contamination into the original data. Two distinct contour maps are produced (figure 5.10A). The three dimensional display of figure 5.10B shows peaks that are much lower than the corresponding peaks in the previous plots, and also the pits are diminished.

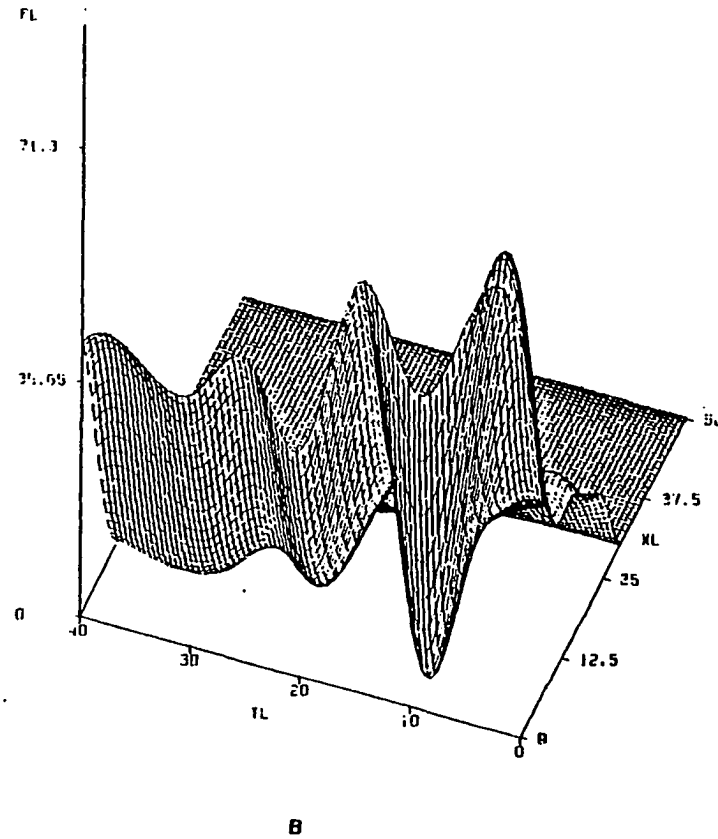
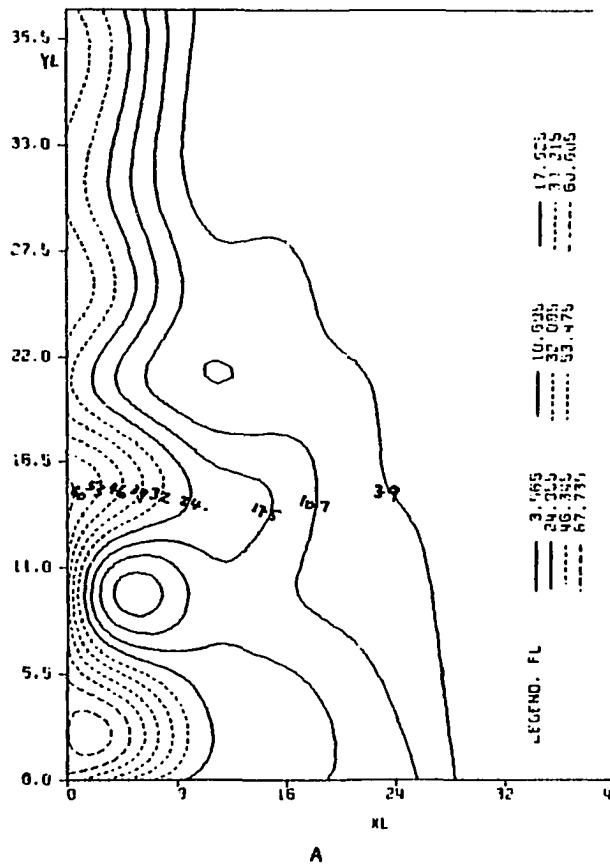


Fig. 5.8: Surface obtained by replacing 10% of data values with zeros (extreme cases).

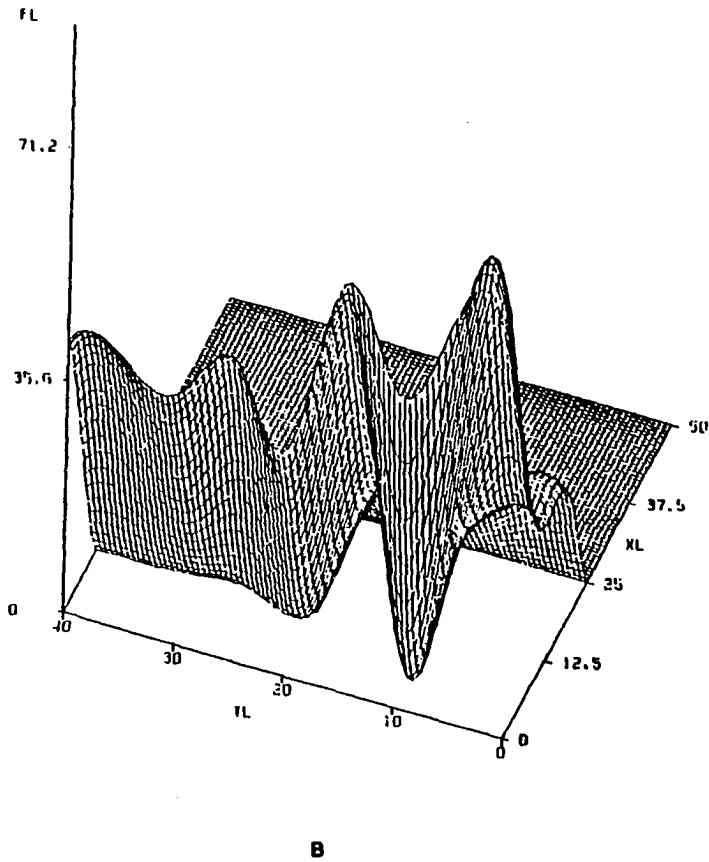
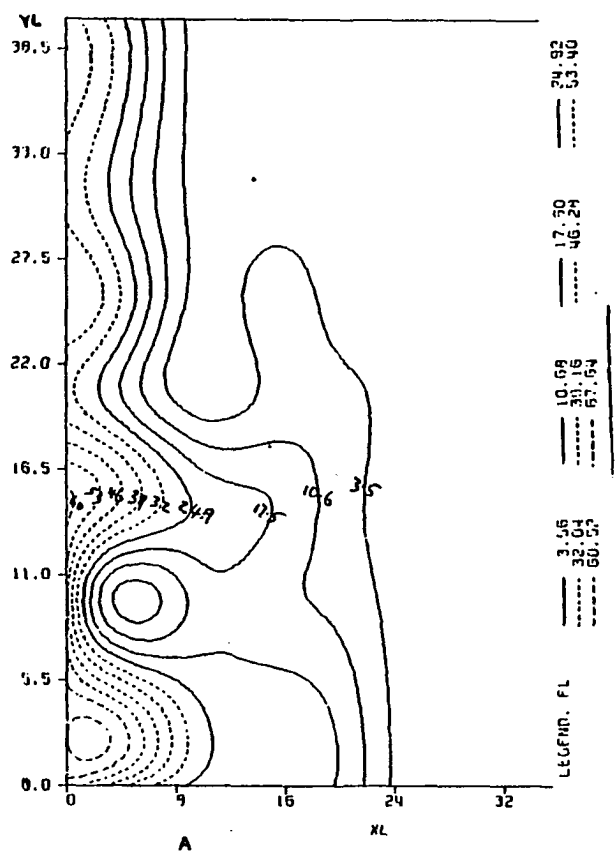
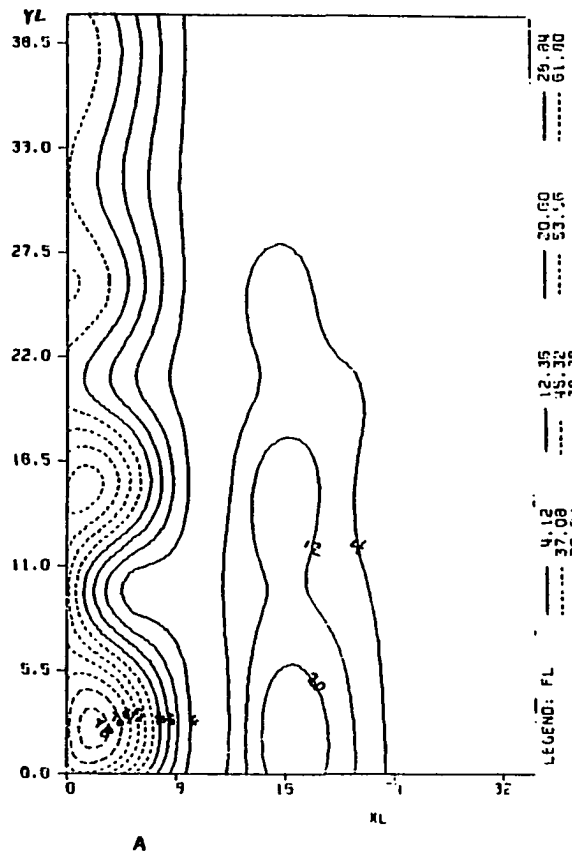
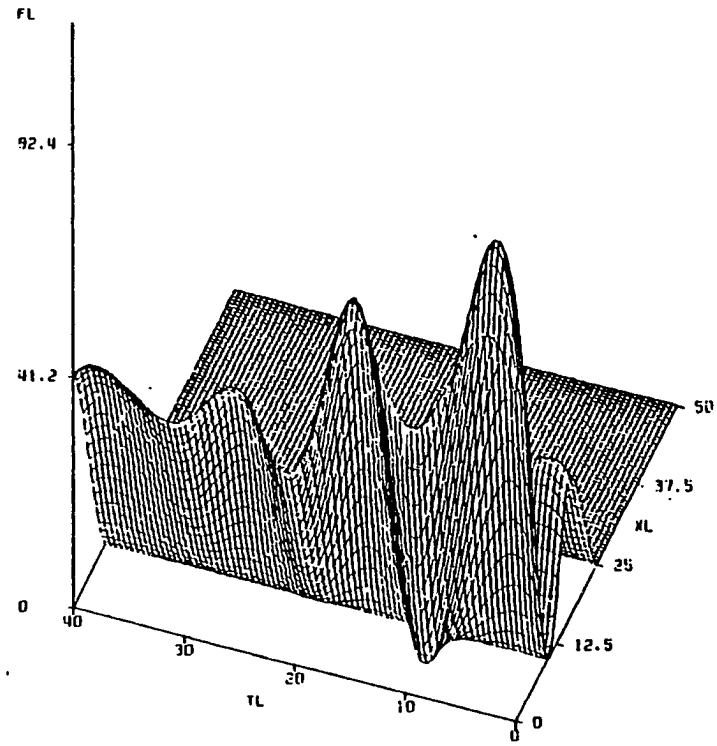


Fig. 5.9: Surface obtained by replacing 20% of data values with zeros (extreme cases).



A



B

Fig. 5.10: Surface obtained by replacing 30% of data points with zeros (extreme cases).

CHAPTER VI

DISCUSSION AND PRACTICAL PETROLEUM ENGINEERING

APPLICATION OF THE PROPOSED MODEL

One of the aims of this study is to develop a practical model that will aid petroleum engineers in the secondary oil recovery operations.

In the application scheme for this model, contour maps [29] have been used extensively to obtain detailed pictorial representation of a function of two variables whose values are known at discrete points. Detailed discussion on contour mapping has been covered in Chapter II, section 1. In reservoir engineering studies, imaginary surfaces comprising of a continuum of all possible reservoir parameter values can be mapped using the proposed model to display the distribution of variables of interest in the reservoir. The distribution of reservoir parameters when there is limited data information is often obscure and difficult to obtain in the absence of an appropriate approximation algorithm. The model of this study has been considered appropriate for use in the study of reservoir parameter distributions.

Similarly a three-dimensional model due to Watkins (31) and modified under the SAS (24) has been employed to obtain a conceptual surface representing appropriate reservoir

parameter. In reservoir engineering, the determination and variation of conceptual surfaces can be directly related to the variation of some corresponding non-spatial functions from point to point. This variation can be regarded as the flow on the conceptual surface, and thus, the generation of this conceptual surface can replace the physical system. An understanding of how the peaks, 'pits' and 'beds' associated with these projections are related to the physical system may relate to the reservoir engineer a desired insight into better ways to optimize his project.

Possibly the area of greatest uncertainty in designing a waterflood project is the quantitative overall knowledge of the variation of rock properties within a reservoir. Though other reservoir parameters such as porosity and connate water saturation vary both areally and vertically within a reservoir, the reservoir parameter whose variation is the most important in influencing waterflood performance is permeability. Permeability is a measure of fluid transmissibility of a rock. Several sources of obtaining good information on permeability are available:

1. Direct measurements of permeability on cores removed from wells.
2. Formation tests during drilling and production.
3. Transmissibilities obtainable from carefully run injection profiles.
4. Inferential information from well Logs,

6.1 Procedure for estimation of flood performance using the results of this model:

- a) From the flow capacity distribution shown in figures 6.1 and 6.2, obtain flow capacity values at fixed contour intervals (here a contour interval of 6 md-ft is convenient).
- b) Using a planimeter method, obtain floodable reservoir volume for the successive contour levels selected.
- c) Calculate water cut and oil recovery by using flow-capacity values (cumulative fraction of the total capacity), and a functional equation (simplifying assumptions were made where necessary).

Derivation of functional equation:

Simplifying assumptions made in this derivation are:

1. flow rate is proportional to flow capacity.
2. each flow contour level has same values of ϕ , S_{Or} , k_{rw} , k_{ro} .
3. Isothermal conditions exist throughout the reservoir.

The procedure of this mathematical analysis is similar to that reported by Stiles (28). The major difference is this model is using a volume weighted value of flow capacity values to calculate the water cut, while Stiles used randomly varying permeability values to obtain his water cut.

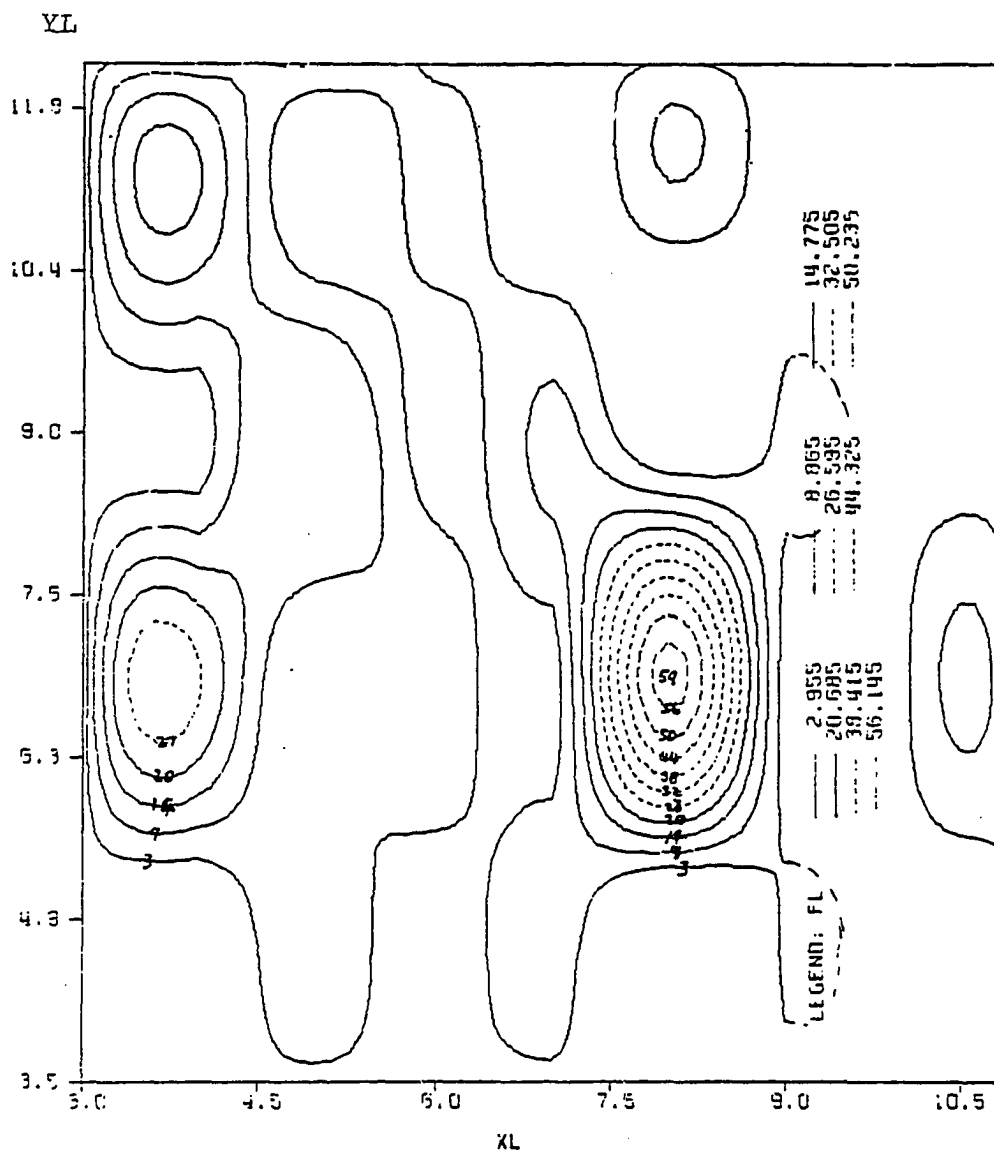


Fig. 6.1: Flow-capacity distribution in the Sitio Grand field (data of ref. 23)

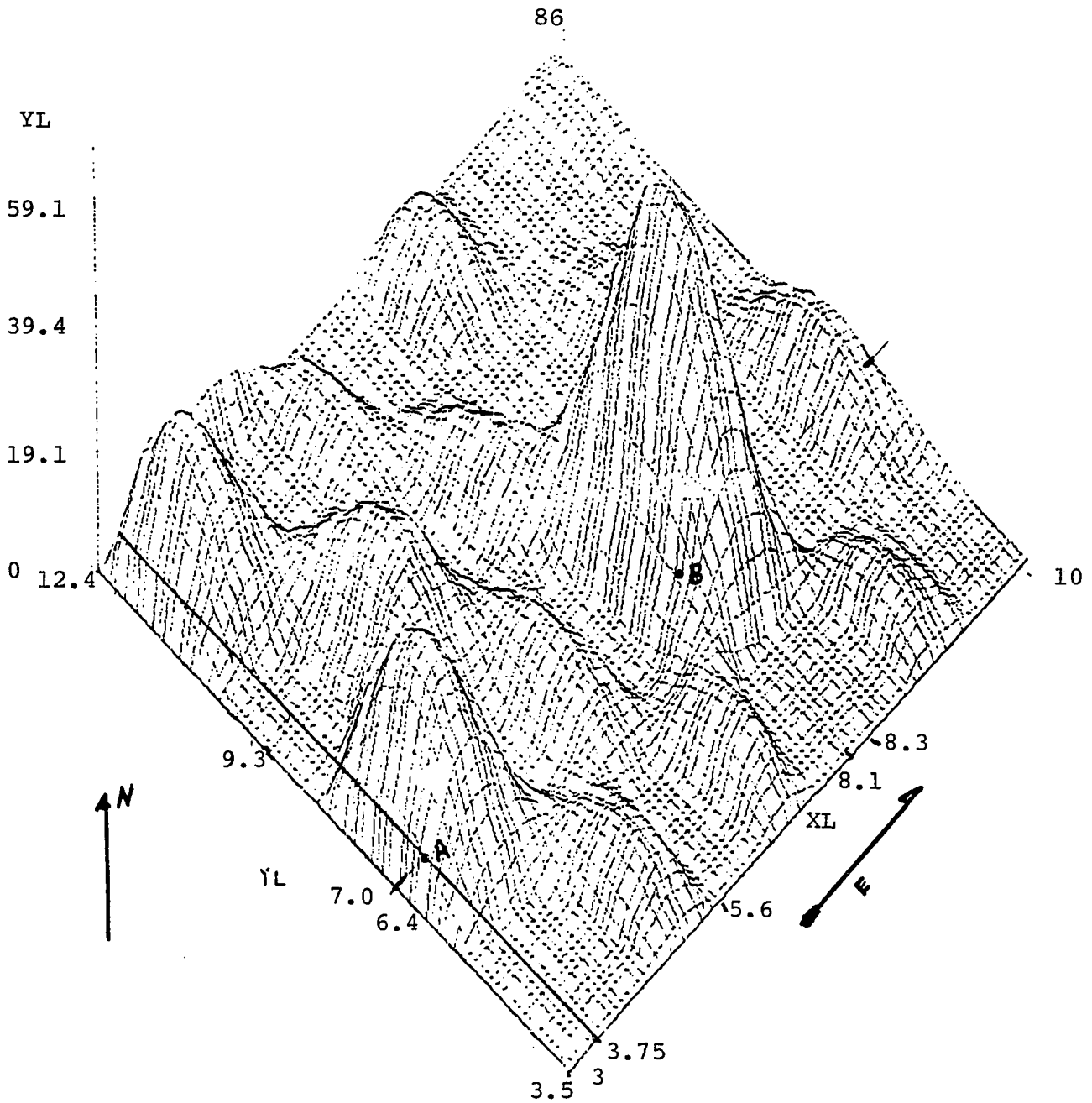


Fig. 6.2: 3-Dimensional plot of flow-capacity distribution in Sitio Grand field (data of ref. 23)

Define water flow rate

$$q_w = \rho_i^* \left(\frac{k_{rw}}{\mu_w} \right) \quad 6.1$$

$$q_o = (i - \rho_i) \left(\frac{k_{ro}}{\mu_o} \right) \left(\frac{1}{\beta_o} \right) \quad 6.2$$

water cut:

$$f_w = \frac{q_w}{q_w + q_o} = \frac{\rho_i \left(\frac{k_{rw}}{\mu_w} \right)}{\rho_i \left(\frac{k_{rw}}{\mu_w} \right) + (1 - \rho_i) \left(\frac{k_{ro}}{\mu_o} \right) \frac{1}{\beta_o}} \quad 6.3$$

$$f_w = \left[1 + \lambda (1 - \rho_i) \right]^{-1} \quad 6.4$$

where:

$$\lambda = \frac{k_{ro}}{k_{rw}} \cdot \frac{\mu_w}{\mu_o} \cdot \frac{1}{\beta_o}$$

$$*\rho_i = (\Sigma \rho_i V_i) / \Sigma V_i$$

ρ_i = flow capacity (weighted value) at point, i

$\mu_o \mu_w$ = oil and water viscosities respectively

k_{rw} , k_{ro} = relative permeabilities to water and oil respectively.

V_i = floodable volume for flow capacity level, i.

Similarly

$$f_o = \frac{(1-\rho_i) \left(\frac{k_{ro}}{\mu_o}\right) \left(\frac{1}{\beta_o}\right)}{\rho_i \left(\frac{k_{rw}}{\mu_w}\right) + (1-\rho_i) \left(\frac{k_{ro}}{\mu_o}\right) \frac{1}{\beta_o}} \quad 6.5$$

Sample Calculation: Contoured data from figure 6.1 is being used to show how the model of this study can aid the reservoir engineer in the estimation of reservoir performance prior to the start of water flooding operations. The necessary data needed in this analysis are given as follows:

$$k_{rw} = 0.3, k_{ro} = 0.7, \phi = 0.2, S_{or} = 0.25, S_w = 0.3 \text{ and } \beta_o = 1.1$$

By using the flow capacity values given in table 6.1, and the flow equation of 6.4 and 6.5, obtain water cut, and recovery values shown in table 6.1. Unit recovery for this reservoir has been estimated to be 458.4 bbls/acre-ft (see equation 6.6).

Figure 6.4 shows the plot of oil recovery versus water cut for the above field. The characteristics of the curves are similar to those reported by Stiles (28) and Johnson (16). A plot of flow-capacity versus oil recovery is shown in figure 6.5. A plot of flow capacity versus water cut is presented in figure 6.6. It is interesting to note that the three plots depicted in the above figures have similar characteristics.

Where V_i = floodable volume for flow capacity level, i.

Table 6.1. Calculation of Reservoir Performance

flow cap. cap. (cum.)	(fraction of total)	water cut (fract.)	Recovery (frac. of total)	Recovery fraction (cum)
--	0.0	0.00	0.21	0.21
59	0.17	0.33	0.143	0.35
115.1	0.33	0.37	0.135	0.48
165.73	0.47	0.43	0.121	0.60
209.66	0.59	0.49	0.109	0.71
248.07	0.7	0.55	0.096	0.81
280.57	0.79	0.65	0.075	0.88
307.87	0.87	0.75	0.05	0.93
327.87	0.93	0.84	0.03	0.96
342.67	0.97	0.93	0.015	0.97
351.57	0.99	0.98	0.0043	0.98
354.57	1.00	1.00	0.0	1.00

$$\text{Unit Recovery} = 7758 \left(\frac{S_{oi} - R_{so} B_o}{B_o} \right) \phi \quad 6.6$$

$$= (7758) \left(\frac{0.6 - (0.25)(1.1)}{1.1} \right) (0.2)$$

$$= 458.4 \text{ bbls/acre-ft}$$

DATA: $K_{rw} = 0.3$

$S_w = 0.3$

$K_{ro} = 0.7$

$R_{so} = 0.25$

$\phi = 0.2$

$B_o = 1.1$

Sweep eff = 0.95

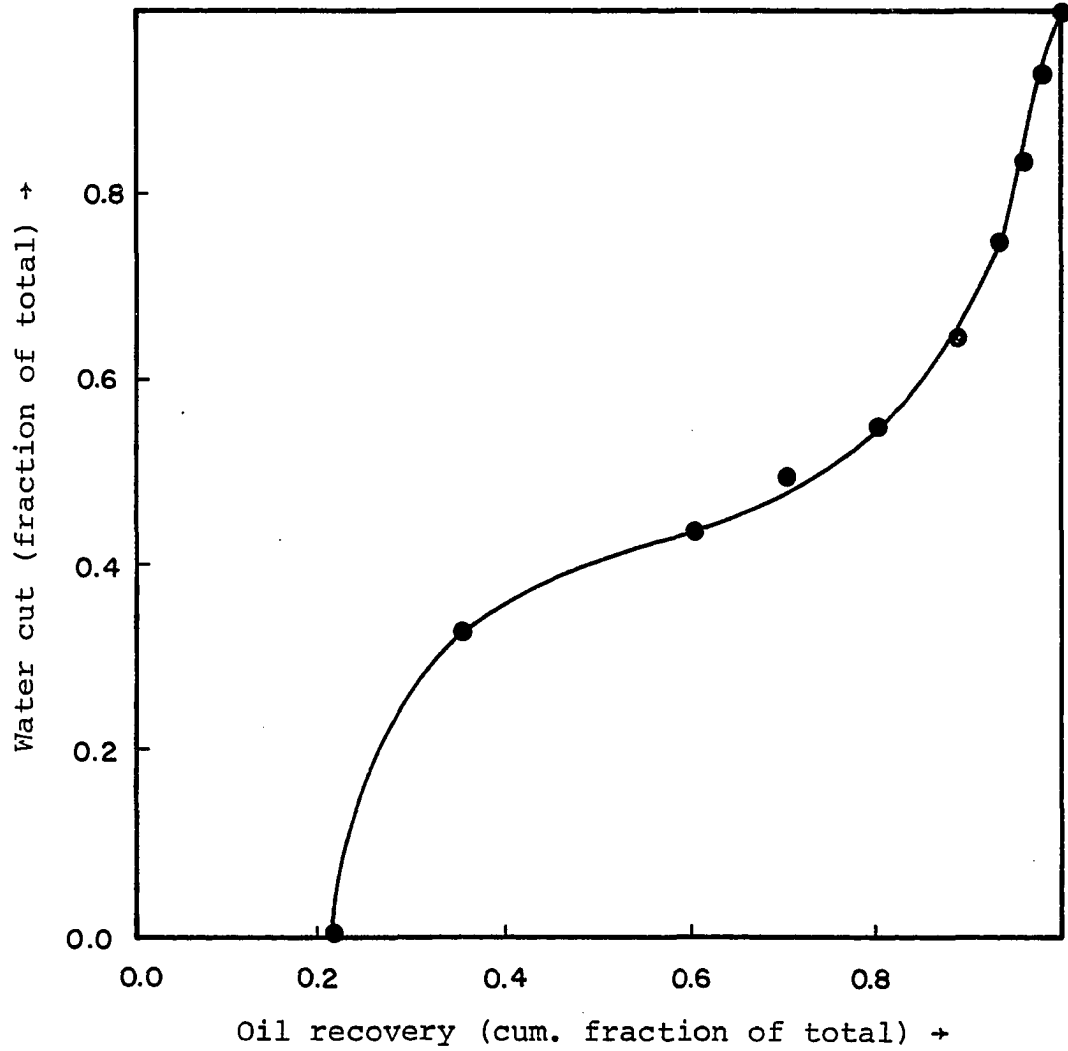


Figure 6.4 Plot of water cut versus oil recovery.

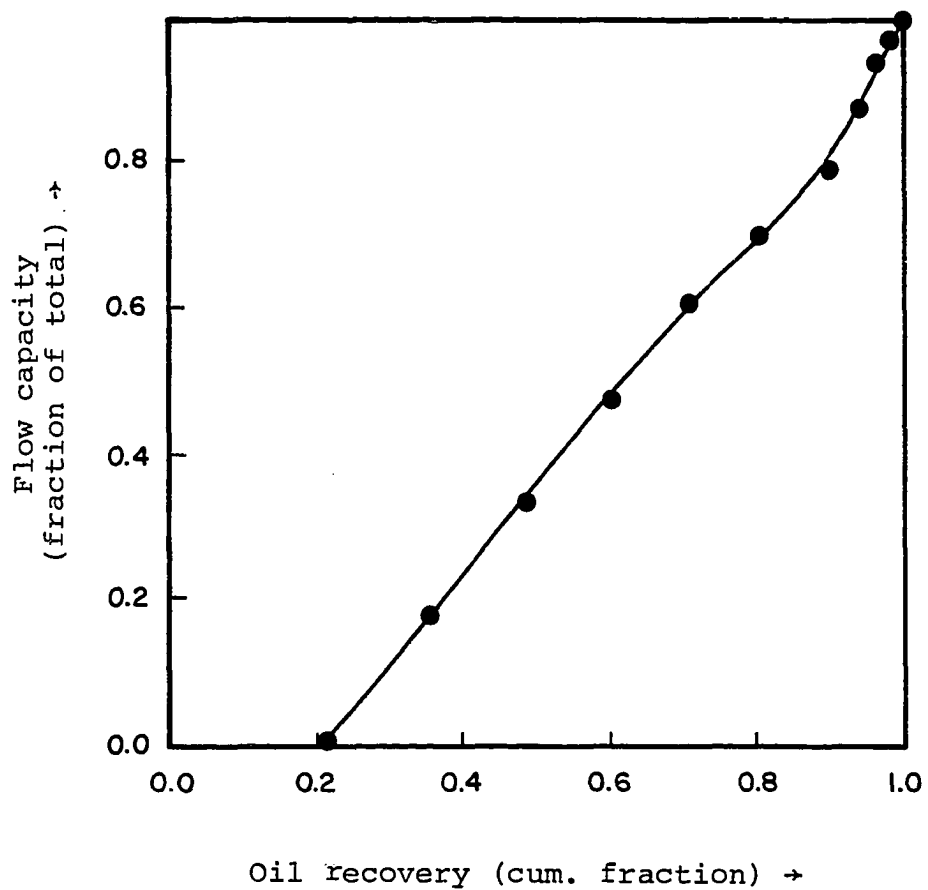


Figure 6.5 Plot of flow capacity versus oil recovery.

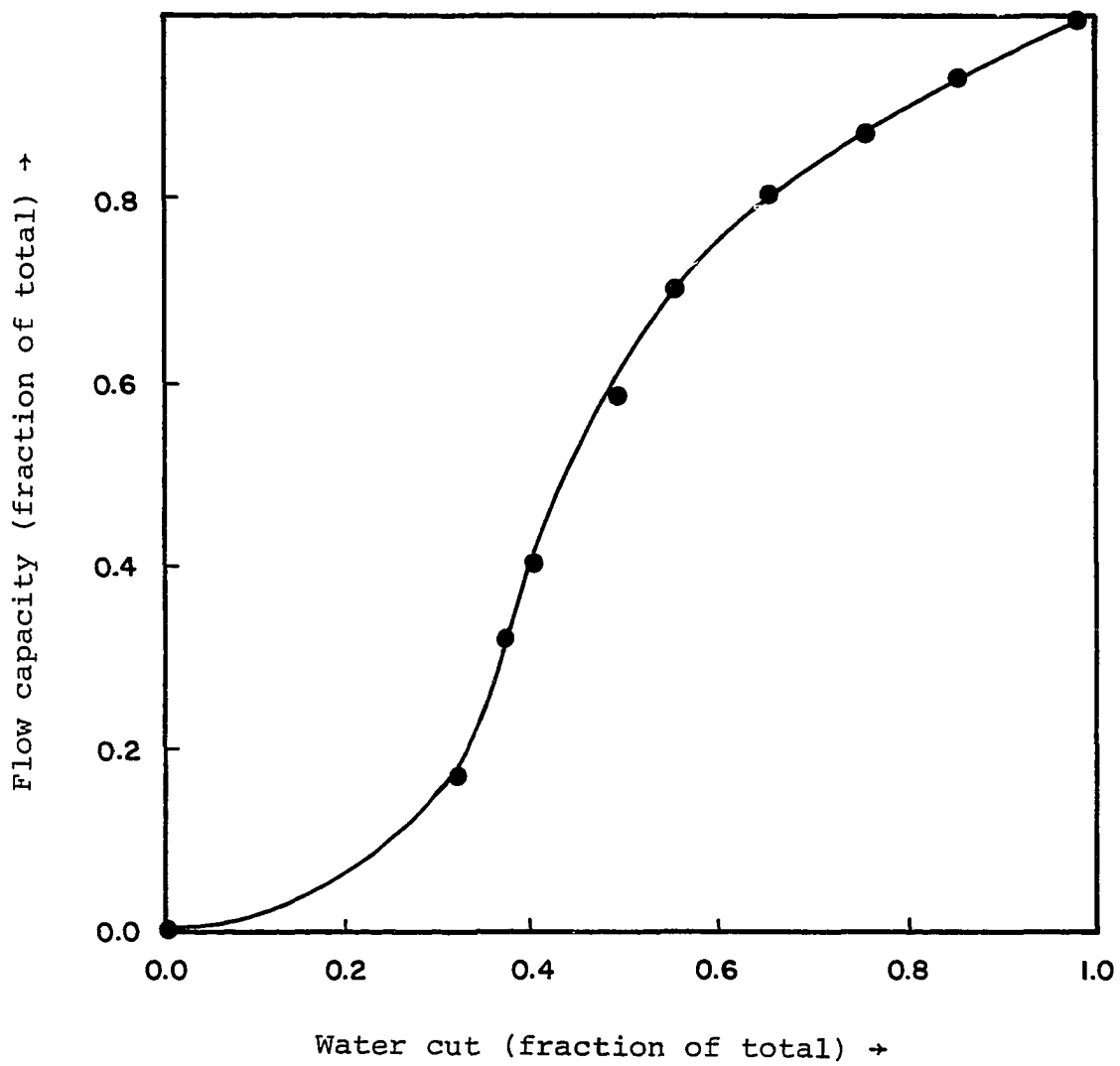


Figure 6.6 Plot of flow capacity versus water cut.

6.2 Determination of Reservoir Productive Volume (Planimeter Technique)

A planimeter (model 80) was used to obtain the bulk volume (V_b) on successive contour levels of the flow capacity distribution. The results of the above measurements are shown in table 6.2. Cumulative values of flow volume (fraction of total) are plotted against cumulative values of flow capacity. Figure 6.7, the result of this plot, shows that a small increase in the floodable volume produces a sharp increase in the flow capacity. Similar observation was reported by Johnson (16) but he used ' ϕh ' product instead of actual reservoir volume.

Table 6.2. Determination of Reservoir Productive Volume

Prod. Cap. Md-ft	Planimeter units	*Planimeter area (in ²)	Area (A _n) (acres)	Contour Interval (md-ft)	ΔV** acre (ft-md)
8	1546	16.3	374	6	
14	76	0.8	18.4	6	1178
20	108	1.14	26.1	6	134
26	48	0.51	11.6	6	113
32	15	0.16	3.6	6	46
38	19	0.20	4.6	6	25
44	5	0.052	1.2	6	18
50	8	0.08	1.9	6	9.3
56	20	0.21	4.8	6	20
59	0	0	0	3	15
					1558

* map scale: 1 inch = 1000 ft, one inch square = 22.96 acres.

NOTE: Calibration constant for the planimeter

$$= 95 \text{ units / (inch)}^2 \text{ or (inch)}^2 / 95 \text{ unit}$$

$$= 0.242 \text{ acres/unit}$$

** use the trapezoidal formula

$$\Delta V = \frac{kh}{2} (A_n + A_{n+1})$$

6.7

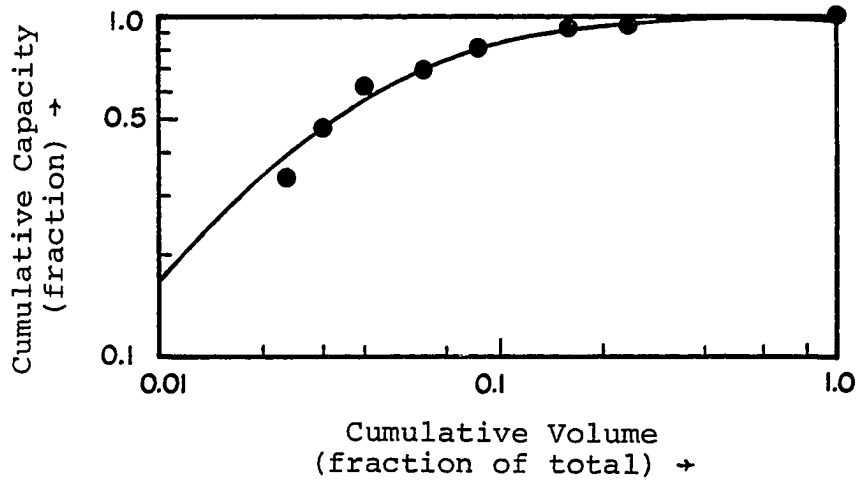


Figure 6.7 Plot of cumulative capacity versus cumulative volume.

Table 6.3. Calculation of Reservoir Volume
(Cum. fraction of total)

Flow Cap. (md)	Cum. Capacity (fraction)	Area (acres)	Vol (Acre ft)	Vol (fraction of total)	Cum vol (fract)
59	0.17	0	15	0.010	0.01
56	0.33	4.8	20	0.013	0.023
50	0.47	1.9	9.3	0.006	0.029
44	0.59	1.2	18.0	0.012	0.041
38	0.7	4.6	25	0.016	0.057
32	0.79	3.6	46	0.03	0.086
26	0.87	11.6	113	0.0725	0.158
20	0.91	26.1	134	0.086	0.244
14	0.97	18.4	1178	.756	1.000
8	0.99	374	0	0	1.000

6.3 Water Injection Plan: Waterflood injection scheme for a reservoir such as the Sitio Grand field could be planned as shown in table 6.4. The schedule is such that more injection water is made available to areas of low flow capacity. This procedure will reduce problems of channelling due to differences in permeability or flow capacity. The underlying assumptions are (1) water injection is a function of flow capacity, floodable volume, and water cut.

(2) Water injection efficiency is 60%.

The water injection equation is given by :

$$I_{inj}^i = \frac{1}{0.6} \left[\frac{\rho_i V_i W_i}{\sum_{i=1}^n \rho_i V_i} \right] \quad 6.8$$

A plot of water injection versus watercut is shown in figure 6.8.

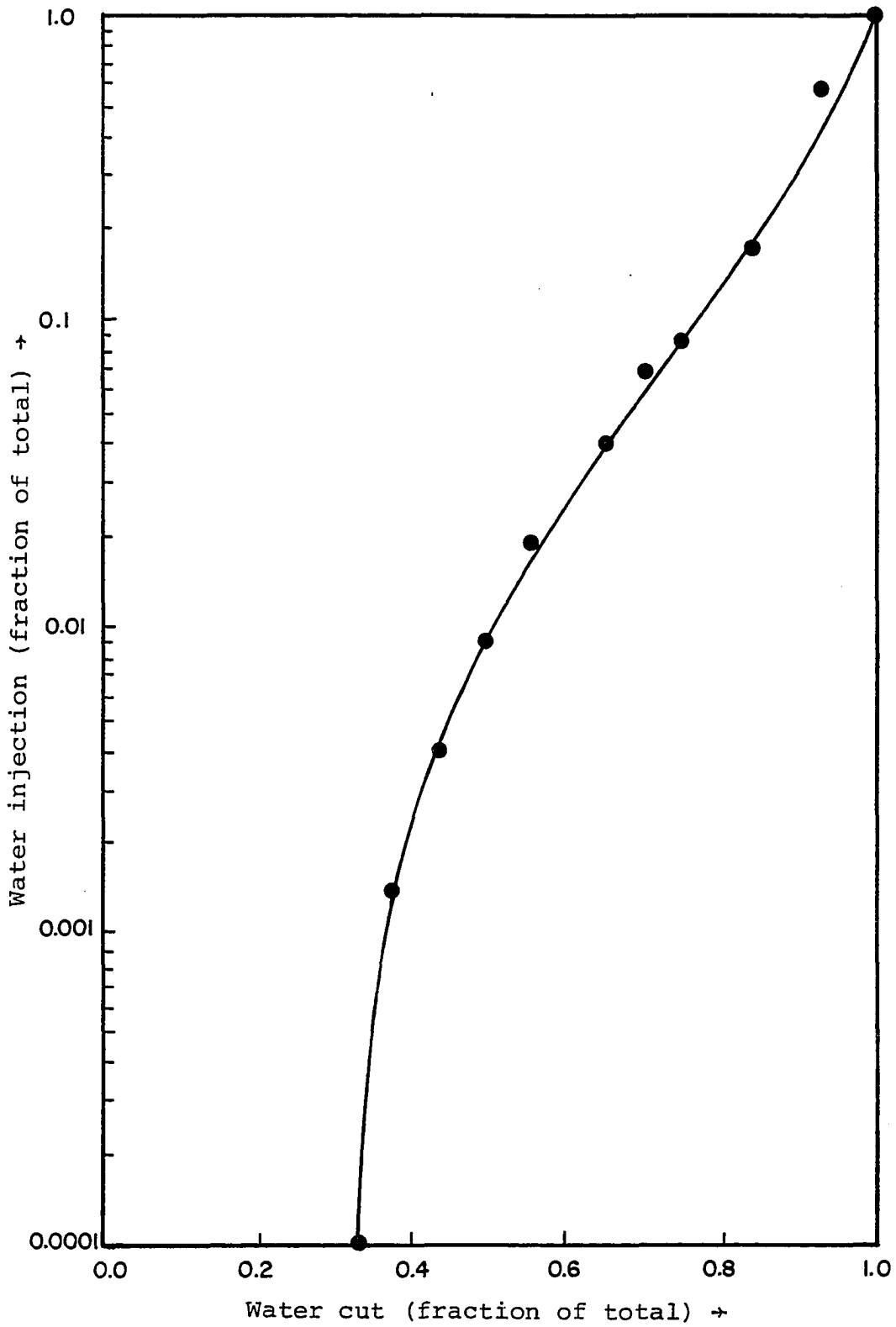


Figure 6.8 Plot of water injection versus water cut.

Table 6.4. Water Injection Plan

ρ (md)	water cut	floodable volume (fraction)	water injection	Cum Water inj (fraction)
0.17	0.33	0.01	0.001	0.0001
0.33	0.37	0.023	0.01	0.0014
0.47	0.43	0.029	0.02	0.004
0.59	0.49	0.041	0.041	0.009
0.7	0.55	0.057	0.075	0.019
0.79	0.65	0.086	0.151	0.039
0.87	0.75	0.158	0.353	0.085
0.92	0.84	0.244	0.65	0.169
0.96	0.93	0.999	3.09	0.57
0.99	0.98	1.000	3.323	1.00

6.4 Limitations of this model

1. Since reservoir performance may be influenced by some other unevaluated parameters, this model's accuracy is limited.
2. Many simplifying assumptions will tend to reduce the quality of the model.
3. Unlike the selective plugging technique, the interpolation part of this study does not redistribute injection water profile. It only indicates its existence. However, the capability of this model to indicate the flow capacity profile, and hence the injection water profile, will be profitably employed in selective plugging procedure by taking advantage of those locations of the reservoir that show relatively high flow capacity distributions. Thus we can economically inject our costly chemicals only in those zones that show abnormally high flow capacity values. In that way we can avoid wasting our 'plugging' chemicals on the zones where they are not needed.

CHAPTER VII

CONCLUSIONS AND RECOMMENDATIONS

1. This model offers an easy and quick means of estimating reservoir performance prior to the start of waterflood-
ing operations by providing flow capacity distribution
of the reservoir under study.
2. It offers an easy and quick means of estimating actual
reservoir floodable volume.
3. The model is useful in the estimation and planning of
waterflood injection schedule.
4. It can be used in the description of reservoir parameter
distribution.
5. The model can be used to represent data as a continuous
surface.
6. The model can be used to interpolate data with a con-
termination level of less than 20%.

RECOMMENDATIONS

1. More reservoir parameters should be incorporated into the program so that better reservoir description could be obtained.
2. Comparison of the performance results of this model should be made with the actual reservoir performance in order to evaluate the reliability of this model.

REFERENCES

1. Ahlberg, J. H., Nilson, E. N. and Walsh, J. L., "The Theory of Splines and Their Applications." Math in Science and Engineering, vol. 38, 266.(1965)
2. Bengtsson, B. E. and Nordbeck, S., "Construction of Isarithms and Isarithmic Maps by Computers," University of Lund, Sweden. BIT 4 87-105 (1964).
3. Birkhoff, G. and Garabedian, H. L., "Smooth Surface Interpolation." J. Math Physics 39 (1960), 258-268.
4. CACM Trans (Algorithm 474) Vol. 5, No. 2, June 1979, page 241.
5. Craig, F. F., "The Reservoir Engineering Aspects of Waterflooding." SPE Monograph, Vol. 2, 101.
6. DeBoor, C., "A Practical Guide to Splines." Springer-Verlag, N.Y. Heidelberg Berlin 1978.
7. DeWight's Natural Gas Well Prod. Histories DALLAS. Jan. 1976.
8. Dougenik, J. A. and Sheehan, D. E. Symap User's Manual Cambridge (Mass.) Lab. for Computer Graphics and Spatial Analysis, Harvard University, 1975.
9. Elkins, L. F. and Skov, A. M., "Determination of Fracture Orientation from Pressure Interference," Trans AIME, (1960) 219, 301-304.
10. Hardy, R. L. Journal of Geophysical Research, Vol. 76, No. 8, 1971.
11. Hutchinson, C. A. Jr., Polasek, T. L. Jr., and Dodge, C. F., "Identification, Classification and Prediction of Reservoir Non-Uniformity Affecting Production Operations." J.P.T. (March 1961) 223-230.
12. International Mathematics and Statistics Libraries, Inc. Edition 8, June 1980.
13. Jacquard, P. and Jain, C., "Permeability Distribution from Field Pressure Data." SPEJ (Dec. 1965) 281-294.

14. Jans, J. O., "A Rapid Method for Obtaining a Two-Dimensional Reservoir Description from Well Pressure Response Data." Journ. Pet. Tech. (Aug. 1962) 909-912.
15. Johnson, C. R., Greenkorn, R. A. and Woods, E. G., "Pulse Testing: A New Method for Describing Reservoir Flow Properties Between Wells." Journ. Pet. Tech. (Dec. 1966) 1599-1604.
16. Johnson, J. P., "Predicting Waterflood Performance by the Graphical Representation of Porosity and Permeability Distributions." Journ. Pet. Tech. (Nov. 1965) vol. 17, 1285.
17. Joseph, N. B., "Selective Plugging of Waterflood Input Wells, Theory, Methods and Results." Journ. Pet. Tech. (March 1957).
18. Kruger, W. D., "Determining Areal Permeability Distribution by Calculations." Journ. Pet. Tech. (July 1961) 691-696.
19. Krumbein, W. C., "Regional and Local Components in Facies Maps." Bull-American Assoc. of Petroleum Geologists, 40, 2163-94 (1956).
20. Miller, M. G. and Lents, M. R., "Performance of Bodcaw Reservoir, Collon Valley Field Cycling Projects New Methods of Predicting Gas-Condensate Reservoir Performance Under Cycling Operations Compared to Field Data." Drilling and Prod. Practice, API (1947) 128-179.
21. Milne, W. E., "Numerical Calculus." Princeton U. Press. Princeton, N.J., 1949, ch. 3.
22. Merriam, D. F. and Harbaugh, J. W. Trend surface analysis of regional and residual components of geology survey. sp. Dist. 11, 1964.
23. Perez-Rosales, C. "Use of Pressure Build up Tests in the Description of Heterogeneous Reservoirs." Society of Petroleum Eng. Journal No. 7451, Annual Fall Tech. Conference Exhib. Oct. 1978, Houston.
24. SAS/Graph Users Guide - 1981 edition, 43-45.
25. Schmalz, J. O. and Rahme, H. S. "Variation in Waterflood Perform. with Variation in Perm. Profile." Journ. Pet. Tech. (July 1950), 9.

26. Schoute, P. H., Goschensche, G. J., "Mehridimensionale Geometrie ā Quatre." Leipsiz 1902.
27. Shepard, D. A., "A Two-Dimensional Interpolation Function for Irregularly Spaced Data." Proc. 1968 ACM Nat. Conf., 517-524.
28. Stiles, W. E. "Use of Permeability Distribution in Waterflood Calculations." Journ. Pet. Tech. (Jan. 1949).
29. Synder, W. V. ACM 531, vol. 4, no. 3 Sept. 1978, 290-294.
30. Tapia, R. A. and Guerva, V. "A Local Procedure for Error Detection and Data Smoothing." MRC Technical Summary Report No. 1452. Maths Research Center University of Wis-Consin, Sept. 1974.
31. Watkins, S. L. Algorithm no. 483, ACM Trans. vol. 1, no. 3, Sept. 1975.
32. Wayne, F. W. and Joe, R. "Selective Plugging of Injection Wells by Insitu Reactions." Journ Pet. Tech. (Jan. 1957).
33. Zieto, G. A. "Interbedding of Shale Breaks and Reservoir Heterogeneities." Journ Pet. Tech. (Oct. 1965) 1223-1228.

APPENDICES

APPENDIX A
FLOW CHART AND NOMENCLATURE FOR THE
SPLINT PREDICTION ALGORITHM

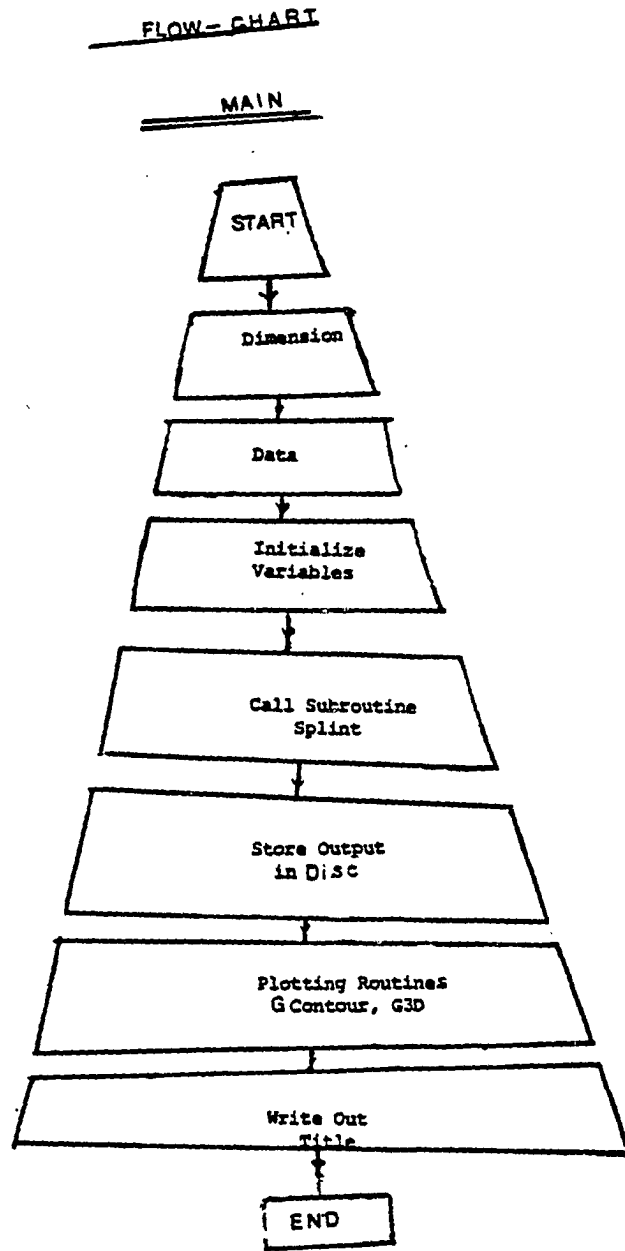


Figure A-1. Flow-chart for this model—Main.

SUB PROGRAM

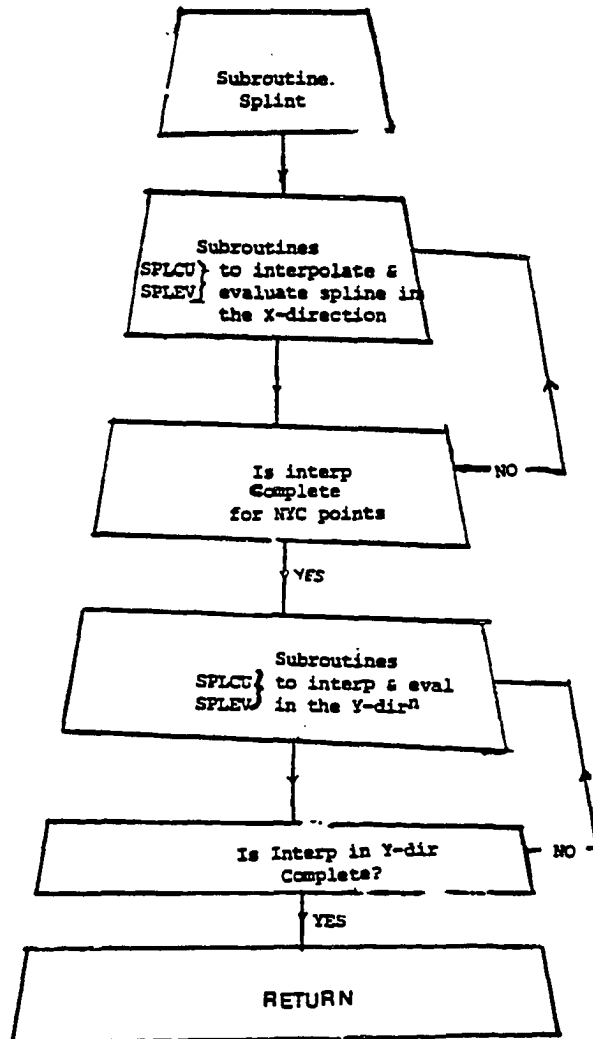


Figure A-2. Flow-chart for Subroutine Splint.

NOMENCLATURE FOR TERMS USED IN THE PROGRAM

- NX Total number of elements in the input vector x
- NY Number of elements in the input vector y
- X Input vector of stretch nx
(x must be in ascending order)
- Y Input vector of length NY
(y must be in ascending order)
- FS NX by NY matrix comprising of values at points specified by vectors X, and y.
- IFD Number of elements of FW in each row
- NXL Number of points along SXL where interpolation are needed
- NYL Number of points along SYL where interpolation are needed
- SXL Vector of length NXL--Input co-ord. points.
(SXL must be order in ascending order)
- SYL Vector of length NYL--input
(SYL must be ordered in ascending order)
- SFL Matrix NXL by NYL containing the interpolated values
- SWK A work vector of max. length the bigger of
(NX-1)*3 and ((NY-1)*3 + NY))
- IFR Is an error parameter.

APPENDIX B
SAMPLE PROGRAM

APPENDIX C

OUT PUT

SFL(SXL,SYL)

58.2 61.8 44.5 66.3 67.3 67.6 67.2 66.4 65.1 63.4 61.5 59.4 57.3 55.1 53.1
 51.2 49.6 48.4 47.7 47.5 47.9 49.0 50.7 52.7 54.9 57.2 59.3 61.0 62.2 62.7
 62.3 60.9 58.7 55.8 52.4 48.9 45.3 41.8 38.8 36.3 34.6 33.8 33.9 34.7 36.0
 37.6 39.4 41.2 43.0 44.5 45.5 46.0 45.9 45.5 44.7 43.7 42.5 41.3 40.1 39.0
 38.2 37.7 37.4 37.4 37.6 37.9 38.4 39.0 39.7 40.5 41.2 41.9 42.6 43.1 43.6
 43.9 43.9 43.8 43.4 42.7 41.7 56.3 61.6 65.5 68.1 69.4 69.7 69.0 67.6 65.5
 62.8 59.8 56.5 53.1 49.7 46.4 43.4 40.8 38.8 37.4 36.9 37.3 38.8 41.1 43.9
 47.2 50.6 53.8 56.7 59.0 60.4 60.8 59.9 57.9 55.0 51.6 47.8 43.9 40.2 36.8
 34.0 32.1 31.2 31.2 32.1 33.5 35.2 37.2 39.3 41.2 42.9 44.0 44.6 44.6 44.1
 43.3 42.2 40.9 39.6 38.4 37.2 36.3 35.8 35.5 35.5 35.7 36.1 36.6 37.3 38.0
 38.8 39.6 40.4 41.1 41.7 42.2 42.5 42.6 42.5 42.0 41.3 40.2 39.3 41.0 43.9
 69.0 70.6 71.9 70.0 68.1 65.3 61.9 57.9 53.6 49.2 44.8 40.5 36.5 33.2 30.5
 29.7 27.9 28.3 30.0 32.8 36.4 40.4 44.7 48.9 52.7 55.9 58.1 59.0 59.5 56.8
 44.0 50.5 46.6 42.5 38.5 34.8 31.8 29.7 28.7 28.8 29.6 31.1 32.9 35.1 37.3
 39.3 41.1 42.3 42.9 42.9 42.5 41.0 40.5 39.2 37.8 36.5 35.3 34.4 33.8 33.5
 32.5 33.7 34.1 34.7 35.4 36.2 37.0 37.9 38.7 39.4 40.1 40.6 40.9 41.0 40.9
 40.4 39.7 38.5 37.3 36.0 35.6 34.2 31.1 31.3 30.2 29.9 29.6 29.6 29.6 29.6
 45.6 40.4 35.4 30.8 26.8 23.6 21.4 20.4 20.8 22.7 25.8 29.9 34.6 39.6 44.5
 49.1 52.9 55.7 57.1 56.9 55.4 52.7 49.2 45.1 40.9 36.7 32.8 29.6 27.4 26.4
 26.3 27.2 29.7 30.0 32.9 35.2 37.3 39.1 40.5 41.1 41.1 40.7 39.8 38.6 37.3
 35.9 34.5 33.3 32.3 31.7 31.4 31.4 31.6 32.1 32.7 33.4 34.2 35.1 35.9 36.8
 37.6 38.2 38.9 39.1 39.2 39.1 38.6 37.8 36.7 35.1 34.7 34.8 34.7 34.7 34.7
 69.7 67.1 63.5 59.0 53.8 48.2 42.4 36.0 31.0 25.7 21.4 17.8 15.4 14.2 14.6
 14.6 20.1 24.5 29.7 35.2 40.7 45.8 50.1 53.3 55.1 55.2 53.7 51.1 47.6 43.5
 39.1 34.8 30.8 27.5 25.2 24.1 24.0 24.9 26.4 28.4 30.6 33.0 35.2 37.1 38.4
 39.1 39.1 38.7 37.8 36.6 35.3 33.8 32.5 31.2 30.2 29.6 29.3 29.3 29.5 30.0
 30.6 31.3 32.1 33.0 33.9 34.8 35.6 36.2 36.8 37.1 37.2 37.1 36.6 35.8 34.6
 48.0 57.0 63.5 67.7 69.7 70.0 65.6 65.9 61.9 57.1 51.6 45.6 39.4 33.2 27.3
 21.8 17.0 13.2 10.5 9.3 9.6 11.8 15.4 20.1 25.6 31.4 37.3 42.7 47.4 50.9
 53.0 53.2 51.9 49.3 45.8 41.7 37.3 32.9 28.9 25.5 23.1 21.9 21.8 22.7 24.2
 26.2 28.4 30.8 33.0 34.9 36.3 36.9 37.0 36.5 35.7 34.5 33.1 31.7 30.3 29.1
 28.1 27.5 27.2 27.1 27.4 27.8 28.4 29.2 30.0 30.9 31.8 32.6 33.4 34.1 34.6
 35.0 35.1 34.0 34.5 33.7 32.5 45.8 55.1 61.8 66.0 68.2 68.4 67.0 64.1 60.0
 55.0 49.3 43.1 36.7 30.3 24.2 18.5 13.5 9.6 6.8 5.5 5.8 8.0 11.7 16.6
 22.2 28.3 34.3 39.9 44.8 48.5 50.7 51.1 49.9 47.4 43.9 39.8 35.4 31.0 26.9
 23.5 21.1 19.9 19.8 20.6 22.0 24.0 26.2 28.6 30.8 32.7 34.0 34.7 34.7 34.3
 33.4 32.3 30.9 29.5 28.1 26.9 25.9 25.3 25.0 25.0 25.2 25.6 26.2 27.0 27.8
 28.0 29.5 30.4 31.2 31.8 32.4 32.7 32.8 32.7 32.2 31.4 30.3 29.6 29.0 29.7
 64.0 66.1 66.3 64.8 61.9 57.8 52.8 47.0 40.8 34.2 27.8 21.6 15.9 10.9 6.9
 4.1 2.7 3.1 5.3 9.0 13.9 19.6 25.7 31.7 37.4 42.4 46.2 48.4 48.8 47.7
 45.2 41.8 37.8 33.4 29.1 25.0 21.0 19.2 18.0 17.8 18.5 20.0 21.9 24.1 26.3
 28.5 30.3 31.7 32.3 32.4 31.9 31.1 30.0 28.6 27.3 25.9 24.7 23.7 23.1 22.8
 22.8 23.0 23.4 24.0 24.7 25.5 26.4 27.2 28.1 28.8 29.5 30.0 30.3 30.5 30.3

29.9 29.1 29.0 41.4 50.6 57.2 61.5 62.6 63.8 62.3 59.4 55.4 50.4 44.7 36.5
 32.1 25.7 19.6 13.0 9.0 5.0 2.2 0.9 1.2 3.4 7.1 11.9 17.5 23.5 29.5
 35.2 40.1 43.4 46.1 46.5 45.4 43.0 39.7 35.7 31.4 27.1 23.2 19.8 17.4 16.1
 17.0 16.6 19.0 19.8 21.9 24.1 26.2 28.0 29.3 29.9 30.0 29.5 29.7 27.6 26.3
 25.0 23.7 22.5 21.6 21.0 20.7 20.0 20.8 21.2 21.8 22.5 23.2 24.1 24.9 25.7
 26.4 27.1 27.6 27.9 28.0 27.9 27.4 26.7 25.6 39.3 48.2 54.6 58.7 60.7 60.9
 59.4 56.6 52.7 47.9 42.3 36.3 30.1 23.9 18.0 12.5 7.7 3.9 1.2 0.0 0.3
 2.2 5.9 10.4 16.1 21.9 27.7 33.2 37.6 41.5 43.7 44.1 43.0 40.7 37.4 33.6
 29.3 25.2 21.3 18.1 15.7 14.4 14.2 14.0 15.1 17.4 19.0 22.0 24.0 25.7 26.9
 27.5 27.5 27.1 26.2 25.2 24.0 22.7 21.5 20.3 19.4 18.8 18.5 18.5 18.7 19.1
 19.6 20.2 21.0 21.8 22.5 23.3 24.0 24.6 25.1 25.4 25.5 25.4 25.0 24.3 23.2
 37.2 45.7 51.7 55.6 57.5 57.7 56.3 53.6 49.9 45.3 40.0 34.3 28.4 22.5 16.8
 11.6 7.1 3.4 0.9 0.0 0.0 0.0 0.0 5.4 9.9 15.1 20.7 26.1 31.3 35.8 39.3
 41.3 41.7 40.6 38.3 35.2 31.4 27.4 23.4 19.6 16.4 14.1 12.9 12.6 13.2 14.4
 16.0 17.9 19.9 21.7 23.3 24.5 25.1 25.1 24.7 23.9 22.9 21.7 20.5 19.3 18.2
 17.3 16.7 16.4 16.4 16.6 16.9 17.4 18.0 18.7 19.5 20.2 20.9 21.6 22.2 22.6
 22.9 23.0 22.9 22.5 21.8 20.8 35.2 43.1 49.7 52.3 54.1 54.3 53.0 50.5 47.0
 42.6 37.7 32.4 26.9 21.4 16.1 11.2 7.0 3.5 1.2 0.0 0.4 2.3 5.5 9.7
 14.5 19.7 24.9 29.7 33.9 37.1 39.9 39.2 38.1 35.9 32.9 29.3 25.4 21.5 17.9
 16.9 12.6 11.4 11.1 11.6 12.7 14.2 16.0 17.8 19.6 21.1 22.1 22.7 22.7 22.3
 21.5 20.6 19.4 18.2 17.1 16.1 15.2 14.7 14.4 14.4 14.5 14.8 15.3 15.9 16.5
 17.2 17.9 18.6 19.2 19.7 20.1 20.4 20.5 20.4 20.0 19.4 18.4 33.2 40.5 45.7
 49.0 50.6 50.7 49.5 47.2 44.0 40.0 35.5 30.6 25.5 20.5 15.6 11.1 7.2 4.1
 2.0 0.9 1.3 3.0 6.0 9.9 14.3 19.1 23.9 28.3 32.1 35.0 26.6 36.8 35.7
 32.5 30.6 27.2 23.5 19.8 16.3 13.4 11.3 10.1 9.8 10.2 11.2 12.5 14.2 15.9
 17.5 18.9 19.9 20.3 20.3 19.9 19.2 18.3 17.2 16.1 15.0 14.0 13.2 12.7 12.4
 12.4 12.5 12.8 13.2 13.8 14.3 15.0 15.6 16.2 16.8 17.3 17.7 18.0 18.0 17.9
 17.0 17.0 17.1 17.1 17.0 17.0 17.1 17.0 17.1 17.0 17.0 17.0 17.0 17.0 17.0
 24.4 19.8 15.4 11.4 7.9 5.1 3.1 2.2 2.6 4.2 6.9 10.4 14.5 18.8 23.1
 27.1 30.5 33.0 34.4 34.4 33.3 31.2 28.4 25.1 21.6 18.1 14.8 12.1 10.0 8.9
 8.6 8.9 9.8 11.0 12.5 14.0 15.5 16.8 17.7 18.1 18.0 17.7 17.0 16.1 15.1
 14.0 13.0 12.1 11.3 10.8 10.6 10.5 10.6 10.9 11.2 11.7 12.3 12.8 13.4 14.0
 14.5 15.0 15.3 15.6 15.7 15.5 15.2 14.7 13.8 29.6 35.4 39.5 42.2 43.4 43.5
 42.6 40.7 39.1 34.9 31.3 27.4 23.4 19.3 15.4 11.9 8.8 6.3 4.6 3.9 4.2
 5.6 8.1 11.2 14.8 18.7 22.5 26.0 28.9 31.1 32.2 32.1 31.0 28.9 26.2 23.1
 19.8 16.5 13.4 10.4 8.7 7.8 7.9 7.7 9.5 9.6 10.9 12.3 13.7 14.8 15.6
 15.9 15.9 15.5 14.9 14.0 13.1 12.1 11.1 10.2 9.5 9.1 8.8 8.7 8.8 9.0
 9.4 9.8 10.3 10.8 11.3 11.9 12.3 12.8 13.1 13.2 13.4 13.3 13.0 12.4 11.7
 28.0 33.0 36.6 39.9 40.0 40.0 36.2 37.6 35.3 32.6 29.4 26.0 22.5 19.0 15.6

12.6 9.9 7.4 6.3 5.7 6.0 7.3 9.4 12.2 15.4 14.7 22.0 25.0 27.6 26.4
 30.2 29.9 27.7 26.7 26.2 21.2 16.1 15.0 12.1 7.7 7.9 6.4 6.5 6.7 7.4
 6.3 9.8 10.6 12.0 13.0 13.7 14.0 13.9 13.8 12.6 12.1 11.2 10.3 9.3 8.5
 7.4 7.4 7.1 7.0 7.1 7.3 7.4 8.0 8.4 8.9 9.4 9.8 10.3 10.6 10.9
 11.1 11.2 11.1 10.8 10.3 9.4 26.5 30.8 32.6 35.7 36.6 36.7 38.3 34.6 39.7
 30.3 27.6 26.9 21.4 16.8 16.3 13.4 11.1 9.3 8.1 7.8 7.9 9.1 10.9 12.2
 14.1 18.9 21.7 24.2 26.3 27.7 28.3 27.9 26.6 24.7 22.2 19.4 16.8 13.6 11.0
 8.7 7.3 6.0 5.4 5.8 6.4 7.2 8.3 9.4 10.4 11.3 11.9 12.1 12.0 11.7
 11.1 10.3 7.8 7.4 7.7 6.9 6.3 5.9 5.4 5.3 5.5 5.7 6.0 6.3 6.7
 7.1 7.5 8.0 8.4 8.7 9.9 9.1 9.2 9.1 8.8 8.4 7.7 28.2 28.7 31.2
 32.8 33.6 33.6 33.0 31.6 30.2 28.3 26.1 23.7 21.3 18.7 16.4 14.2 12.4 10.9
 10.0 7.6 7.7 7.9 12.8 14.3 14.6 14.2 21.5 23.3 25.2 24.2 26.6 26.0 24.7
 22.6 20.4 17.8 19.1 12.4 9.9 7.8 6.2 5.3 4.9 5.0 5.3 6.3 7.2 8.1
 9.1 7.8 10.4 10.8 10.4 10.0 9.4 8.7 7.9 7.1 6.3 5.3 4.9 4.5 4.2
 4.1 4.1 4.3 4.3 4.4 5.1 5.8 5.9 6.3 6.4 6.9 7.1 7.3 7.2 7.2
 7.0 6.6 4.0 24.1 24.9 28.9 30.2 30.0 30.8 30.3 29.4 28.1 26.8 24.6 22.7
 20.7 18.7 14.8 19.1 13.6 12.4 11.7 11.4 12.7 12.8 13.9 15.6 17.8 19.4 21.3
 22.9 24.2 24.9 25.0 24.3 23.0 21.1 18.9 16.4 13.8 11.3 9.0 7.1 5.6 4.7
 4.3 4.4 4.8 5.5 6.3 7.1 7.9 8.6 9.0 9.2 9.0 8.8 8.0 7.3 6.6
 5.8 5.0 4.3 3.7 3.3 3.0 2.9 2.9 3.0 3.2 3.4 3.7 4.1 4.4 4.7
 5.0 5.3 5.3 5.7 5.7 5.4 5.4 5.0 4.5 23.1 25.4 27.0 28.0 24.8 28.4
 29.0 27.3 28.2 28.9 23.5 21.9 20.3 18.7 17.2 18.4 14.7 13.9 13.2 13.0 13.3
 14.6 15.2 16.4 14.1 14.7 21.2 22.4 23.3 23.6 23.6 22.8 21.8 19.6 17.8 16.2
 12.8 10.4 5.3 4.5 5.1 4.2 2.9 3.9 4.3 4.9 5.6 6.3 7.0 7.6 8.3
 4.0 7.7 7.5 6.9 6.2 5.4 4.7 3.9 3.2 2.6 2.2 2.0 1.8 1.8 1.9
 2.4 2.3 2.5 2.8 3.1 3.4 3.7 4.0 4.2 4.3 4.3 4.2 4.3 3.7 3.2
 22.4 24.2 25.4 26.2 26.6 26.5 26.1 25.6 24.7 23.7 22.8 21.3 20.0 18.7 17.5
 14.5 14.6 14.5 14.5 14.3 14.9 14.2 14.2 17.3 18.6 14.9 21.0 22.0 22.6 22.8
 22.8 21.6 22.2 14.4 16.4 14.2 11.9 9.7 7.7 6.0 4.7 3.8 3.6 3.6 3.4
 4.4 5.1 5.3 4.4 4.9 7.2 7.2 7.0 6.6 4.0 5.3 4.6 3.8 3.0 2.4
 1.8 1.4 1.1 1.0 0.9 1.0 1.1 1.3 1.5 1.8 2.1 2.4 2.6 2.9 3.0
 3.2 3.2 3.1 3.9 2.6 2.1 21.7 23.3 24.3 24.7 25.2 25.1 24.6 24.3 23.6
 22.7 21.8 20.8 19.7 18.7 17.8 16.9 16.2 13.6 15.3 15.3 15.5 16.1 16.9 17.9
 14.9 14.9 20.4 21.6 22.0 22.0 21.4 20.7 19.3 17.5 15.5 13.4 11.2 9.2 7.3
 5.7 4.5 3.7 3.4 3.4 3.7 4.2 4.4 5.4 6.0 6.5 6.7 6.7 6.5 6.0
 5.4 4.7 4.0 3.2 2.4 1.7 1.2 0.7 0.5 0.3 0.2 0.3 0.4 0.4 0.4
 1.0 1.3 1.6 1.8 2.0 2.2 2.3 2.3 2.3 2.1 1.7 1.3 21.6 22.4 23.4
 24.1 24.3 24.2 23.9 23.8 22.8 22.1 21.3 20.4 19.5 18.7 17.9 17.2 16.6 16.1
 15.9 15.6 14.1 14.6 17.3 16.1 14.0 14.9 20.6 21.2 21.5 21.4 20.9 19.9 18.8
 16.8 14.9 12.8 10.9 8.8 7.0 6.3 4.3 3.4 3.4 3.4 3.7 4.2 4.7 5.3
 6.9 6.3 6.3 6.3 6.2 5.7 5.1 4.4 3.4 2.8 2.0 1.3 0.7 0.3 0.0
 0.0 0.0 0.0 0.0 0.0 0.3 0.5 0.4 1.0 1.2 1.5 1.6 1.7 1.7 1.7
 1.8 1.2 0.7 21.8 22.8 23.2 23.6 23.7 23.4 23.4 22.9 22.4 21.7 21.0 20.2
 19.4 18.4 17.9 17.2 16.7 16.3 16.1 16.1 16.3 16.7 17.4 18.2 19.0 19.7 20.4
 20.9 21.1 20.9 20.4 19.4 18.0 16.3 14.8 12.8 10.8 8.6 6.8 5.4 4.3 3.7
 3.4 3.3 3.4 4.4 4.4 4.4 4.4 4.3 4.5 4.4 4.4 4.4 4.4 4.4 4.4
 2.4 1.4 1.1 0.5 0.0 0.0 0.0 0.0 0.0 0.0 0.0 0.0 0.1 0.4 0.4

0.9 1.1 1.3 1.4 1.4 1.3 1.1 0.6 0.3 21.4 22.4 23.0 23.4 23.5 23.4
 23.1 22.7 22.2 21.5 20.8 20.0 19.3 19.5 17.8 17.2 16.7 16.3 16.1 16.0 16.2
 16.7 17.2 18.0 18.7 19.9 20.1 20.5 20.7 20.5 20.0 19.0 17.7 16.0 14.2 12.3
 10.3 8.5 6.9 5.4 4.4 3.8 3.5 3.6 3.9 4.4 5.0 5.6 6.1 6.5 6.6
 6.5 6.2 5.7 5.0 4.2 3.6 2.8 1.7 1.0 0.3 0.3 0.0 0.0 0.0 0.0
 0.0 0.0 3.0 0.0 0.2 3.4 6.7 0.0 1.1 1.2 1.2 1.1 0.9 0.6 0.1
 21.8 22.4 23.1 23.4 23.8 23.4 23.1 22.7 22.1 21.4 20.7 19.9 19.1 18.4 17.7
 17.0 16.5 16.1 15.7 15.9 15.0 14.3 17.0 17.7 18.4 19.1 19.7 20.1 20.3 20.2
 16.7 14.7 12.4 10.0 8.3 12.1 10.1 14.5 6.9 5.2 4.5 3.4 3.4 3.9 4.2
 4.7 5.2 5.8 6.4 6.7 6.9 6.8 6.6 5.9 5.1 4.3 3.5 2.6 1.7 0.9
 0.3 0.0 0.0 0.0 0.0 0.0 3.0 0.0 0.0 0.1 0.4 0.6 0.8 0.8 1.0
 1.1 1.1 1.0 0.4 0.5 0.1 21.4 22.4 23.2 23.4 23.7 23.6 23.3 22.8 22.2
 21.8 20.7 19.8 19.0 18.2 17.4 16.7 16.2 15.7 15.4 15.3 15.3 15.9 16.5 17.2
 17.0 18.6 19.2 19.7 19.9 19.8 19.4 18.8 17.2 15.7 13.9 12.1 10.3 8.5 7.0
 5.7 4.7 4.2 4.0 4.1 4.5 5.0 5.6 6.1 6.7 7.0 7.2 7.8 8.6 6.1
 5.2 4.5 3.6 2.7 1.8 1.0 0.3 0.0 0.0 0.0 0.0 0.0 0.0 0.0 0.0
 0.0 3.1 0.4 0.7 0.9 1.0 1.2 1.2 1.1 0.9 0.6 0.1 21.7 22.8 23.4
 23.8 23.9 23.8 23.8 23.0 22.3 21.6 20.7 19.8 18.9 18.0 17.2 16.4 15.7 15.2
 14.9 14.6 14.4 13.3 12.9 12.6 12.3 12.1 12.1 12.7 13.2 13.5 13.5 13.1 12.2 12.0
 15.5 13.9 12.1 10.3 8.4 7.1 5.9 5.0 4.4 4.3 4.4 4.6 5.3 5.9 6.5
 6.9 7.3 7.4 7.3 6.9 6.3 5.5 4.7 3.8 2.8 1.9 1.1 0.4 0.0 0.0
 0.0 0.0 0.0 0.0 0.0 0.0 0.0 0.2 0.5 0.8 1.0 1.2 1.3 1.3 1.2
 1.0 0.7 0.2 21.8 22.9 23.7 24.1 24.2 24.1 23.7 23.2 22.5 21.6 20.7 19.7
 18.7 17.6 16.8 16.0 15.3 14.7 14.3 14.3 14.2 14.6 13.8 12.7 12.7 12.4 12.1
 11.7 11.0 10.0 10.7 11.9 12.8 13.4 13.8 13.1 12.4 11.4 10.4 9.9 9.3 8.7
 8.6 8.8 9.1 9.6 10.2 10.7 11.2 11.8 12.4 13.0 13.6 14.2 14.8 15.4 16.0
 3.0 2.1 1.3 0.6 0.0 0.0 0.0 0.0 0.0 0.0 0.0 0.0 0.1 0.4 0.6
 0.9 1.1 1.3 1.4 1.4 1.3 1.1 0.8 0.3 21.9 23.0 23.8 24.3 24.4 24.2
 23.4 23.3 22.5 21.6 20.6 19.6 18.5 17.5 16.5 15.6 14.6 14.1 13.7 13.5 13.5
 13.0 12.4 12.1 12.9 13.7 14.5 15.3 16.1 16.9 17.7 18.5 19.3 20.1 20.9 21.7
 10.3 8.9 7.2 6.4 5.5 5.0 4.9 5.1 5.4 5.8 6.4 7.0 7.6 7.7
 7.5 7.1 6.5 5.7 4.9 4.0 3.1 2.2 1.4 0.7 0.2 0.0 0.0 0.0 0.0
 0.0 0.0 0.0 0.2 0.5 0.8 1.0 1.2 1.4 1.6 1.5 1.3 1.0 0.5
 21.8 23.0 23.8 24.3 24.4 24.3 23.9 23.3 22.6 21.3 20.5 19.4 18.3 17.2 16.1
 15.1 14.3 13.6 13.1 12.8 12.6 12.1 12.4 12.3 12.1 11.9 11.6 11.3 11.0 10.7
 17.6 17.0 16.1 14.9 12.5 12.0 10.8 9.0 7.7 6.6 5.8 5.3 5.2 5.3 5.4
 4.0 3.5 3.5 3.3 3.6 3.6 3.6 3.0 2.4 2.4 2.4 2.9 3.1 2.2 1.4
 0.5 0.2 0.0 0.3 0.0 0.0 0.0 0.0 0.1 0.3 0.6 0.9 1.1 1.3 1.5
 1.6 1.6 1.5 1.4 1.1 0.6 21.6 22.8 23.7 24.1 24.3 24.1 23.7 23.1 22.2
 21.3 20.2 19.1 18.0 16.8 15.7 14.7 12.8 13.0 12.8 12.2 12.1 12.4 12.9 13.5
 14.2 15.0 15.7 16.3 16.9 17.3 18.5 18.3 18.5 18.4 13.1 11.6 10.4 9.1 7.9
 6.8 6.1 5.6 5.5 5.5 5.7 6.1 6.4 6.4 7.1 7.3 7.2 7.1 6.7 6.1
 5.4 4.6 3.4 3.0 2.2 1.5 0.8 0.4 0.1 0.0 0.0 0.0 0.0 0.0 0.2
 0.4 0.7 0.6 1.1 1.3 1.5 1.6 1.6 1.6 1.4 1.1 0.7 21.3 22.5 23.3
 23.8 23.9 23.7 23.3 22.7 21.9 20.7 19.9 18.7 17.6 16.4 15.3 14.3 13.3 12.6
 12.0 11.6 11.5 11.7 12.1 12.7 13.4 14.1 14.7 15.3 15.4 16.0 16.9 18.4 14.7
 13.8 12.7 11.2 10.3 9.1 8.0 7.0 6.3 5.9 5.7 5.7 5.6 6.0 6.3 6.3

0.7 0.8 0.9 0.5 0.1 3.0 4.0 0.2 3.5 2.7 2.3 1.0 0.9 0.4 0.2
0.0 0.0 0.0 0.0 0.1 0.3 0.5 0.7 0.9 1.1 1.3 1.4 1.5 1.5 1.5
1.3 1.1 0.7 20.9 22.1 22.0 23.2 23.3 23.2 22.2 22.1 21.3 20.4 19.4 18.3
17.1 16.0 14.9 13.9 12.9 12.1 11.2 11.1 11.0 11.1 11.0 11.0 11.0 12.8 13.1 13.7
14.2 14.6 14.8 14.8 14.8 13.9 13.1 12.2 11.1 10.1 9.0 8.0 7.2 6.5 6.1
5.4 5.7 5.4 5.0 0.0 0.1 0.2 0.2 0.1 0.1 0.1 0.1 0.1 0.1 0.1 0.1
2.4 1.8 1.2 0.8 0.8 0.2 0.1 0.0 0.0 0.0 0.2 0.3 0.5 0.6 0.8
1.0 1.2 1.3 1.4 1.4 1.3 1.2 1.0 0.7 20.4 21.5 22.2 22.6 22.7 22.5
22.1 21.3 20.7 19.8 19.6 17.7 16.6 15.8 14.5 13.4 12.5 11.7 11.1 10.7 10.4
10.5 10.7 11.1 11.0 12.1 12.4 13.1 13.4 13.7 13.7 13.4 12.9 12.3 11.8 10.7
9.4 8.9 9.1 7.3 6.7 6.2 5.6 5.0 5.7 5.4 5.0 5.7 5.6 5.5 5.4
5.1 4.7 4.2 3.7 3.2 2.6 2.1 1.6 1.1 0.7 0.8 0.2 0.1 0.1 0.1
0.1 0.2 0.3 0.4 0.6 0.7 0.9 1.0 1.1 1.2 1.2 1.1 1.0 0.9 0.6
10.9 20.4 21.6 21.4 21.9 21.7 21.3 20.7 20.0 19.1 18.2 17.2 16.1 15.1 14.0
13.0 12.1 11.4 10.7 10.2 10.0 9.9 10.0 10.3 10.7 11.1 11.5 11.9 12.2 12.4
12.5 12.3 11.9 11.5 10.9 10.2 9.5 8.7 8.0 7.4 6.8 6.4 6.0 5.7 5.5
5.4 5.2 5.1 4.9 4.8 4.7 4.2 3.9 3.5 3.0 2.6 2.1 1.7 1.3 0.9
0.6 0.4 0.3 0.2 0.1 0.1 0.1 0.2 0.3 0.4 0.5 0.6 0.7 0.8 0.9
0.9 0.9 0.9 0.9 0.7 0.5 19.3 20.1 20.7 20.9 21.0 20.4 19.4 19.0 19.2
18.4 17.8 17.5 17.5 17.4 17.4 17.4 17.4 17.4 17.4 17.4 17.4 17.4 17.4 17.4
6.8 10.1 13.4 13.2 11.0 11.2 11.2 11.1 10.9 10.4 10.1 9.6 9.1 8.5 7.9
7.4 6.9 6.4 6.3 5.8 5.7 5.0 4.5 4.2 3.9 3.7 3.3 3.0 2.6
2.3 1.9 1.4 1.3 1.0 0.7 0.5 0.4 0.3 0.2 0.1 0.1 0.2 0.2 0.2
0.3 0.4 0.5 0.5 0.4 0.7 0.7 0.7 0.6 0.5 0.4 0.4 0.4 0.4 0.4
20.0 20.0 19.6 19.5 18.9 18.3 17.6 16.7 15.9 14.9 14.0 13.1 12.2 11.4 10.7
10.3 9.8 9.1 8.6 8.0 7.4 6.8 6.2 5.6 5.0 4.4 3.8 3.2 2.6 2.0
9.7 9.4 9.0 8.6 8.2 7.8 7.3 6.8 6.4 5.9 5.5 5.1 4.6 4.2 3.9
3.5 3.1 2.8 2.5 2.1 1.9 1.6 1.3 1.1 0.9 0.7 0.5 0.4 0.3 0.2
0.2 0.2 0.2 0.2 0.2 0.2 0.2 0.3 0.3 0.4 0.4 0.4 0.5 0.5 0.4
0.4 0.4 0.3 18.0 18.6 18.9 19.1 19.0 18.8 18.5 18.0 17.4 16.7 16.0 15.2
14.3 13.8 12.4 11.8 11.0 10.3 9.7 9.2 8.6 8.5 8.3 8.2 8.3 8.3 8.0
8.6 8.7 8.7 8.9 8.9 8.9 8.8 8.6 8.4 8.2 7.9 7.5 7.1 6.7 6.3
5.4 5.3 4.7 4.2 3.7 3.2 2.8 2.3 2.0 1.6 1.3 1.1 0.9 0.7 0.6
0.5 0.4 0.4 0.3 0.3 0.2 0.2 0.2 0.2 0.2 0.2 0.2 0.2 0.2 0.2
0.2 0.2 0.2 0.2 0.2 0.2 0.2 0.2 0.2 17.4 17.8 18.1 18.1 18.1 17.8
17.5 17.0 16.5 15.9 15.2 14.5 13.7 12.9 12.2 11.4 10.7 10.0 9.4 8.9 8.4
8.1 7.8 7.7 7.6 7.6 7.6 7.6 7.7 7.8 7.8 7.9 7.9 7.9 7.9 7.8
7.6 7.4 7.2 6.9 6.8 6.1 5.5 5.0 4.4 3.8 3.2 2.6 2.1 1.6 1.2
0.9 0.5 0.4 0.3 0.2 0.2 0.2 0.2 0.2 0.2 0.2 0.2 0.2 0.2 0.2
0.2 0.1 0.1 0.1 0.1 0.1 0.1 0.0 0.0 0.0 0.0 0.0 0.0 0.1 0.1
16.8 17.1 17.2 17.2 17.1 16.9 16.5 16.1 15.6 15.0 14.4 13.7 13.1 12.4 11.7
11.0 10.3 9.7 9.1 8.6 8.1 7.7 7.4 7.2 7.0 6.9 6.8 6.8 6.8 6.8
6.9 7.0 7.0 7.1 7.1 7.1 7.1 7.0 6.8 6.6 6.2 5.8 5.2 4.6 4.0
3.4 2.7 2.1 1.8 1.6 0.4 0.2 0.1 0.0 0.0 0.0 0.0 0.0 0.0 0.0
0.1 0.1 0.2 0.2 0.2 0.2 0.2 0.1 0.1 0.0 0.0 0.0 0.0 0.0 0.0
0.0 0.0 0.0 0.0 0.0 0.0 18.2 18.4 18.4 18.3 18.2 18.0 18.6 18.2 18.7

